

Contributions Towards Practical Cognitive Radios Systems

Thesis by
Mahdi Ben Ghorbel

In Partial Fulfillment of the Requirements

For the Degree of

Doctor of Philosophy (*Electrical Engineering*)

King Abdullah University of Science and Technology (KAUST)

Thuwal, Makkah Province

Kingdom of Saudi Arabia

July, 2013

The thesis of Mahdi Ben Ghorbel is approved by the examination committee

Committee Chairperson: Dr Mohamed-Slim Alouini

Committee Member: Dr Meriem Taous Laleg

Committee Member: Dr Ahmed Sultan Salem

Committee Member: Dr Karim Abed-Meriem

ABSTRACT

Contributions Towards Practical Cognitive Radios Systems

Mahdi Ben Ghorbel

Cognitive radios is one of the hot topics for emerging and future wireless communication. It has been proposed as a suitable solution for the spectrum scarcity caused by the increase in frequency demand. The concept is based on allowing unlicensed users, called cognitive or secondary users, to share the unoccupied frequency bands with their owners, called the primary users, under constraints on the interference they cause to them. The objective of our work is to propose some enhancements to cognitive radio systems while taking into account practical constraints. Cognitive radios requires a capability to detect spectrum holes (spectrum sensing) and a scheduling flexibility to avoid the occupied spectrum and selectively use the empty spectrum (dynamic resource allocation). Thus, the work is composed of two main parts. The first part focuses on cooperative spectrum sensing. We compute in this part the analytical performance of cooperative spectrum sensing under non identical and imperfect channels. Different schemes are considered for the cooperation between users such as hard binary, censored information, quantized, and soft information. The second part focuses on the dynamic resource allocation. We first propose low-cost resource allocation algorithms that use location information to estimate the interference to primary users to replace absence of instantaneous channel state information. We extend these algorithms to handle practical implementation constraints such as dis-

crete bit-loading and collocated subcarriers allocations. We then propose a reduced dimension approach based on the grouping of subcarriers into clusters and performing the resource allocation over clusters of subcarriers instead of single subcarriers. This approach is shown to reduce the computational complexity of the algorithm with limited performance loss. In addition, it is valid for a generic set of resource allocation problems in presence of co-channel interference between users.

DEDICATIONS

to my mother and father,

to my wife,

to my sister and brothers,

to all my big family and friends,

to all people who supported me,

ACKNOWLEDGEMENTS

I would like to sincerely thank my supervisor Dr Mohamed-Slim Alouini for his valuable feedback and continuous guidance throughout this work.

I would like also to thank Dr Haewoon Nam (Assistant Professor at Hanyang University, Korea) and Dr Mamoun Guenash (Research Engineer at Bell Labs, Belgium) for their valuable support and advices for fulfilling this work.

I thank also all the members of our research group for their continuous encouragement and help, and providing a great environment for work.

Lastly, I would like to thank KAUST for providing support and resources for this research work.

TABLE OF CONTENTS

Examination Committee Approval	2
Copyright	3
Abstract	4
Dedications	6
Acknowledgements	7
Acronyms	11
List of Figures	12
List of Tables	14
1 Introduction	15
1.1 Motivation for Cognitive Radios: The Spectrum Scarcity Problem . . .	15
1.2 Cognitive Radios Concept	17
1.3 Proposed Models for Cognitive Radios	17
1.4 Main Challenges in Cognitive Radio Systems	19
1.4.1 Spectrum Sensing	19
1.4.2 Dynamic Resource Allocation	20
1.5 Thesis Objectives	20
2 Cooperative Spectrum Sensing under Imperfect Reporting Channels	22
2.1 Introduction	22
2.2 System and Channel Model	24
2.2.1 System Model	24
2.2.2 Cooperation Schemes	26
2.2.3 Channel Model	27

2.3	Performance of Cooperative Spectrum Sensing under Imperfect Reporting Channels	28
2.3.1	Binary Local Decision Scheme	29
2.3.2	Tertiary (Censored) Local Decision Scheme	39
2.3.3	Quantized Local Decision Scheme	44
2.3.4	Soft Information Scheme	49
2.4	Numerical Results	53
2.4.1	Effect of Imperfect Channels and Non Identical Average SNRs	54
2.4.2	Applications of the Performance Analysis to System Parametrization	60
2.4.3	Application of the Performance Analysis for Different Network Topologies	65
2.5	Conclusion	69
3	Location-based Resource Allocation	72
3.1	Introduction	72
3.2	System Model	74
3.3	Estimating Interference from Location Information	75
3.3.1	Interference Estimation using Location Information	76
3.3.2	Interference Constraint in the Cognitive System	78
3.4	Resource Allocation Algorithms based on Location Information	79
3.4.1	Downlink	79
3.4.2	Uplink	85
3.4.3	Practical Implementation Algorithms for Resource Allocation	88
3.5	Simulation Results	92
3.5.1	Effect of the Use of Location Information	93
3.5.2	Optimality of the Proposed Algorithms	94
3.5.3	Effect of the Users' Spatial Distribution	95
3.5.4	Effect of the Interference Threshold	96
3.5.5	Effect of the Number of Primary Users	96
3.5.6	Practical Algorithms Performance	97
3.6	Conclusion	98
4	Reduced-Dimension Power Allocation over Clustered Channels under Cochannel Interference	101
4.1	Introduction	101
4.2	System Model	103

4.3	Problem Formulation	104
4.3.1	Utility Function	104
4.3.2	Power and Rate Constraints	105
4.3.3	Subcarriers Clustering	106
4.4	Reduced Dimension Power Allocation	107
4.4.1	Optimization Problem	107
4.4.2	Per-cluster Subproblems Decomposition	109
4.4.3	Interference Constraint per Cluster	112
4.5	Numerical and Simulation Results	113
4.5.1	Effect of Subcarriers Clustering	114
4.5.2	Effect of Interference Thresholds	116
4.6	Conclusion	118
5	Conclusion	119
5.1	Summary	119
5.2	Future Research Work	120
	References	121
	Appendices	128

ACRONYMS

Symbol	Meaning
AWGN	Additive White Gaussian Noise
BFSK	Binary-Frequency Shift Keying
BPSK	Binary Phase-Shift Keying
CDF	Complementary Density Function
CROC	Complementary Receiver Operating Characteristic
CSI	Channel State Information
DRA	Dynamic Resource Allocation
FCC	Federal Communication Commission
FDMA	Frequency-Division Multiple Access
GPS	Global Positioning System
I.I.D	Identically and Independently Distributed
KKT	Karush-Kuhn-Tucker
LI	Location Information
MGF	Moment Generating Function
OFDMA	Orthogonal Frequency-Division Multiple Access
PAM	Pulse-Amplitude Modulation
PDF	Probability Density Function
RF	Radio Frequency
SINR	Signal-to-Interference and Noise Ratio
SNR	Signal-to-Noise Ratio
TDD	Time Division Duplex

LIST OF FIGURES

1.1	Spectrum occupancy in USA	16
1.2	Proposed cognitive radios model versus the classic models.	19
2.1	System model for cooperative spectrum sensing.	25
2.2	Binary and tertiary decision for binary test hypothesis.	26
2.3	Quantized local decision rule with 4 regions.	27
2.4	Constellation for reporting channel under tertiary decision.	41
2.5	Constellation for reporting channel under quantized decision.	46
2.6	Performance of cooperative spectrum sensing	55
2.7	Effect of identical average SNR hypothesis on the sensing performance	56
2.8	Comparison between tertiary and binary local decision schemes	57
2.9	CROC curves for different quantization sizes (M)	59
2.10	Cooperative error probability for different quantification sizes	59
2.11	Cooperative error probability for soft cooperation scheme.	60
2.12	Comparison between different binary reporting decision constellations	61
2.13	Performance of cooperative spectrum sensing for different fusion rules	62
2.14	Comparison between tertiary and binary local decision scenarios for perfect reporting channels	63
2.15	Cooperative error probability function of the fusion decision threshold and the target error probability	64
2.16	Cooperative error probability function of the fusion decision threshold with perfect reporting channel	65
2.17	Distributed cooperative spectrum sensing model.	66
2.18	Distributed cooperative spectrum sensing performance	67
2.19	Cluster-based cooperative spectrum sensing scheme.	68
2.20	Different clustering strategies.	69
2.21	Comparison between the clustering strategies on performance of cluster- based spectrum sensing.	70

3.1	Effect of the location information use instead of the channel state information on the total capacity of the network.	93
3.2	Comparison between the total capacity obtained using the proposed algorithm and the exhaustive search algorithm.	94
3.3	Downlink capacity of various schemes as a function of p_ϵ	95
3.4	Impact of interference threshold on the network capacity for the proposed algorithm	96
3.5	Impact of the number of primary users on the cognitive network performances.	97
3.6	Discrete rate and fixed power constraints effect on the performance of the resource allocation.	98
3.7	Effect of discretization of the capacities and allocation of collocated subchannels on the performance of the cognitive network.	99
4.1	Block diagram for cognitive radios system with co-channel interference.	103
4.2	Rate regions reduced dimension power allocation	115
4.3	Power allocation on clusters of subcarriers	115
4.4	Rate region of two users for different interference constraints per cluster.	116
4.5	Rate region of two users versus the clustering ρ and the interference factors ϵ	117
4.6	Comparison of the interference at the primary user with the different interference constraints with reduced dimension.	118

LIST OF TABLES

2.1	Parameters for common binary modulations.	33
3.1	Different resource allocation scenarios for Fig. 3.7.	99

Chapter 1

Introduction

1.1 Motivation for Cognitive Radios: The Spectrum Scarcity Problem

The last two decades were marked by a revolution in the area of wireless communications. The great advances in research in this field lead to 1) emergence of variety of devices/ technologies with different objectives and uses, and 2) improvement of the performances of the wireless networks especially regarding achievable rate and energy consumption. However, with these great advancements, the spectrum, considered as a limited national resource, is threatened by saturation in the coming few years. As an example, we refer to the USA spectrum allocation table in Fig. 1.1 which shows the rarity of available empty slots.

Many approaches were investigated to tackle this problem of spectrum scarcity by trying to enhance the efficiency of the spectrum usage. Among these techniques

- Multiple receive and transmit antennas [1], which exploits new spatial dimension in order to increase throughput and efficiency without requiring additional spectrum.
- Adaptive multi-level modulation and coding [2], which optimizes the use of the available slots by adapting the modulation depending on the channel condition

in stead of static modulations designed to support worst-case scenario previously.

- Millimeter wave communications, where new spectrum slot of very high frequency compared to the currently used spectrum bands is under study for use in communications. The challenge consists in the high attenuation of such frequencies. [3]
- Spectrum sharing which attracted research after statistics showing very low real use of the spectrum allocated. The cognitive radio concept was firstly proposed by Mitola in 1999. [4]

1.2 Cognitive Radios Concept

Starting from a conclusion of the Federal Communication Commission (FCC) which states that around 90% of the licensed frequency remain idle [5], cognitive radio systems have received a great deal of attention to improve the spectrum efficiency. The concept consists in allowing some secondary users, called cognitive users, to opportunistically access and share the spectrum with the licensed users, called primary users, under certain interference condition. This principle requires certain intelligence of the secondary users to 1) detect the primary users use of the spectrum, and 2) adapt their transmission rapidly in order to profit from the detected spectrum holes and optimize their throughput while respecting the allowed interference levels.

1.3 Proposed Models for Cognitive Radios

In literature, proposed cognitive radios models can be classified into three main approaches:

1. **Interweave scenario** [4], in which secondary users can transmit only in the spectrum holes of the primary user. This approach requires an accurate spectrum sensing. It guarantees zero interference to the primary user but the secondary users throughput is limited.
2. **Underlay scenario** [6], in which secondary users can share the spectrum with the primary users under a low interference constraint. This approach achieves better performance for the secondary users and do not need spectrum sensing. However, it requires the knowledge of the interference channel between the secondary transmitter and the primary receiver.
3. **Overlay scenario** [7], in which secondary user will play the role of a relay for the primary user transmission and simultaneously transmit its own data without interfering the primary transmission via orthogonal multiplexing. This approach assumes collaboration between primary and secondary users via share of codebooks which is not always practical especially in secure communications.

In this work we will consider a generic scenario between the interweave and underlay scenarios explained above, as follows: The secondary users perform spectrum sensing, then

- if the primary user is not there (idle/absent), the secondary user can transmit without any limit of interference (like the interweave scenario)
- if the primary is present and active, the secondary user can transmit under a tolerable interference constraint (like the underlay scenario)

This approach provides higher transmission opportunities for the secondary users as shown in Fig. 1.2. In addition, the two original scenarios could be re-obtained from this generic scheme, the interweave by setting the interference thresholds to zero when

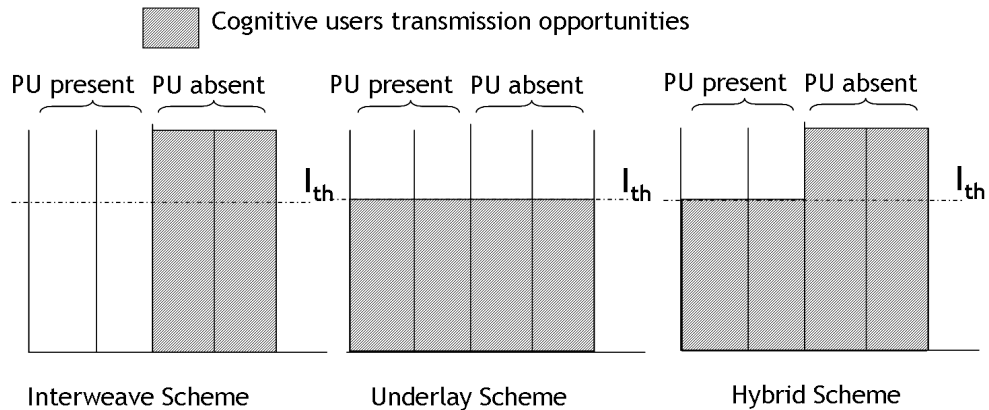


Figure 1.2: Proposed cognitive radios model versus the classic models.

the user is present, and the underlay by setting the primary user occupancy to present in all subcarriers.

This generic model can be decomposed into two main parts.

- **Spectrum sensing**, where detection of the spectrum occupancy is performed.
- **Dynamic resource allocation**, where the transmission scheduling is optimized to avoid generating harmful interference to the primary users and maximize the use of the empty spectrum.

1.4 Main Challenges in Cognitive Radio Systems

Due to the nature of cognitive radios, different challenges are faced in order to achieve a realistic model. In what follows, we summarize some particular challenges related to each part of our system model.

1.4.1 Spectrum Sensing

Spectrum sensing consists in detecting the occupancy of the spectrum by primary users. Thus, the reliability of this sensing is of paramount importance as high miss-detection probability will lead to a loss of important transmission opportunities and

on the other hand high false-alarm probability will lead to a high risk of interference to the primary users. In order to improve spectrum sensing performance, usually cognitive users will cooperate together in order to overcome shadowing and fading effects. Thus, cooperation parameters should also be well selected in order to optimize the sensing performance.

1.4.2 Dynamic Resource Allocation

Dynamic Resource allocation (DRA) is the ability of allocating the available secondary user resources, mainly spectrum and power, in order to optimize their throughput while respecting the interference condition. Thus, proposing low-complex dynamic resource allocation algorithms in the context of cognitive radios is more challenging in order to take-advantage from the spectrum vacancies before the conditions change. In addition, in absence of collaboration between primary and secondary users, knowledge of the instantaneous interference channels towards the primary users is a challenging problem.

1.5 Thesis Objectives

In this thesis, we target some specific problems within the cognitive radios concept that we will focus on by taking into consideration some practical constraints in order to achieve practical cognitive radio systems.

In particular, in chapter 2, we focus on the performance evaluation of cooperative spectrum sensing. Specifically, we target to compute the performance of cooperative spectrum sensing under independent but non identically distributed sensing and reporting channels. We consider different cooperation schemes and target derivation of closed-form expressions for global probabilities of detection and false alarm.

In chapter 3, we target the problem of knowledge of interference channels. We

propose the use of location information to estimate this interference. In particular, we formulate and solve optimization problems using this location information for downlink and uplink DRA. We propose also algorithms considering specific practical implementation constraints such as discrete rate and collocated channels.

Next, in chapter 4, we tackle a DRA problem in presence of co-channel interference between users. We propose an approach to reduce the complexity of the problem using grouping of subcarriers. We study the efficiency of the approach in terms of complexity and performance.

Finally, we draw in chapter 5 the main conclusions of this work and enumerate some possible extensions.

Chapter 2

Cooperative Spectrum Sensing under Imperfect Reporting Channels

2.1 Introduction

Spectrum sensing, in which the decision of presence or absence of a primary user is made, is the first and the key step in cognitive radio systems. The purpose of spectrum sensing is to guarantee no interference to the primary users while maximizing the available spectrum for the secondary users' use. [8, 9] review the main algorithms employed for spectrum sensing by comparing them and highlighting the advantages and disadvantages of each method.

Cooperative spectrum sensing has been extensively studied in the literature [10, 11, 12, 13, 14, 15]. For instance, [16] and [17] provide a detailed review of most of the works done in this area and highlight the main advantages and the limits. Among the elements for cooperative spectrum sensing, the process of combining local sensing results in the fusion center, such as the "AND" rule and the "OR" rule, to make the final decision is discussed in [12, 18]. In particular, the used cooperation scheme is a

key subject for spectrum sensing due to its effect on performance. The general known schemes are binary hard and fully soft information, [19] compares performance of these two schemes. Other schemes are suggested such as the quantized scheme [20] and the censored scheme (called also tertiary scheme) [21, 22, 23] where local users do not take decision when they are not sure about their decision. In addition, [24, 18, 25] derive optimal parameters for cooperative spectrum sensing, such as decision thresholds, fusion rule, and number of cooperating users.

Most of the aforementioned results assume 1) fading channels from primary users to secondary users, where local sensing is done, but perfect channels from the secondary users to the fusion center, where reporting local decisions is error free, and 2) identical average signal-to-noise ratio (SNR) for the channel from the primary user to the secondary users. In reality, however, errors may occur when local decisions are transmitted over the fading channels from the secondary users to the fusion center. These errors over the reporting channels obviously plague the accuracy of the global decision made by the fusion center. Therefore, it is of paramount importance to investigate the effect of imperfect reporting channels on the performance of cooperative spectrum sensing techniques. In addition, average SNR for the secondary users are not identical in general due to the difference of the distance from the primary user to each secondary user in practice. This heterogeneous user scenario is certainly worth being studied to evaluate its effect on the performance of cooperative spectrum sensing techniques.

Motivated by these observations, we investigate in this work the effect of these two common assumptions and compute closed-form expressions of the average cooperative detection and the false alarm probabilities under imperfect and non-identically distributed reporting channels under different cooperation schemes.

Imperfect reporting channel has been a subject of study in multiple related works. In [26], cooperative spectrum sensing performance under imperfect reporting channels

was derived for both hard binary and soft local decisions without focusing on the local detector neither on the channels characteristics. In [27], imperfect reporting channels were considered but with assumption of identically distributed channels.

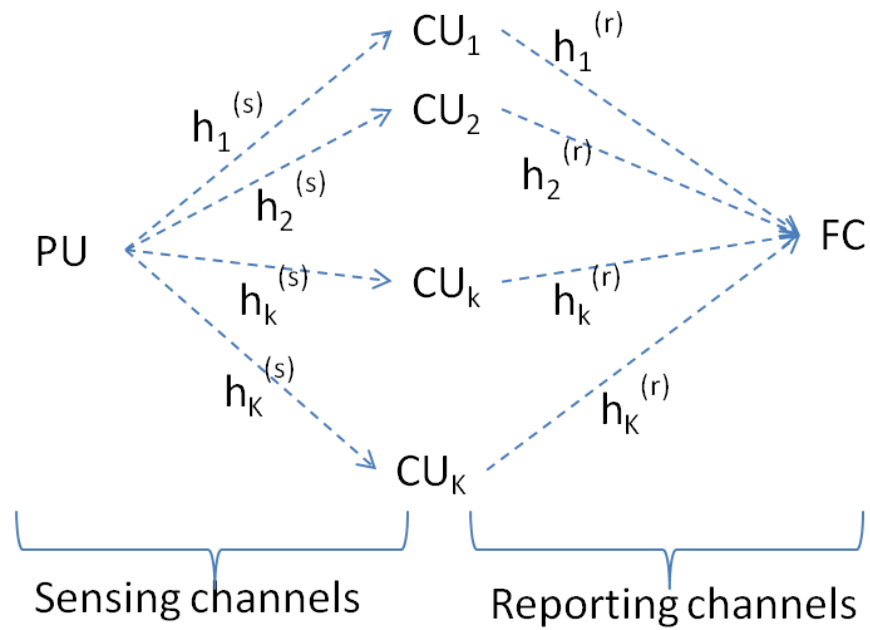
In the remainder of this chapter, we introduce in section 2.2 the system model . In section 2.3, we develop the cooperative error probability expressions for the different cooperation schemes. Then, section 2.4 presents simulation results along with the discussion analysis of these results. Finally, section 2.5 draws conclusions.

2.2 System and Channel Model

2.2.1 System Model

We consider a cognitive network that consists of a single primary user, K secondary users, and a fusion center (ref Fig. 2.1). The objective is to cooperatively sense the presence or absence of a primary user on a certain frequency band. We denote by H_1 and H_0 the states of presence/activity and absence/inactivity of the primary user. The channels complex gains are denoted as follows. $h_k^{(s)}$, $1 \leq k \leq K$ represents the channel from the primary user to the k -th secondary user, called “sensing channels”. $h_k^{(r)}$, $1 \leq k \leq K$ denotes the channel from the k -th secondary user to the fusion center, called “reporting channels”. A fusion center can be one of the secondary users or an extra node with an external connection (i.e. a cluster head or a base station). Each user performs spectrum sensing individually using energy detection then according to the cooperation scheme will forward its decision or measurement to the fusion center where a global decision based on a defined fusion rule will be taken.

The main objective of this work is to determine the performance of cooperative spectrum sensing system by computing the analytical expressions of the global average probabilities of detection and false alarm under imperfect and not necessarily identical sensing and reporting channels.



PU: Primary User
CU: Cognitive User
FC: Fusion Center

Figure 2.1: System model for cooperative spectrum sensing.

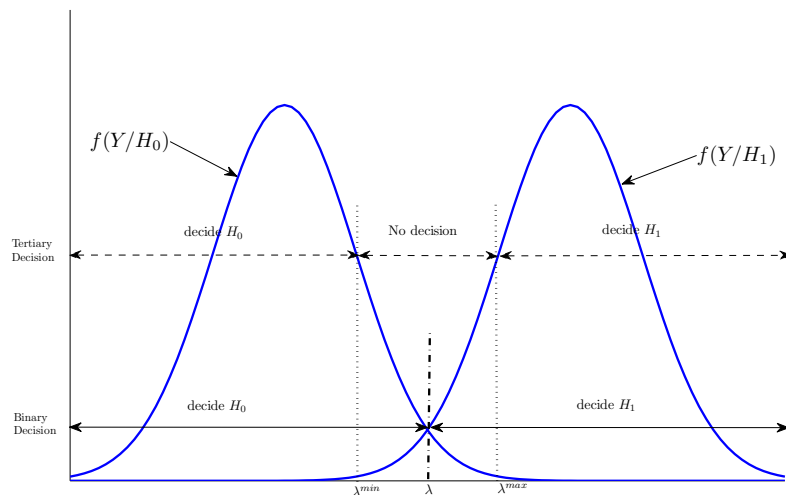


Figure 2.2: Binary and tertiary decision for binary test hypothesis.

2.2.2 Cooperation Schemes

We will consider the following cooperation schemes between local users in order to take global decision

- **Local Binary Decision Scheme**

This is the classic hard binary cooperation scheme, where each local user will take a binary decision H_0 or H_1 which correspond to the inactivity (or absence) and activity (or presence) of primary users, respectively. Then, this decision is sent to the fusion center where a global decision will be taken.

- **Local Tertiary (Censored) Decision Scheme**

In this scheme, as illustrated in Fig. 2.2, an additional state H_x is added to express an uncertainty about the activity of primary users. Thus, a local decision in tertiary scenario can take one of the three states: H_0 , H_x , or H_1 where H_x will represent that the user is uncertain about the presence or absence of the primary user.

- **Local Quantized Decision Scheme**

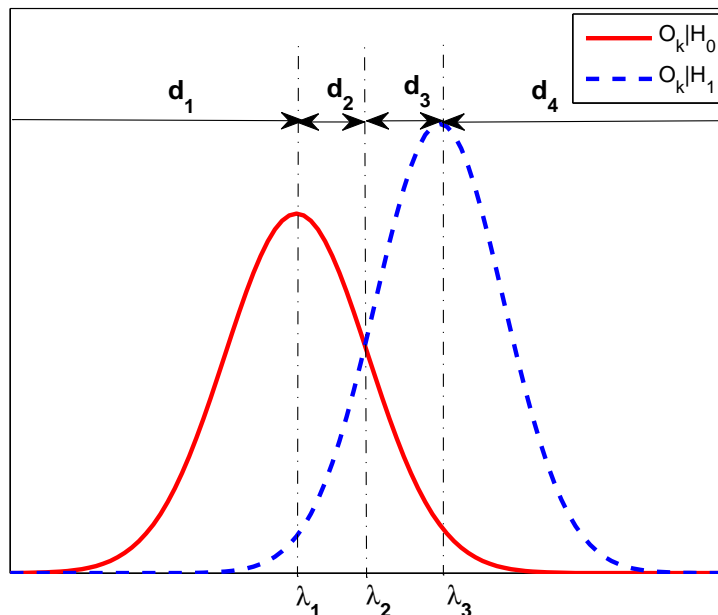


Figure 2.3: Quantized local decision rule with 4 regions.

Each user performs spectrum sensing individually and take a local decision in the format of a quantized hard decision as illustrated in Fig.2.3 and then forwards it to the fusion center which takes the global decision based on a certain fusion rule.

- **Soft Cooperation Scheme**

In this scheme, local users do not take any decision but they forward directly the measured signal/energy to the fusion center where the global decision will be taken based on all measurements taken at different sensing nodes.

2.2.3 Channel Model

To evaluate the performance of the cognitive radio systems in generalized fading environments while maintaining analytical tractability of the analytical derivations, we model the envelope of the channels by a Nakagami-m distribution [28]. Thus, the instantaneous received power γ is modeled by a Gamma probability density function

(PDF) given by [29]

$$f_{\gamma}(\gamma) = \frac{\gamma^{m-1}}{\Gamma(m)} \left(\frac{m}{\bar{\gamma}}\right)^m \exp\left(-\frac{m\gamma}{\bar{\gamma}}\right), \quad \gamma > 0, \quad m > 0, \quad (2.1)$$

where m is the Nakagami multipath fading parameter and $\bar{\gamma}$ is the average received power.

The Rayleigh distribution can be obtained from the Nakagami- m distribution by setting the fading parameter $m = 1$. In this case, the PDF of the power described in 2.1 reduces to an exponential distribution. In addition, [30] and the references therein show that this Gamma PDF can also model the shadowing effects by setting $m = 1/(\exp((\frac{\sigma_s}{8.686})^2) - 1)$, where σ_s is the shadowing variance. It is also shown in [30] that this PDF can fit the Generalized- K PDF and can such be used to model the mixed effect of fading and shadowing using a simple moment matching technique.

2.3 Performance of Cooperative Spectrum Sensing under Imperfect Reporting Channels

The objective of this section is to compute the global performance of a cooperative spectrum sensing under imperfect and non-identical channels. For this goal, we first start by developing the expressions of average probabilities of detection and false alarm at local users, then express the average probabilities of reporting errors, and finally deduce the global average probabilities at a fusion center as function of the previous expressions. The development proceeds for the different cooperation schemes stated in section 2.2.2.

2.3.1 Binary Local Decision Scheme

Local Decision Performance

Measurements taken by the k -th secondary user at a certain time instant j can be modeled as a binary hypothesis test as follows

$$\begin{aligned} H_1 : y_k(j) &= h_k^{(s)} s(j) + v_k(j) \\ H_0 : y_k(j) &= v_k(j), \end{aligned} \tag{2.2}$$

where $y_k(j)$ is the received j -th sample of the primary user signal at the k -th secondary user, $h_k^{(s)}$ is the sensing channel between the primary user and the k -th secondary user, $s(j)$ is the unknown deterministic transmitted signal by the primary user, and $v_k(j)$ is a zero-mean additive white Gaussian noise (AWGN) with variance σ_v^2 . We assume that the sensing time is smaller than the coherence time of the channel. Then, the sensing channel $h_k^{(s)}$ can be viewed as time-invariant during the sensing process. Moreover, we assume that the status of the PU remains unchanged during the spectrum sensing process. If prior knowledge of the primary user signal is unknown, the energy detection method is optimal for detecting zero-mean constellation signals [31].

Suppose that the k -th user takes measurements over a detection interval of $2N$ samples, where $2N$ is the time-bandwidth product. Thus, the observed energy at this user is given as

$$\tilde{O}_k = \sum_{j=0}^{2N-1} |y_k(j)|^2. \tag{2.3}$$

The sum of the squares of $2N$ standard Gaussian random variables follows a chi-square

distribution of $2N$ degrees of freedom as

$$O_k \triangleq \frac{\tilde{O}_k}{\sigma_v^2} \sim \begin{cases} \chi_{2N}^2(a_k), & H_1 \\ \chi_{2N}^2, & H_0, \end{cases} \quad (2.4)$$

where $a_k = \frac{|h_k^{(s)}|^2}{\sigma_v^2} \sum_{j=0}^{2N-1} |s(j)|^2$ is the non-centrality parameter of the non-central chi-square.

Binary Local Decision

A local decision is taken by the binary hypothesis testing rule as follows

$$u_k^{(bin)} = \begin{cases} H_1, & \text{if } O_k \geq \lambda_k \\ H_0, & \text{otherwise,} \end{cases} \quad (2.5)$$

where λ_k is the decision threshold for the k -th user.

The local probabilities of detection and false alarm over AWGN channels are expressed, respectively, as [32]

$$P_{u_k}^{(d)}(\gamma_k^{(s)}) = P_{u_k}^{(1|1)}(\gamma_k^{(s)}) = Pr[O_k > \lambda_k | H_1] = Q_N\left(\sqrt{2\gamma_k^{(s)}}, \sqrt{\lambda_k}\right), \quad (2.6)$$

and

$$P_{u_k}^{(f)}(\gamma_k^{(s)}) = P_{u_k}^{(1|0)}(\gamma_k^{(s)}) = Pr[O_k > \lambda_k | H_0] = \frac{\Gamma(N, \frac{\lambda_k}{2})}{\Gamma(N)}, \quad (2.7)$$

where, $\gamma_k^{(s)} = |h_k^{(s)}|^2 \frac{E_s}{\sigma_v^2}$ the instantaneous SNR of the sensing channel between the primary user and the k -th user, $E_s = \sum_{j=0}^{2N-1} |s(j)|^2$ is the energy transmitted by the primary user over the $2N$ samples, $\Gamma(x) = \int_0^\infty t^{x-1} e^{-t} dt$ is the Gamma function, $\Gamma(x, a) = \int_a^\infty t^{x-1} e^{-t} dt$ is the incomplete Gamma function, and $Q_M(x, a) = \left(\frac{1}{x}\right)^{M-1} \int_a^\infty t^M \exp\left(-\frac{t^2+x^2}{2}\right) I_{M-1}(tx) dt$ is the generalized Marcum-Q function with

$I_{M-1}(\cdot)$ the modified Bessel function of first kind and of order $M - 1$.

$P_{u_k}^{(1|1)}(\gamma_k^{(s)})$ (respectively $P_{u_k}^{(1|0)}(\gamma_k^{(s)})$) is denoted by the probability that the k -th user makes a local decision of H_1 when the instantaneous SNR is $\gamma_k^{(s)}$ given that the actual state of the primary user is H_1 (respectively H_0).

The average probabilities of detection and false alarm for the k -th user are obtained by averaging (2.6) and (2.7) over the channel SNR distribution presented in (2.1) as

$$P_{u_k}^{(d)} = P_{u_k}^{(1|1)} = \int_0^\infty P_{u_k}^{(d)}(\gamma_k^{(s)}) f_\gamma(\gamma_k^{(s)}) d\gamma_k^{(s)} \triangleq F_N(m_k^{(s)}, \bar{\gamma}_k^{(s)}, \lambda_k), \quad (2.8)$$

and

$$P_{u_k}^{(f)} = P_{u_k}^{(1|0)} = \int_0^\infty P_{u_k}^{(f)}(\gamma_k^{(s)}) f_\gamma(\gamma_k^{(s)}) d\gamma_k^{(s)} = \frac{\Gamma(N, \frac{\lambda_k}{2})}{\Gamma(N)}, \quad (2.9)$$

We now only need to get a closed form expression of the integral

$$F_n(m, \bar{\gamma}, \lambda) \triangleq \int_0^\infty Q_n(\sqrt{2\gamma}, \sqrt{\lambda}) \frac{\gamma^{m-1}}{\Gamma(m)} \left(\frac{m}{\bar{\gamma}}\right)^m e^{-\frac{m\gamma}{\bar{\gamma}}} d\gamma. \quad (2.10)$$

Using [29, eq. (B.52)], $F_n(m, \bar{\gamma}, \lambda)$ can be determined recursively using the following relation

$$F_n(m, \bar{\gamma}, \lambda) = F_{n-1}(m, \bar{\gamma}, \lambda) + \left(\frac{m}{m + \bar{\gamma}}\right)^m \frac{e^{-\frac{\lambda}{2}} \left(\frac{\lambda}{2}\right)^{n-1}}{(n-1)!} {}_1F_1\left(m, n; \frac{\lambda\bar{\gamma}}{2(m + \bar{\gamma})}\right), \quad (2.11)$$

where ${}_1F_1(a, b; c)$ is the confluent hypergeometric function [33].

In the case of an integer fading parameter m , $F_n(m, \bar{\gamma}, \lambda)$ is computed for $n = m$ using [29, eq. (B.51)] as

$$F_m(m, \bar{\gamma}, \lambda) = e^{-\frac{m\lambda}{2(m + \bar{\gamma})}} \sum_{j=0}^{m-1} \frac{1}{j!} \left(\frac{m\lambda}{2(m + \bar{\gamma})}\right)^j, \quad (2.12)$$

and (2.12), (2.11) is deduced as a finite sum

$$\begin{aligned}
F_n(m, \bar{\gamma}, \lambda) &= e^{-\frac{m\lambda}{2(m+\bar{\gamma})}} \sum_{j=0}^{m-1} \frac{1}{j!} \left(\frac{m\lambda}{2(m+\bar{\gamma})} \right)^j \\
&+ \left(\frac{m}{m+\bar{\gamma}} \right)^m e^{-\frac{\lambda}{2}} \sum_{j=m}^{n-1} \frac{1}{j!} \left(\frac{\lambda}{2} \right)^j {}_1F_1 \left(m, j+1; \frac{\lambda\bar{\gamma}}{2(m+\bar{\gamma})} \right).
\end{aligned} \tag{2.13}$$

For non-integer m , a closed form expression for this integral was derived in [34] but it is expressed as a function of an infinite sum which should be capped for practical evaluations.

Reporting Decision

When a secondary user reports its local decision to the corresponding fusion center, the local decision may be incorrectly delivered to the fusion center in practice, which later affects the global decision made by the fusion center.

When a user makes a binary local decision, the user can transmit this decision to the fusion center using a binary modulated signal. A unified form for the conditional bit error rate (BER) for various modulations in AWGN channel when the received SNR is $\gamma_k^{(r)}$ is written as [35, eq. (8.100)]

$$P_{c,u_k}^{(e)}(\gamma_k^{(r)}) = \frac{\Gamma(b, a\gamma_k^{(r)})}{2\Gamma(b)}, \tag{2.14}$$

where a and b are the parameters according to the modulation used. Table 2.1 shows the different parameter values for binary modulations, such as binary phase-shift keying (BPSK) or binary-frequency shift keying (BFSK).

A delivery error of the local decision made by the k -th user to the fusion center in fading channel can be written as an average of the error probability in AWGN

Table 2.1: Parameters for common binary modulations.

	Coherent detection	Non coherent detection
BPSK	$(a = 1, b = 1/2)$	$(a = 1, b = 1)$
BFSK	$(a = 1/2, b = 1/2)$	$(a = 1/2, b = 1)$

channel over the SNR distribution as follows

$$P_{c,u_k}^{(e)} = P_{c,u_k}^{(1|0)} = P_{c,u_k}^{(0|1)} = \int P_{c,u_k}^{(e)}(\gamma_k^{(r)}) f_\gamma(\gamma_k^{(r)}) d\gamma_k^{(r)}, \quad (2.15)$$

where $\gamma_k^{(r)}$ is the instantaneous SNR of the reporting channel between the k -th secondary user and the fusion center, $f_\gamma(\gamma_k^{(r)})$ is the PDF of $\gamma_k^{(r)}$, and $P_{c,u_k}^{(e)}(\gamma_k^{(r)})$ is the reporting error probability from the k -th user to the fusion center over AWGN channel.

Substituting (2.1) and (2.14) and using [36, eq. (15)], the equation (2.15) can be rewritten as

$$\begin{aligned} P_{c,u_k}^{(e)} &= P_{c,u_k}^{(1|0)} = P_{c,u_k}^{(0|1)} \\ &= \frac{\Gamma(m_k^{(r)} + b)}{2\Gamma(b)\Gamma(m_k^{(r)} + 1)} \frac{(m_k^{(r)})^{m_k^{(r)}} (a\bar{\gamma}_k^{(r)})^b}{(m_k^{(r)} + a\bar{\gamma}_k^{(r)})^{m_k^{(r)} + b}} {}_2F_1\left(1, m_k^{(r)} + b; m_k^{(r)} + 1; \frac{m_k^{(r)}}{m_k^{(r)} + a\bar{\gamma}_k^{(r)}}\right), \end{aligned} \quad (2.16)$$

where ${}_2F_1(a, b; c; x)$ is the Gaussian hypergeometric function [33].

Fusion Decision Performance

Once the local decisions are collected, the fusion center takes a global decision according to a defined fusion rule of the received local decisions. The weights are assigned depending on the reliability of each local decision.

We start by discussing a general weighted fusion decision rule. Then, we derive the

performance for some special cases to compare the results with the known formulas in literature.

Weighted Sum Fusion Decision: In this rule, the fusion center assigns a weight for each user's local decision and then sums all the weighted decisions to compare them with a threshold. The weights can be based on some a-priori information about the users' local decisions or reporting error reliability in terms of the average sensing SNR or average reporting SNR.

The fusion rule is as follows

$$c^{(bin)} = \begin{cases} H_1, & \text{if } \sum_{k=1}^K \omega_k I_u(u_k^{(bin)} = H_1) \geq \rho \\ H_0, & \text{otherwise,} \end{cases} \quad (2.17)$$

where ω_k represents the weight associated with the local decision of the k -th user (i.e. $\sum_{k=1}^K \omega_k = 1$), ρ is the threshold of the fusion decision in the range of $[0, 1]$, and $I_u(x)$ is the indicator function defined as $I_u(x) = 1$ if x is true and 0 otherwise (i.e. $I_u(u_k^{(bin)} = H_1) = 1$ (respectively $I_u(u_k^{(bin)} = H_1) = 0$) if the fusion center receives H_1 (respectively H_0) from the k -th user).

With this fusion decision rule and generalizing the formula in [37], the probability that a global decision of H_1 is made (i.e. primary user is present) is expressed as

$$Pr[c = H_1] = \sum_{l \in \{\mathbf{V}^{(\rho)}, \mathbf{W}^{(\rho)}\}} \prod_{k_1 \in \mathbf{v}_l} (Pr[\{c, u_{k_1}\} = H_1]) \prod_{k_0 \in \mathbf{w}_l} (Pr[\{c, u_{k_0}\} = H_0]), \quad (2.18)$$

where $\{\mathbf{V}^{(\rho)}, \mathbf{W}^{(\rho)}\} = \{\{\mathbf{v}_1, \mathbf{w}_1\}, \{\mathbf{v}_2, \mathbf{w}_2\}, \dots, \{\mathbf{v}_L, \mathbf{w}_L\}\}$ is the set containing all combinations of users who are reporting to the fusion center and satisfying the equation

$$\sum_{k \in \mathbf{v}_l} \omega_k \geq \rho, \quad (2.19)$$

\mathbf{v}_l is the set of the indices of the users who made a local decision H_1 (i.e., $\mathbf{v}_l = \{j\}$, $\forall j$, such that $I_u(u_j = H_1) = 1$) and \mathbf{w}_l is the set of the indices of the users who declared a local decision H_0 (i.e., $\mathbf{w}_l = \{k\}$, $\forall k$, such that $I_u(u_k = H_1) = 0$). By definitions, $\forall l$, $\mathbf{v}_l \cup \mathbf{w}_l = \{1, 2, \dots, K\}$. Note that l in the summation indicates that $\{\mathbf{v}_l, \mathbf{w}_l\}$ is selected out of $\{\mathbf{V}^{(\rho)}, \mathbf{W}^{(\rho)}\}$ for the subsequent products. For instance, if $l = 2$, \mathbf{v}_2 and \mathbf{w}_2 are used in the subsequent products. In addition, k_1 is the user index in \mathbf{v}_l and k_0 is the user index in \mathbf{w}_l . In (2.18), $Pr[\{c, u_k\} = H_1]$ is the probability that the fusion center determines the local decision of the k -th user is H_1 . This probability is not exactly equal to the probability of local decision H_1 at the k -th user due to probable errors that can occur over the reporting channel.

By conditioning (2.18) over H_1 and H_0 , the probabilities of detection and false-alarm at fusion center can be written respectively as

$$P_c^{(d)} = Pr[c = H_1 | H_1] \quad (2.20)$$

$$= \sum_{l \in \{\mathbf{V}^{(\rho)}, \mathbf{W}^{(\rho)}\}} \prod_{k_1 \in \mathbf{v}_l} (P_{c, u_{k_1}}^{(bin)}[H_1 | H_1]) \prod_{k_0 \in \mathbf{w}_l} (1 - P_{c, u_{k_0}}^{(bin)}[H_1 | H_1]), \quad (2.21)$$

and

$$P_c^{(f)} = Pr[c = H_1 | H_0] \quad (2.22)$$

$$= \sum_{l \in \{\mathbf{V}^{(\rho)}, \mathbf{W}^{(\rho)}\}} \prod_{k_1 \in \mathbf{v}_l} (P_{c, u_{k_1}}^{(bin)}[H_1 | H_0]) \prod_{k_0 \in \mathbf{w}_l} (1 - P_{c, u_{k_0}}^{(bin)}[H_1 | H_0]), \quad (2.23)$$

where $P_{c, u_k}^{(bin)}[H_1 | H_1]$ (respectively $P_{c, u_k}^{(bin)}[H_1 | H_0]$) is the probability that the fusion center estimated a decision H_1 from the decision received from the k -th user when the real state of the primary user is H_1 (respectively H_0). Since errors can occur in delivering a local decision from each user to the fusion center, $P_{c, u_k}^{(bin)}[H_1 | H_1]$ is the sum of two possible cases: 1) the local decision is H_1 and no error in reporting, and 2) incorrect local decision is made as H_0 but this decision is received as H_1 due to an

error occurred over the reporting channel. Similarly, $P_{c,u_k}^{(bin)}[H_1|H_0]$ is the sum of two cases when the actual state of the primary user is H_0 . Thus, these are expressed as

$$P_{c,u_k}^{(bin)}[H_1|H_1] = P_{u_k}^{(d)}(1 - P_{c,u_k}^{(e)}) + (1 - P_{u_k}^{(d)})P_{c,u_k}^{(e)}, \quad (2.24)$$

$$P_{c,u_k}^{(bin)}[H_1|H_0] = P_{u_k}^{(f)}(1 - P_{c,u_k}^{(e)}) + (1 - P_{u_k}^{(f)})P_{c,u_k}^{(e)}, \quad (2.25)$$

with

- $P_{u_k}^{(d)}$ and $P_{u_k}^{(f)}$ are the local probabilities of detection and false alarm of the k -th secondary user defined in (2.8) and (2.9), respectively.
- $P_{c,u_k}^{(e)}$ is the probability of error when sending a local decision from the k -th user to the i -th fusion center and is defined in (2.16).

Uniform Weighting Rule: In this case, all reported local decisions are assigned equal weights (i.e., $\omega_k = \frac{1}{K}, \forall k \in \{1 \leq k \leq K\}$), the fusion rule is re-written as

$$c^{(bin)} = \begin{cases} H_1, & \text{if } \frac{1}{K} \sum_{k=1}^K I_u(u_k^{(bin)} = H_1) \geq \rho \\ H_0, & \text{otherwise.} \end{cases} \quad (2.26)$$

This fusion rule can be interpreted that at least $n \triangleq \lceil \rho K \rceil$ out of the K reporting users need to report H_1 to the i -th fusion center in order to decide globally by the fusion center that the primary user is present. Note that $\lceil x \rceil$ is the nearest integer to x towards infinity. This fusion rule is simple and generic, the OR rule is obtained by choosing ρ such that $n = 1$, the AND rule is obtained by setting $\rho = 1$ which gives $n = K$, and 50% rule by choosing $\rho_c = 1/2$.

Following this decision rule, due to the non-identical average SNRs and variable decision thresholds for the users, the global probabilities of detection and false alarm are modeled as obtaining at least n successes in K independent non-identical Bernoulli

trials. Thus, by applying the formula derived in [37], the probability that the global decision of H_1 is made (i.e. primary user is present) is expressed as

$$Pr[c = H_1] = \sum_{l=n}^K \sum_{j_1+j_2+\dots+j_K=l} \prod_{k=1}^K (Pr[\{c, u_k\} = H_1])^{j_k} (1 - Pr[\{c, u_k\} = H_1])^{1-j_k}, \quad (2.27)$$

where the first summation adds up the possibilities that the number of users l declaring H_1 for their local decisions is equal or higher than n . The second summation considers all the combinations on selecting l users out of the K users to report H_1 , where $j_k = 1$ if the k -th user declares H_1 , otherwise $j_k = 0$. In total, there are $L = \binom{K}{l} = \frac{K!}{l!(K-l)!}$ total combinations on selecting l users out of the K users. In the subsequent product, the probabilities of reporting H_1 or H_0 for the users reporting to the fusion center are multiplied.

The probabilities of detection and false alarm of the fusion center are deduced by conditioning (2.27) over H_1 and H_0 , respectively, as

$$P_c^{(d)} = Pr[c = H_1 | H_1] \quad (2.28)$$

$$= \sum_{l=n}^K \sum_{j_1+j_2+\dots+j_K=l} \prod_{k=1}^K (P_{c,u_k}^{(bin)}[H_1 | H_1])^{j_k} (1 - P_{c,u_k}^{(bin)}[H_1 | H_1])^{1-j_k}, \quad (2.29)$$

and

$$P_c^{(f)} = Pr[c = H_1 | H_0] \quad (2.30)$$

$$= \sum_{l=n}^K \sum_{j_1+j_2+\dots+j_K=l} \prod_{k=1}^K (P_{c,u_k}^{(bin)}[H_1 | H_0])^{j_k} (1 - P_{c,u_k}^{(bin)}[H_1 | H_0])^{1-j_k}, \quad (2.31)$$

where $P_{c,u_k}^{(bin)}[H_1 | H_1]$ and $P_{c,u_k}^{(bin)}[H_1 | H_0]$ are shown in (2.24) and (2.25), respectively.

Special Case of Perfect Reporting Channels: In this special case, the average reporting SNR ($\bar{\gamma}_k^{(r)}$) goes to infinity and thus the reporting error probabilities are

null ($P_{c,u_k}^{(e)} = 0, \forall k$). Thus the probabilities of detection and false alarm of local users received at the fusion center are exactly equal to the probabilities of decision and false alarm of local users (i.e. $P_{c,u_k}^{(bin)}[H_1|H_1] = P_{u_k}^{(d)}$ and $P_{c,u_k}^{(bin)}[H_1|H_0] = P_{u_k}^{(f)}$). Then, the global detection and false alarm probabilities in (2.28) and (2.30) are simplified to

$$P_c^{(d)} = \sum_{l=n}^K \sum_{j_1+j_2+\dots+j_K=l} \prod_{k=1}^K (P_{u_k}^{(d)})^{j_k} (1 - P_{u_k}^{(d)})^{1-j_k}, \quad (2.32)$$

and

$$P_c^{(f)} = \sum_{l=n}^K \sum_{j_1+j_2+\dots+j_K=l} \prod_{k=1}^K (P_{u_k}^{(f)})^{j_k} (1 - P_{u_k}^{(f)})^{1-j_k}. \quad (2.33)$$

Special Case of Identical Sensing and Reporting Average SNRs: In this special case, $\bar{\gamma}_k^{(s)} = \bar{\gamma}^{(s)}, \forall k$ and $\bar{\gamma}_k^{(r)} = \bar{\gamma}^{(r)}, \forall k$. Thus, the probabilities of detection, false alarm, and reporting error are equal for all users for each of them ($P_{u_k}^{(d)} = P_u^{(d)}$, $P_{u_k}^{(f)} = P_u^{(f)}$, and $P_{c,u_k}^{(e)} = P_{c,u}^{(e)}, \forall k$). Then, the global detection and false alarm probabilities in (2.28) and (2.30) are simplified thanks to this uniformity among the users as follows

$$P_c^{(d)} = \sum_{l=n}^K \binom{K}{l} (P_{c,u}^{(bin)}[H_1|H_1])^l (1 - P_{c,u}^{(bin)}[H_1|H_1])^{K-l}, \quad (2.34)$$

and

$$P_c^{(f)} = \sum_{l=n}^K \binom{K}{l} (P_{c,u}^{(bin)}[H_1|H_0])^l (1 - P_{c,u}^{(bin)}[H_1|H_0])^{K-l}, \quad (2.35)$$

where

$$P_{c,u}^{(bin)}[H_1|H_1] = P_u^{(d)}(1 - P_{c,u}^{(e)}) + (1 - P_u^{(d)})P_{c,u}^{(e)}, \quad (2.36)$$

$$P_{c,u}^{(bin)}[H_1|H_0] = P_u^{(f)}(1 - P_{c,u}^{(e)}) + (1 - P_u^{(f)})P_{c,u}^{(e)}. \quad (2.37)$$

Special Case of Identical Average SNRs and Perfect Reporting Channels

This special case combines the two previous special cases (i.e. $P_{u_k}^{(d)} = P_u^{(d)}, P_{u_k}^{(f)} =$

$P_u^{(f)}$, and $P_{c,u_k}^{(e)} = 0, \forall k$). The global probabilities are deduced with ideal conditions of identical channels and perfect reporting channels as [18]

$$P_c^{(d)} = \sum_{l=n}^K \binom{K}{l} (P_u^{(d)})^l (1 - P_u^{(d)})^{K-l}, \quad (2.38)$$

and

$$P_c^{(f)} = \sum_{l=n}^K \binom{K}{l} (P_u^{(f)})^l (1 - P_u^{(f)})^{K-l}. \quad (2.39)$$

2.3.2 Tertiary (Censored) Local Decision Scheme

Local Decision Performance

The tertiary local decision rule is expressed as

$$u_k^{(ter)} = \begin{cases} H_1, & \text{if } O_k > \lambda_k^{max} \\ H_0, & \text{if } O_k < \lambda_k^{min} \\ H_x, & \text{otherwise.} \end{cases} \quad (2.40)$$

Since there are three states for a local decision although the actual state of the primary user is binary, we compute the probabilities of a local decision for the k -th user with

an instantaneous SNR $\gamma_k^{(s)}$ as

$$\begin{aligned}
P_{u_k}^{(1|1)}(\gamma_k^{(s)}) &= Pr[O_k > \lambda_k^{max} | H_1] = Q_N\left(\sqrt{2\gamma_k^{(s)}}, \sqrt{\lambda_k^{max}}\right), \\
P_{u_k}^{(x|1)}(\gamma_k^{(s)}) &= Pr[\lambda_k^{min} < O_k < \lambda_k^{max} | H_1] = 1 - [P_{u_k}^{(0|1)}(\gamma_k^{(s)}) + P_{u_k}^{(1|1)}(\gamma_k^{(s)})] \\
P_{u_k}^{(0|1)}(\gamma_k^{(s)}) &= Pr[O_k < \lambda_k^{min} | H_1] = 1 - Q_N\left(\sqrt{2\gamma_k^{(s)}}, \sqrt{\lambda_k^{min}}\right), \\
P_{u_k}^{(1|0)}(\gamma_k^{(s)}) &= Pr[O_k > \lambda_k^{max} | H_0] = \frac{\Gamma(N, \frac{\lambda_k^{max}}{2})}{\Gamma(N)}, \\
P_{u_k}^{(x|0)}(\gamma_k^{(s)}) &= Pr[\lambda_k^{min} < O_k < \lambda_k^{max} | H_0] = 1 - [P_{u_k}^{(1|0)}(\gamma_k^{(s)}) + P_{u_k}^{(0|0)}(\gamma_k^{(s)})], \\
P_{u_k}^{(0|0)}(\gamma_k^{(s)}) &= Pr[O_k < \lambda_k^{min} | H_0] = 1 - \frac{\Gamma(N, \frac{\lambda_k^{min}}{2})}{\Gamma(N)}.
\end{aligned} \tag{2.41}$$

Similar to the binary case, using the distribution of $\gamma_k^{(s)}$ in (2.1), we can deduce $P_{u_k}^{(t|v)}$ as

$$P_{u_k}^{(t|v)} = \int_0^\infty P_{u_k}^{(t|v)}(\gamma_k^{(s)}) f_\gamma(\gamma_k^{(s)}) d\gamma_k^{(s)}, \quad t = 0, x, 1 \text{ and } v = 0, 1, \tag{2.42}$$

from which we obtain the average probabilities of a local decision for the k -th user similarly to the binary case as

$$\begin{aligned}
P_{u_k}^{(1|1)} &= F_N(m_k^{(s)}, \bar{\gamma}_k^{(s)}, \lambda_k^{max}), \\
P_{u_k}^{(x|1)} &= F_N(m_k^{(s)}, \bar{\gamma}_k^{(s)}, \lambda_k^{min}) - F_N(m_k^{(s)}, \bar{\gamma}_k^{(s)}, \lambda_k^{max}) \\
P_{u_k}^{(0|1)} &= 1 - F_N(m_k^{(s)}, \bar{\gamma}_k^{(s)}, \lambda_k^{min}), \\
P_{u_k}^{(1|0)} &= \frac{\Gamma(N, \frac{\lambda_k^{max}}{2})}{\Gamma(N)}, \\
P_{u_k}^{(x|0)} &= \frac{\Gamma(N, \frac{\lambda_k^{min}}{2})}{\Gamma(N)} - \frac{\Gamma(N, \frac{\lambda_k^{max}}{2})}{\Gamma(N)}, \\
P_{u_k}^{(0|0)} &= 1 - \frac{\Gamma(N, \frac{\lambda_k^{min}}{2})}{\Gamma(N)}.
\end{aligned} \tag{2.43}$$

where $F_n(m, \bar{\gamma}, \lambda)$ as defined in (2.13).

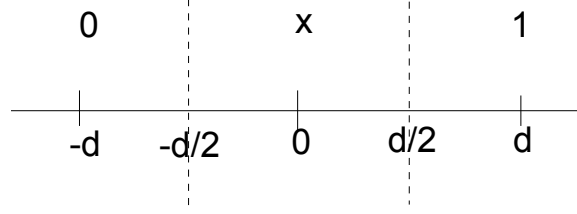


Figure 2.4: Constellation for reporting channel under tertiary decision.

Tertiary Information Reporting Probabilities

For a tertiary local decision reporting probabilities, we need to compute the probability of receiving a state t given that a state v was transmitted between 3 different possibilities. Even if, for energy optimization reason, we do not really report the state H_x but rather report H_0 and H_1 only but at the receiver side (fusion center), the detection will be a test between three possible states (no transmission (H_x , transmission of H_0 , and transmission of H_1)). We use the constellation shown in Fig. 2.4. The probability that the state t is received when the received SNR is $\gamma_k^{(r)}$ given that the state v was sent for AWGN channels is written as

$$P_{c,u_k}^{(t|v)}(\gamma_k^{(r)}) = \begin{cases} Q\left(\alpha_{t,v}\sqrt{\gamma_k^{(r)}}\right), & \text{if } t \in \{0, 1\}, \\ 1 - [P_{c,u_k}^{(0|v)}(\gamma_k^{(r)}) + P_{c,u_k}^{(1|v)}(\gamma_k^{(r)})], & \text{if } t = x, \end{cases} \quad \forall v \in \{0, 1, x\}, \quad (2.44)$$

where $Q(x) = \frac{1}{\sqrt{2\pi}} \int_x^\infty \exp(-\frac{t^2}{2}) dt$ is the Gaussian Q function and $\alpha_{t,v}$ defined as

$$\alpha_{t,v} = \begin{cases} 3/2\sqrt{3/2}; & \text{for } (t, v) \in \{(1, 0), (0, 1)\}, \\ -1/2\sqrt{3/2}; & \text{for } (t, v) \in \{(1, 1), (0, 0)\}, \\ 1/2\sqrt{3/2}; & \text{for } (t, v) \in \{(1, x), (0, x)\}. \end{cases} \quad (2.45)$$

In order to obtain the average reporting probabilities, we integrate (2.44) over the

SNR distributed as in (2.1). Thus, we obtain an integral in the following format

$$G(\alpha, m, \bar{\gamma}) \triangleq \int_0^\infty Q(\alpha\sqrt{\gamma}) \frac{\gamma^{m-1}}{\Gamma(m)} \left(\frac{m}{\bar{\gamma}}\right)^m \exp\left(-\frac{m\gamma}{\bar{\gamma}}\right) d\gamma. \quad (2.46)$$

Using [29, eq. (B.6)], this integral can be solved as

$$G(\alpha, m, \bar{\gamma}) = (2m)^{m-1} \frac{\Gamma(m + \frac{1}{2})}{\Gamma(m)} \sqrt{\frac{\bar{\gamma}}{\pi}} \frac{\alpha}{(2m + \alpha^2 \bar{\gamma})^{m + \frac{1}{2}}} \times {}_2F_1\left(1, m + \frac{1}{2}; m + 1; \frac{2m}{2m + \alpha^2 \bar{\gamma}}\right), \quad \alpha \geq 0. \quad (2.47)$$

Thus, the average error probabilities for the k -th user over the fading reporting channels are given as

$$P_{c,u_k}^{(t|v)} = \begin{cases} 1 - G(1/2\sqrt{3/2}, m_k^{(r)}, \bar{\gamma}_k^{(r)}), & \text{if } (t, v) = (0, 0) \text{ and } (1, 1), \\ G(3/2\sqrt{3/2}, m_k^{(r)}, \bar{\gamma}_k^{(r)}), & \text{if } (t, v) = (1, 0) \text{ and } (0, 1), \\ G(1/2\sqrt{3/2}, m_k^{(r)}, \bar{\gamma}_k^{(r)}), & \text{if } (t, v) = (0, x) \text{ and } (1, x), \\ 1 - P_{c,u_k}^{(0|0)} - P_{c,u_k}^{(1|0)}, & \text{if } (t, v) = (x, 0), \\ 1 - P_{c,u_k}^{(0|x)} - P_{c,u_k}^{(1|x)}, & \text{if } (t, v) = (x, x), \\ 1 - P_{c,u_k}^{(0|1)} - P_{c,u_k}^{(1|1)}, & \text{if } (t, v) = (x, 1). \end{cases} \quad (2.48)$$

Fusion Decision Performance

For tertiary local decisions, we consider only uniform weighting fusion decision, the generalization to the weighted case can be deduced similarly to the binary case. The main difference of the tertiary fusion with comparison to the binary decision is that the users who take local decisions H_x are not considered in taking the global decision due to their high uncertainty, thus their decisions are discarded from the fusion sum.

The fusion rule for tertiary local decisions is given as

$$c^{(ter)} = \begin{cases} H_1, & \text{if } \frac{1}{T} \sum_{k=1}^K I_u(u_k^{(ter)} = H_1) \geq \rho \\ H_0, & \text{otherwise,} \end{cases} \quad (2.49)$$

where $T = \sum_{k=1}^K [I_u(u_k^{(ter)} = H_0) + I_u(u_k^{(ter)} = H_1)]$ is the number of reporting users who decided either H_1 or H_0 to discard the uncertain users (i.e. users who reported H_x).

In order to derive the performance for this tertiary case, conditioning over the number of certain users T allows to obtain similar expressions of the global probabilities of detection and false alarm as the binary case with an additional sum which incorporate all possible values of T

$$P_c^{(d)} = \sum_{T=0}^K \sum_{n=\lceil \rho T \rceil}^T \sum_{l \in \{\mathbf{U}^{(K-T)}, \mathbf{V}^{(n)}, \mathbf{W}^{(T-n)}\}} \prod_{k_x \in u_l} (P_{c, u_{k_x}}^{(ter)}[H_x | H_1]) \prod_{k_1 \in \mathbf{v}_l} (P_{c, u_{k_1}}^{(ter)}[H_1 | H_1]) \prod_{k_0 \in \mathbf{w}_l} (P_{c, u_{k_0}}^{(ter)}[H_0 | H_1]), \quad (2.50)$$

and

$$P_c^{(f)} = \sum_{T=0}^K \sum_{n=\lceil \rho T \rceil}^T \sum_{l \in \{\mathbf{U}^{(K-T)}, \mathbf{V}^{(n)}, \mathbf{W}^{(T-n)}\}} \prod_{k_x \in u_l} (P_{c, u_{k_x}}^{(ter)}[H_x | H_0]) \prod_{k_1 \in \mathbf{v}_l} (P_{c, u_{k_1}}^{(ter)}[H_1 | H_0]) \prod_{k_0 \in \mathbf{w}_l} (P_{c, u_{k_0}}^{(ter)}[H_0 | H_0]), \quad (2.51)$$

where $\{\mathbf{U}^{(K-T)}, \mathbf{V}^{(n)}, \mathbf{W}^{(T-n)}\} = \{\{\mathbf{u}_1, \mathbf{v}_1, \mathbf{w}_1\}, \{\mathbf{u}_2, \mathbf{v}_2, \mathbf{w}_2\}, \dots, \{\mathbf{u}_L, \mathbf{v}_L, \mathbf{w}_L\}\}$ represents all combinations out of K users who reported their decisions to fusion center such that $K - T$ users in \mathbf{u}_l decided H_x , n users in \mathbf{v}_l decided H_1 , and $T - n$ users in \mathbf{w}_l decided H_0 . Note that in the probabilities expressions there are three sums, the first one is over T the number of users who took a decision H_0 or H_1 to cover all

possibilities of probable number of users reporting H_x , the second sum is over n , the number of users who decided H_1 , such that it satisfy the fusion rule ($n \geq \rho T$), the third sum over l to cover all permutations of users out of the K users.

In (2.50) and (2.51), the probability that the fusion center receives the local decision H_t from the k -th user when the actual state is H_v is written as

$$P_{c,u_k}^{(ter)}[H_t|H_v] = P_{c,u_k}^{(t|0)}P_{u_k}^{(0|v)} + P_{c,u_k}^{(t|x)}P_{u_k}^{(x|v)} + P_{c,u_k}^{(t|1)}P_{u_k}^{(1|v)}, \quad \forall t \in \{0, x, 1\}, \quad \forall v \in \{0, 1\}, \quad (2.52)$$

with

- $P_{u_k}^{(t|v)}, \forall t \in \{0, x, 1\}, \quad \forall v \in \{0, 1\}$ are the local probabilities of decision of the k -th user and are defined in (2.43),
- $P_{c,u_k}^{(t|v)}, \forall t, v \in \{0, x, 1\}$ are the reporting probabilities that the fusion center receives H_v given that the k -th user reports H_t and are defined in (2.48).

2.3.3 Quantized Local Decision Scheme

Local Decision Performance

The local decision rule for the quantized decision with M states, $d_i, 1 \leq i \leq M$, is taken following the hypothesis testing rule

$$u_k^{(quant)} = \begin{cases} d_1, & \text{if } O_k < \lambda_{k,1}, \quad \text{for } i = 1 \\ d_i, & \text{if } \lambda_{k,i} \leq O_k < \lambda_{k,i+1}, \quad \forall 2 \leq i \leq M-1 \\ d_M, & \text{if } O_k \geq \lambda_{k,M-1}, \quad \text{for } i = M, \end{cases} \quad (2.53)$$

where $\lambda_{k,i}, 1 \leq i \leq M-1$ are the decision thresholds for the k -th cognitive user. We define $\lambda_{k,0} = 0$ and $\lambda_{k,M} = \infty$.

The local decision probabilities over AWGN channels, given the instantaneous

SNR $\gamma_k^{(s)}$, are expressed as

$$P_{u_k}[d_i|H_v, \gamma_k^{(s)}] = Pr[\lambda_{k,i-1} \leq O_k < \lambda_{k,i}|H_v, \gamma_k^{(s)}] = F_{O_k|H_0, \gamma_k^{(s)}}(\lambda_{k,i}) - F_{O_k|H_0, \gamma_k^{(s)}}(\lambda_{k,i-1}), \quad (2.54)$$

$$\forall v \in \{0, 1\}, \quad \forall 1 \leq i \leq M-1, \quad \forall 1 \leq k \leq K,$$

which can be rewritten, using [32], as

$$P_{u_k}[d_i|H_0, \gamma_k^{(s)}] = \frac{\Gamma(N, \frac{\lambda_{k,i-1}}{2})}{\Gamma(N)} - \frac{\Gamma(N, \frac{\lambda_{k,i}}{2})}{\Gamma(N)}, \quad (2.55)$$

$$P_{u_k}[d_i|H_1, \gamma_k^{(s)}] = Q_N\left(\sqrt{2\gamma_k^{(s)}}, \sqrt{\lambda_{k,i-1}}\right) - Q_N\left(\sqrt{2\gamma_k^{(s)}}, \sqrt{\lambda_{k,i}}\right). \quad (2.56)$$

Averaging (2.55) and (2.56) over the distribution of the SNR given in (2.1), we deduce the expression of the local average probabilities of decisions similarly to the binary and tertiary cases as

$$P_{u_k}[d_i|H_0] = \frac{\Gamma(N, \frac{\lambda_{k,i-1}}{2})}{\Gamma(N)} - \frac{\Gamma(N, \frac{\lambda_{k,i}}{2})}{\Gamma(N)}, \quad (2.57)$$

$$P_{u_k}[d_i|H_1] = F_N(m_k^{(s)}, \bar{\gamma}_k^{(s)}, \lambda_{k,i-1}) - F_N(m_k^{(s)}, \bar{\gamma}_k^{(s)}, \lambda_{k,i}), \quad (2.58)$$

where $F_n(m, \bar{\gamma}, \lambda)$ as defined in (2.13).

Reporting Decision Performance

We consider a pulse-amplitude modulation (PAM) of M symbols for the reporting of quantized local decisions from secondary user to the fusion center as in Fig. 2.5.

Thus, the probability that symbol d_j is received when d_i was sent over an AWGN

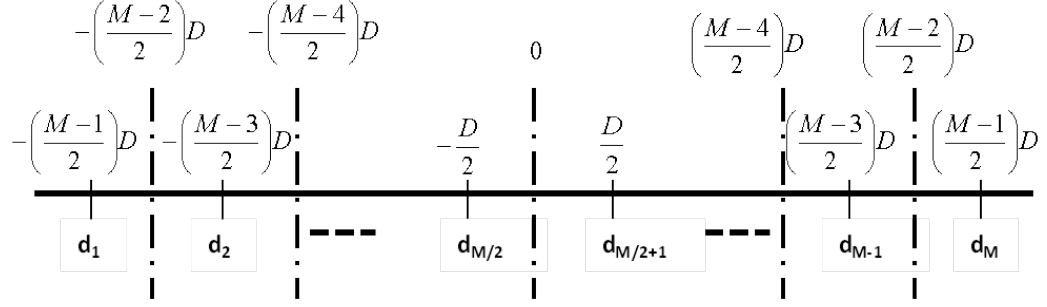


Figure 2.5: Constellation for reporting channel under quantized decision.

channel can be written as

$$P_{c,u_k}[d_j|d_i, \gamma_k^r] = \begin{cases} \frac{1}{\sqrt{2\pi}} \int_{-\infty}^{\nu_j} \exp(-\frac{(t-\mu_i)^2}{2}) dt, & \text{if } j = 1 \\ \frac{1}{\sqrt{2\pi}} \int_{\nu_{j-1}}^{\nu_j} \exp(-\frac{(t-\mu_i)^2}{2}) dt, & \text{if } 1 < j < M \\ \frac{1}{\sqrt{2\pi}} \int_{\nu_{j-1}}^{\infty} \exp(-\frac{(t-\mu_i)^2}{2}) dt, & \text{if } j = M, \end{cases} \quad (2.59)$$

where

- $\mu_i = (-\frac{M+1}{2} + i)D$, $1 \leq i \leq M$ is the position of the i -th symbol in the constellation.
- $\nu_j = (-\frac{M}{2} + j)D$, $1 \leq j \leq M - 1$ is the position of the j -th threshold of detection in the constellation.

The reporting energy is then $E_r = \frac{1}{M} \sum_{i=1}^M \mu_i^2 = \frac{D^2(M^2-1)}{12}$.

Thus, (2.59) can be rewritten as

$$P_{c,u_k}[d_j|d_i, \gamma_k^{(r)}] = \begin{cases} 1 - Q\left(\alpha_{i,j} \sqrt{\gamma_k^{(r)}}\right), & \text{if } j = 1 \\ Q\left(\alpha_{i,j-1} \sqrt{\gamma_k^{(r)}}\right) - Q\left(\alpha_{i,j} \sqrt{\gamma_k^{(r)}}\right), & \text{if } 1 < j < M \\ Q\left(\alpha_{i,j-1} \sqrt{\gamma_k^{(r)}}\right), & \text{if } j = M, \end{cases} \quad (2.60)$$

where $\alpha_{i,j} = \frac{1}{\sqrt{E_r}}(\mu_i - \nu_j) = \sqrt{\frac{12}{M^2-1}}(-\frac{1}{2} + i - j)$, $1 \leq i \leq M$, $1 \leq j \leq M - 1$,

The average reporting probability over the SNR is then determined by

$$P_{c,u_k}[d_j|d_i] = \int P_{c_k}[d_j|d_i, \gamma_k^{(r)}] f_{\gamma_k^{(r)}}(\gamma_k^{(r)}) d\gamma_k^{(r)}, \quad \forall 1 \leq i, j \leq M, \quad (2.61)$$

which can be re-written in function of $G(\alpha, m, \bar{\gamma})$ defined in (2.47) as

$$P_{c,u_k}[d_j|d_i] = \begin{cases} 1 - G(\alpha_{i,j}, m_k^{(r)}, \bar{\gamma}_k^{(r)}), & \text{if } j = 1 \\ G(\alpha_{i,j-1}, m_k^{(r)}, \bar{\gamma}_k^{(r)}) - G(\alpha_{i,j}, m_k^{(r)}, \bar{\gamma}_k^{(r)}), & \text{if } 1 < j < M \\ G(\alpha_{i,j}, m_k^{(r)}, \bar{\gamma}_k^{(r)}), & \text{if } j = M. \end{cases} \quad (2.62)$$

Fusion Decision Performance

We consider the following fusion rule for the quantized decisions

$$c^{(quant)} = \begin{cases} H_1, & \text{if } \sum_{k=1}^K w_k I_c^{(quant)}(u_k) \geq \rho, \\ H_0, & \text{otherwise,} \end{cases} \quad (2.63)$$

where $I_c^{(quant)}(x)$ is a mapping function that the fusion center uses to map the local quantized decisions to a pre-defined values α_j for each decision d_j (i.e. $I_c^{(quant)}(d_j) = \alpha_j, \forall 1 \leq j \leq M$), w_k is a weighting factor for the decision taken by k -th user, and ρ is the fusion decision threshold.

This decision rule can be interpreted as if the fusion center assigns a value for each local decision then takes a weighted sum of all values of different local users decisions and compares this weighted sum to a fusion threshold.

Thus,

$$P_c[d_1] = Pr[u_1 = d_{j_1}, \dots, u_K = d_{j_K}, \sum_{k=1}^K w_k \alpha_{j_k} \geq \rho] \quad (2.64)$$

$$= \sum_{\sum_{k=1}^K w_k \alpha_{j_k} \geq \rho} Pr[u_1 = d_{j_1}, \dots, u_K = d_{j_K}] \quad (2.65)$$

$$= \sum_{\sum_{k=1}^K w_k \alpha_{j_k} \geq \rho} \prod_{k=1}^K P_{c,u_k}[d_{j_k}]. \quad (2.66)$$

Thus, the probabilities of detection and false alarm at the fusion center are deduced, respectively, as

$$P_c^{(f)} = P_c[d_1|H_0] = \sum_{\sum_{k=1}^K w_k \alpha_{j_k} \geq \rho} \prod_{k=1}^K P_{c,u_k}[d_{j_k}|H_0] \quad (2.67)$$

$$P_c^{(d)} = P_c[d_1|H_1] = \sum_{\sum_{k=1}^K w_k \alpha_{j_k} \geq \rho} \prod_{k=1}^K P_{c,u_k}[d_{j_k}|H_1], \quad (2.68)$$

with $P_{c,u_k}[d_j|H_u]$, $j \in \{1, 2, \dots, M\}$, $u \in \{0, 1\}$ is the probability that the fusion center estimates that the k -th user decided d_j while the real state is H_u and defined as

$$P_{c,u_k}[d_j|H_u] = \sum_{i=1}^M P_{c,u_k}[d_j|d_i] P_{u_k}[d_i|H_u], \quad (2.69)$$

$$\forall u \in \{0, 1\}, \forall 1 \leq j \leq M.$$

In (2.69), $P_{c_k}[d_j|d_i]$ is the average reporting probability that the user k send d_i while the fusion center estimate d_j defined in (2.62), and $P_{u_k}[d_i|H_u]$ is the local probability of decision d_i by the user k given H_u defined in (2.57) and (2.58). Thus,

$$P_c^{(f)} = \sum_{\sum_{k=1}^K w_k \alpha_{j_k} \geq \rho} \prod_{k=1}^K \sum_{i=1}^M P_{c,u_k}[d_{j_k}|d_i] P_{u_k}[d_i|H_0] \quad (2.70)$$

$$P_c^{(d)} = \sum_{\sum_{k=1}^K w_k \alpha_{j_k} \geq \rho} \prod_{k=1}^K \sum_{i=1}^M P_{c,u_k}[d_{j_k}|d_i] P_{u_k}[d_i|H_1]. \quad (2.71)$$

2.3.4 Soft Information Scheme

In this scheme, the local users will not take any decision. The measured signals are directly forwarded to the fusion center. The fusion center is the only entity who will take a decision based on the collected measurements from the different users.

The received signal at the fusion center from user k at instant j can be written as

$$y_{c,k}(j) = \begin{cases} g_k h_k^{(r)} \left(h_k^{(s)} s(j) + v_k(j) \right) + v_c(j) & \text{if } H_1 \\ g_k h_k^{(r)} v_k(j) + v_c(j) & \text{if } H_0, \end{cases} \quad (2.72)$$

where g_k is the k -th user amplification gain, $v_c(j)$ is zero-mean additive white Gaussian noise (AWGN) at the fusion center with variance σ_v^2 .

Taking into considerations the measurements of $2N$ samples from K users, the observed energy at the fusion center is written as

$$O_c = \sum_{k=1}^K \sum_{j=0}^{2N-1} |y_{c,k}(j)|^2. \quad (2.73)$$

The objective is to compute the average detection and false alarm and probabilities defined respectively as

$$P_c^{(d)} = Pr[O_c > \lambda_c | H_1] \quad (2.74)$$

$$P_c^{(f)} = Pr[O_c > \lambda_c | H_0], \quad (2.75)$$

where λ_c is the decision threshold at the fusion center.

From (2.72), we deduce the distribution of $y_{c,k}(j)$ as

$$y_{c,k}(j) \sim \begin{cases} \mathcal{N}\left(h_k|^{(s)}h_k^{(r)}g_k s(j), |h_k^{(s)}|^2|h_k^{(r)}|^2|s(j)|^2g_k^2 + \sigma_v^2(1 + |h_k^{(r)}|^2g_k^2)\right) & \text{if } H_1 \\ \mathcal{N}\left(0, \sigma_v^2(1 + |h_k^{(r)}|^2g_k^2)\right) & \text{if } H_0, \end{cases} \quad (2.76)$$

where $\mathcal{N}(\mu, \sigma^2)$ is the Gaussian (Normal) distribution of mean μ and variance σ^2 .

Noting that the $y_{c,k}(j)$ have different variances due to the imperfect non identical reporting channels, the distribution of O_c for AWGN channels is not simply a chi-square. The problem is more challenging in this case.

The system configuration can be modeled as multiple branches relay communication. In each branch, a secondary user will behaves like a relay node who forwards its local measurement to the fusion center over fading channels. Thus, the total observed energy can be re-written as sum of energy observations per branch as

$$O_c = \sum_{k=1}^K O_{c,k}, \quad (2.77)$$

where $O_{c,k}$ is the observed energy coming through the user k expressed as

$$O_{c,k} = \sum_{j=0}^{2N-1} |y_{c,k}(j)|^2. \quad (2.78)$$

Thus, the well known moment generating (MGF) approach can be used. In the following, we will first derive the averaged MGF per branch then deduce the MGF of the total signal in order to finally compute the false-alarm and detection probabilities.

Given the expression of $y_{c,k}(j)$ in (2.72), the observed energy at each branch $O_{c,k}$ given the SNR can be written as a central chi-square in absence of the primary user and as a non central chi-square with a non-centrality parameter $\gamma_k^{(T)}$ when the primary user is present, where $\gamma_k^{(T)}$ is the end-to-end SNR through branch k which

can be written using [eq(20),[38]] as

$$\gamma_k^{(T)} = \frac{E_s}{N_k} |h_k^{(s)}|^2 |h_k^{(r)}|^2, \quad (2.79)$$

where N_k is the total noise over the k -th branch expressed as

$$N_k = \sigma_v^2 (1 + \Omega_k^{(r)} g_k^2), \quad (2.80)$$

with $\Omega_k = E[|h_k|^2]$.

Then, we redefine

$$O_{c,k} \triangleq \alpha_{c,k} \tilde{O}_{c,k}, \quad (2.81)$$

where

$$\tilde{O}_{c,k} \sim \begin{cases} \chi_{2N}^2(1), & \text{if } H_1 \\ \chi_{2N}^2(0), & \text{if } H_0, \end{cases} \quad (2.82)$$

and

$$\alpha_{c,k} = \begin{cases} \gamma_k^{(T)} = \frac{E_s}{\sigma_v^2 (1 + \Omega_k^{(r)} g_k^2)} |h_k^{(s)}|^2 |h_k^{(r)}|^2, & \text{if } H_1 \\ \frac{1}{E[|y_{c,k}(j)|^2 | H_0]} = \frac{1}{\sigma_v^2 (1 + \Omega_k^{(r)} g_k^2)}, & \text{if } H_0. \end{cases} \quad (2.83)$$

Thus, the moments of $O_{c,k}$ are deduced as

$$E[O_{c,k}^i] = E[\alpha_{c,k}^i] E[\tilde{O}_{c,k}^i], \forall i, \quad (2.84)$$

with

- using [eq(2.35) and (2.45),[29]]

$$E[\tilde{O}_{c,k}^i] = \begin{cases} 2^i \exp(-\frac{1}{2}) \frac{\Gamma(N+i)}{\Gamma(N)} {}_1F_1(N+i, N, \frac{1}{2}), & \text{if } H_1 \\ 2^i \frac{\Gamma(N+i)}{\Gamma(N)}, & \text{if } H_0, \end{cases} \quad (2.85)$$

- using [eq(28), [38]]

$$E[\alpha_{c,k}^i] = \begin{cases} \frac{\Gamma(m_k^{(s)}+i) \Gamma(m_k^{(r)}+i)}{\Gamma(m_k^{(s)}) \Gamma(m_k^{(r)})} \left(\frac{\bar{\gamma}_k^{(T)}}{\beta_k^{(s)}}\right)^i \left(\frac{\bar{\gamma}_k^{(T)}}{\beta_k^{(r)}}\right)^i, & \text{if } H_1 \\ \frac{1}{\sigma_v^2(1+\Omega_k^{(r)}g_k)}, & \text{if } H_0, \end{cases} \quad (2.86)$$

where $\bar{\gamma}_k^{(T)} = E[\gamma_k^{(T)}] = \frac{E_s \Omega_k^{(s)} \Omega_k^{(r)}}{\sigma_v^2 (1 + \Omega_k^{(r)} g_k^2)}$ and $\beta_k = \frac{\Gamma(m_k+i)}{\Gamma(m_k)}$.

Then, we deduce $\mathcal{M}_{O_{c,k}}(s)$, the MGF of $O_{c,k}$ in function of the moments $E[O_{c,k}^i]$ as

$$\mathcal{M}_{O_{c,k}}(s) = \sum_{i=0}^{\infty} \frac{(-1)^i}{i!} E[O_{c,k}^i] s^i. \quad (2.87)$$

Although this infinite series is absolutely convergent, it converges slowly and has to be truncated for practical computations. Pade Approximation [39] is known to give the best approximation of this series. It can be written in this format:

$$\hat{\mathcal{M}}_{O_{c,k}}(s) = \frac{\sum_{i=0}^p a_i s^i}{1 + \sum_{i=0}^q b_i s^i}, \quad (2.88)$$

where the coefficients a_i and b_i can be determined by solving the so-called Pade equations. A detailed explanation on the use of Pade approximation and error computations can be found in [40] and the references therein.

Once the expressions of $\mathcal{M}_{O_{c,k}}(s)$ are obtained, the total observation signal $\mathcal{M}_{O_c}(s)$ MGF is deduced as the product of the all the MGF of each observation's MGF:

$$\mathcal{M}_{O_c} = \prod_{k=1}^K \mathcal{M}_{O_{c,k}}. \quad (2.89)$$

Given the MGF, the cumulative distribution function (CDF) is computed using the Inverse Laplace Transformation technique as

$$\mathcal{F}_{O_c}(x) = \mathcal{L}^{-1} \left\{ \frac{1}{s} \mathcal{M}_{O_c}(s) \right\}. \quad (2.90)$$

A simple derivation of the Laplace Transform can be found by re-writing the MGF as fractional expansion in the following format

$$\mathcal{M}_{O_c}(s) = \sum_{i=1}^I \frac{\nu_i}{s - \mu_i}, \quad (2.91)$$

where ν_i and $\mu_i (i = 1 \dots I)$ are respectively the residues and poles of $\mathcal{M}_{O_c}(s)$.

Thus, the CDF is finally deduced as

$$F_{O_c}(x) = 1 + \sum_{i=1}^I \frac{\nu_i}{\mu_i} \exp(\mu_i x), \quad (2.92)$$

Finally, the average cooperative detection and false alarm probabilities are concluded as

$$P_c^{(d)} = 1 - F_{O_c}(\lambda_c | H_1) \quad (2.93)$$

$$P_c^{(f)} = 1 - F_{O_c}(\lambda_c | H_0). \quad (2.94)$$

2.4 Numerical Results

Consider a cognitive network composed of $K = 10$ users. The users are geographically uniformly distributed inside a circle of radius $d = 1$ km around the primary user. The fusion center is selected as the closest user to the centroid of the users. The fading parameters are taken all identical $m_k^{(s)} = m_k^{(r)} = 8$, $\forall k$ (which yields to shadowing variance $\sigma_s^2 = 10$ dB). The secondary users take their local decision over a sensing interval of $N = 100$ samples. The noise variance at the receivers is set to $\sigma_v^2 = 0$ dB. The average SNRs will be estimated using the distance-based pathloss equation

$$\bar{\gamma} = E_t \frac{\xi}{d^\eta}, \quad (2.95)$$

where E_t is the transmitted energy, ξ is the pathloss in a reference distance (1 km) with the transmit and receive antenna gains, d is the distance between the transmitting and receiving user, and η the pathloss exponent. ξ and η are fixed in the simulations to 1 and 3, respectively. The primary user's transmission energy is set to $E_s = 10$ dB while the reporting energy will be the main variable parameter in order to show the effect of imperfect reporting channels on the sensing performance. The weighting factors for local decision, w_k , are set equally (i.e. $w_k = \frac{1}{K}$, $\forall 1 \leq k \leq K$). The performance measure is the global error probability written as $P^{(e)} = \alpha P^{(f)} + (1 - \alpha)(1 - P^{(d)})$, where $\alpha \in [0, 1]$ is a weighting parameter selected to tune the effect of probability of false alarm and miss-detection on the global error probability according to the system requirements.

2.4.1 Effect of Imperfect Channels and Non Identical Average SNRs

Binary Local Decision Scheme

In this part, we will focus on the binary local decision scheme. Binary local decision is considered with non coherent BPSK constellation ($a = 1$, $b = 1$) for reporting the decisions. The binary local decision thresholds for the local hypothesis testing rule are determined assuming equal prior probabilities of the two states H_0 and H_1 .

Effect of Imperfect Reporting Channel

Fig. 2.6 plots the global cooperative error probability at the fusion center with $\alpha = 1/2$ for different levels of the primary user transmission energy, denoted by E_s , as function of the reporting energy of the secondary users, denoted by E_r , to the fusion center. It is noted that the reporting energy highly affects the sensing performance especially for high transmission energy of the primary user. For instance, for $E_s = 15$ dB, the loss

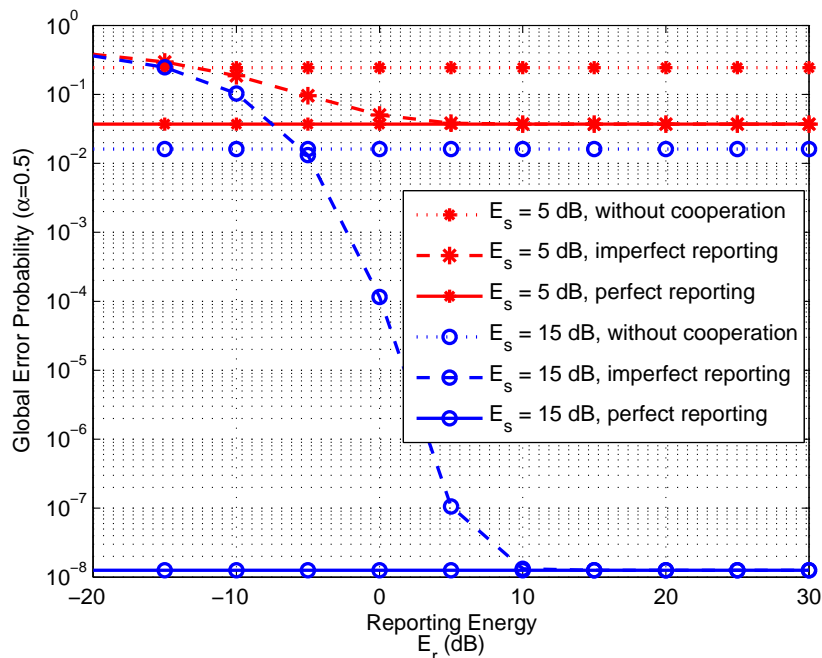


Figure 2.6: Performance of cooperative spectrum sensing function of the reporting energy E_r for different primary user transmission energy levels E_s . The local decision is binary while the fusion rule is the uniform weighting fusion rule with $\rho = 0.5$.

in the error probability compared to the perfect reporting case could achieve 10^{-7} by selecting a reporting power $E_r < -10$ dB and the cooperation effect becomes negative (the error with cooperation for $E_s < -5$ dB is higher than without cooperation). On the other hand, this performance analysis could be exploited in optimizing the reporting power. For example, for $E_s = 15$ dB, $E_r = 10$ dB is required to achieve the perfect reporting power performance while it is only 5 dB for $E_s = 5$ dB.

Performance Comparison between Identical and Non Identical Channels

Fig. 2.7 compares the performance of cooperative sensing techniques for identically and independently distributed (i.i.d.) channels with that for non i.i.d. channels. For the case of i.i.d channels, the average SNR for all users equals to the arithmetic mean of the users' average SNRs. The difference between the curves for perfect and imperfect reporting channels shows the necessity of considering non identical

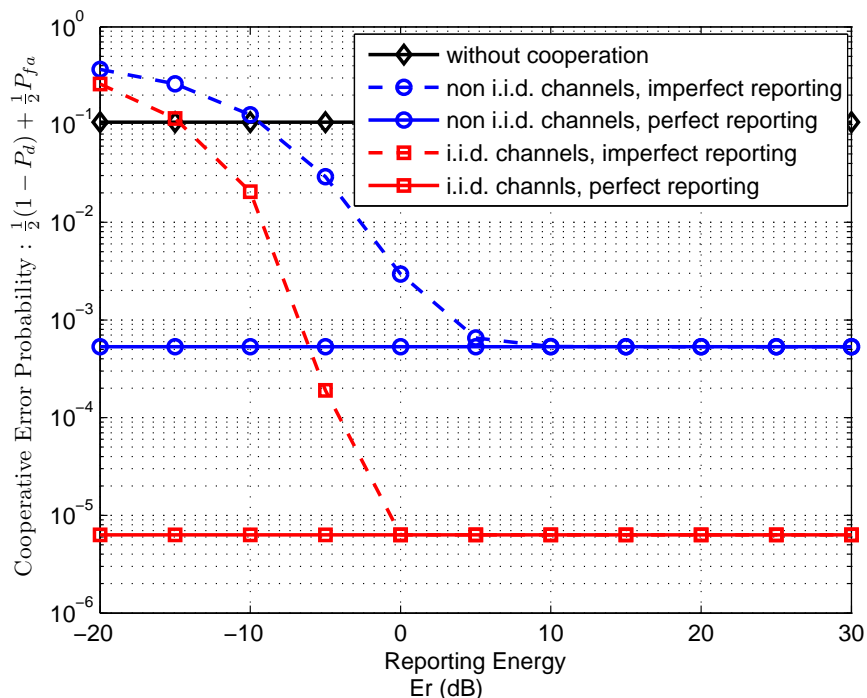


Figure 2.7: Effect of identical average SNR hypothesis on the sensing performance for binary local decision, uniform weighting fusion rule, $\rho = 0.5$, and $E_s = 10$ dB.

average SNRs in computing the performance of cooperative spectrum sensing systems in order to guarantee accurate parametrization of the cognitive system. This figure also shows the cooperative gain by comparing the global error probability at the fusion center and the average error probability of individual users. Even though the cooperative gain could attain 10^{-2} for perfect reporting channels, in case of imperfect reporting channels, the cooperation effect becomes negative for low reporting SNRs ($E_r < -10$ dB for this set up).

Tertiary Local Decision Scheme

In this paragraph we will show the advantages of tertiary local decision by comparing its performance in terms of global error probability to the binary local decision. The local tertiary decision thresholds λ^{min} and λ^{max} are chosen around the binary threshold λ such that for each user k , $P_k^{(ter)}[H_x|H_1] = P_k^{(ter)}[H_x|H_0] = \epsilon$ where $\epsilon \in [0, 1]$

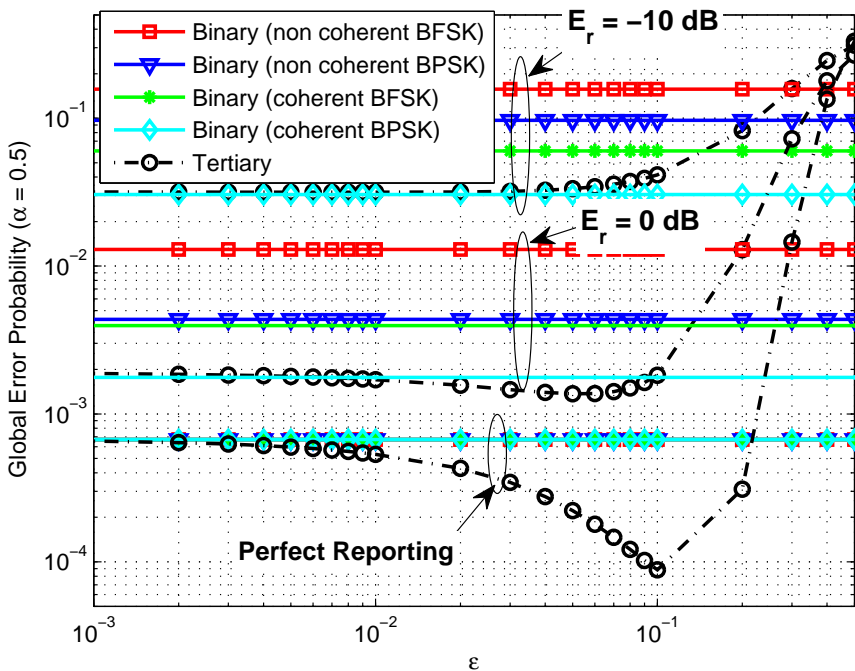


Figure 2.8: Comparison between tertiary and binary local decision schemes with $E_s = 10$ dB and uniform weighting fusion rule ($\rho = 0.5$).

is a parameter that we will use to control the interval of the uncertainty state. In Fig. 2.8, we plot the global probability as a function of ϵ to compare the performance when the tertiary decision is used versus that of the binary decision with the various constellations presented in Table 2.1. The comparison is done for various levels of the reporting energy E_r . The simulation results show that there exists an ϵ_0 such that the tertiary strategy performs better than all the binary constellations for $\epsilon \leq \epsilon_0$ and that an optimal ϵ^* which minimizes the global error probability exists since the tertiary curves in function of ϵ are continuous and convex. We note when ϵ is close to 1, the tertiary strategy become very bad and that is explained by the fact that the interval of uncertainty is very large so most of the users will take a local decision H_x .

Quantized Local Decision Scheme

The local decision thresholds are selected such that we obtain equal decision probabilities over each interval (i.e. $|P_{u_k}[d_i|H_1] - P_{u_k}[d_i|H_0]| = \text{Constant}, \forall 1 \leq i \leq M$). The fusion mapping function for the local decisions is set to obtain symmetric weights around 0 such that

$$[\alpha_1, \alpha_2, \dots, \alpha_M] = \left[-\frac{M}{2}, -\frac{M}{2} - 1, \dots, -1, 1, \dots, \frac{M}{2} - 1, \frac{M}{2} \right]$$

The fusion decision threshold is variable in the figures in the interval $[-M/2, M/2]$. Due to computational complexity exponentially increasing with the number of users and number of quantification levels, for this simulation, we use only $k = 5$ users.

In Fig. 2.9, we plot the the miss-detection probability versus the false alarm probability for different number of local decision levels M for the case of perfect reporting channels. The sensing performance increases as M increases (lower probabilities of error). Thus, increasing the number of reported decisions has a good impact on the cooperative performance thanks to the increase of the reported information.

In Fig. 2.10, we plot the cooperative error probability with $\alpha = \frac{1}{2}$ in function of the reporting energy for different number of quantification levels M . As deduced from the previous figure, for perfect reporting channels, the higher the number of quantification levels M , the lower the cooperative error probability. However, for low reporting SNRs (equivalently, low reporting energy), a higher cooperative error probability is obtained for the highest number of quantification levels due to the reporting errors. We note also that for lower quantification levels, lesser reporting energy is needed to achieve the same performance as perfect reporting channel. Thus, a trade-off between the number of quantification levels for the hard decision and the reporting energy controls our system configuration depending on the required system performance.

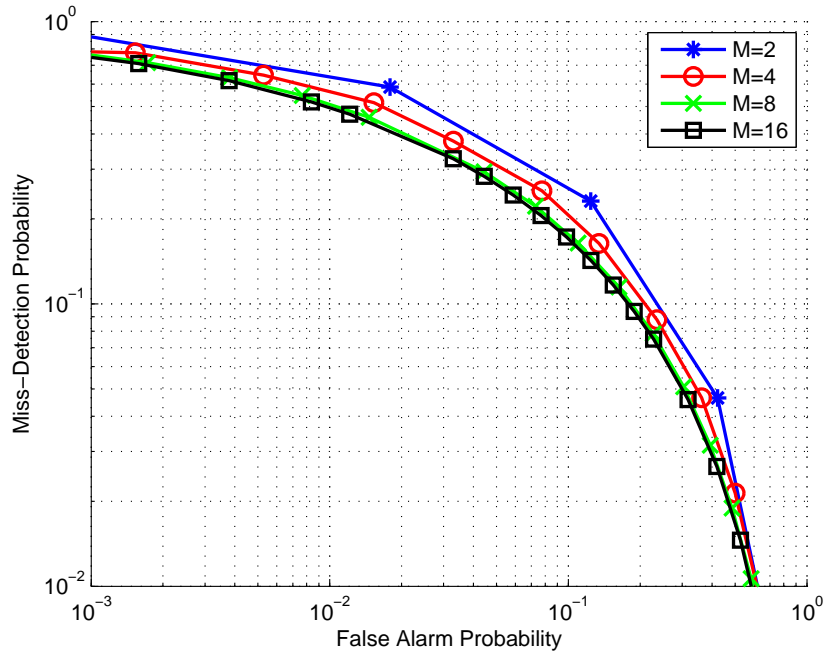


Figure 2.9: Complementary Receiver operating characteristic (CROC) curves for different quantization sizes (M) with perfect reporting channels and fusion decision threshold $\rho = 0$.

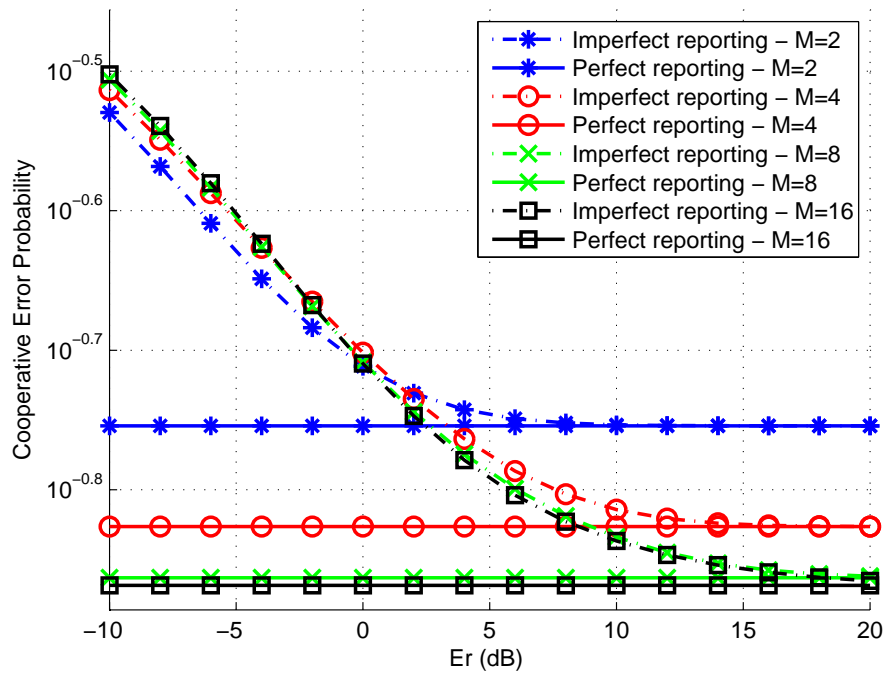


Figure 2.10: Cooperative error probability for $\alpha = \frac{1}{2}$ with different quantization sizes (M) and fusion decision threshold $\rho = 0$.

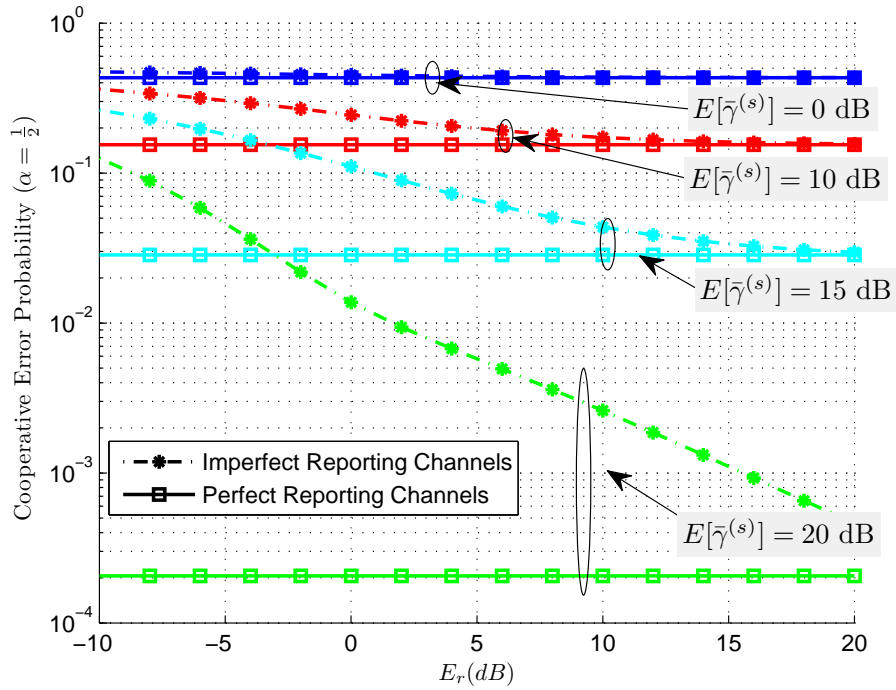


Figure 2.11: Cooperative error probability for soft cooperation scheme.

Soft Cooperation Scheme

In Fig. 2.11, we plot the cooperative error probability with the soft cooperation scheme under perfect and non perfect reporting channels. In this scheme, we observe also the effect of imperfect reporting channels which penalize the performance of the spectrum sensing even in high sensing SNR.

2.4.2 Applications of the Performance Analysis to System Parametrization

Reporting Energy Optimization with Binary Local Decision Scheme

In Fig. 2.12, we plot global error probability in function of the weighting parameter α for the different constellations of binary information reporting presented in Table. 2.1. This figure allow us to verify the classification of the bit-error rate of the different

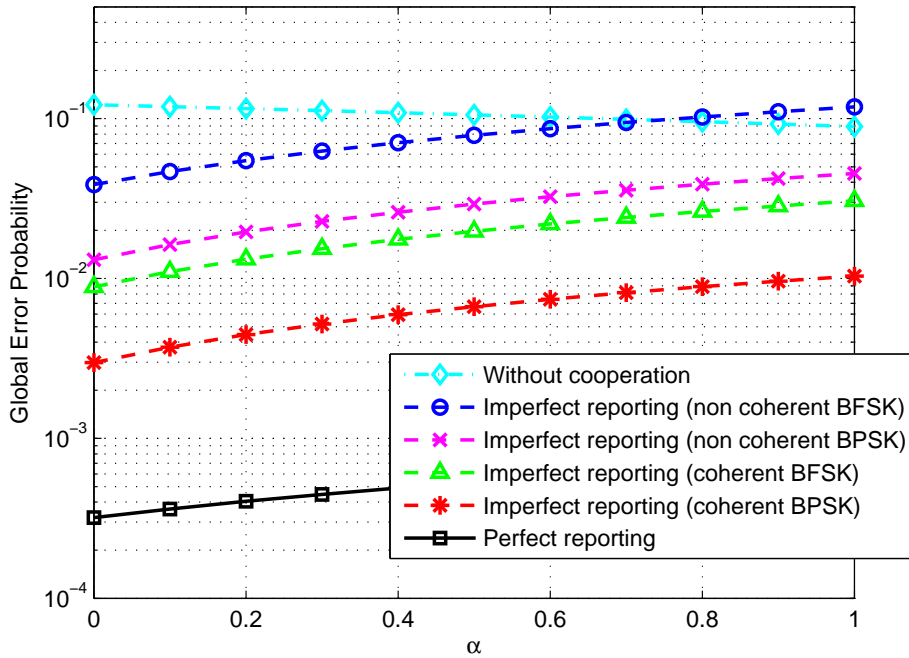


Figure 2.12: Comparison between different binary reporting decision constellations with $E_s = 10$ dB and counting fusion rule ($\rho = 0.5$).

constellations as in [35]. Secondly, this figure allow us to interpret the effect of the weighting factor α which represent the weight of the false alarm error in the global error probability (respectively, $1 - \alpha$ represents the weighting of the miss-detection error). α is generally fixed according to the system specifications and will allow to determine the system parameters in order to achieve targeted level of error probability.

Fusion Rule Weights Choice

Fig. 2.13 illustrates the global error probability with $\alpha = 1/2$ with different fusion rules as a function of the fusion decision threshold when $E_s = 10$ dB. Three weighting schemes are considered: 1) uniform weighting, 2) weighting proportional to the sensing SNR, and 3) weighting proportional to the reporting SNR. With the assumption of perfect reporting channels, the weighting based on the sensing SNR achieves the best performance since reporting channels do not play any role in this case while

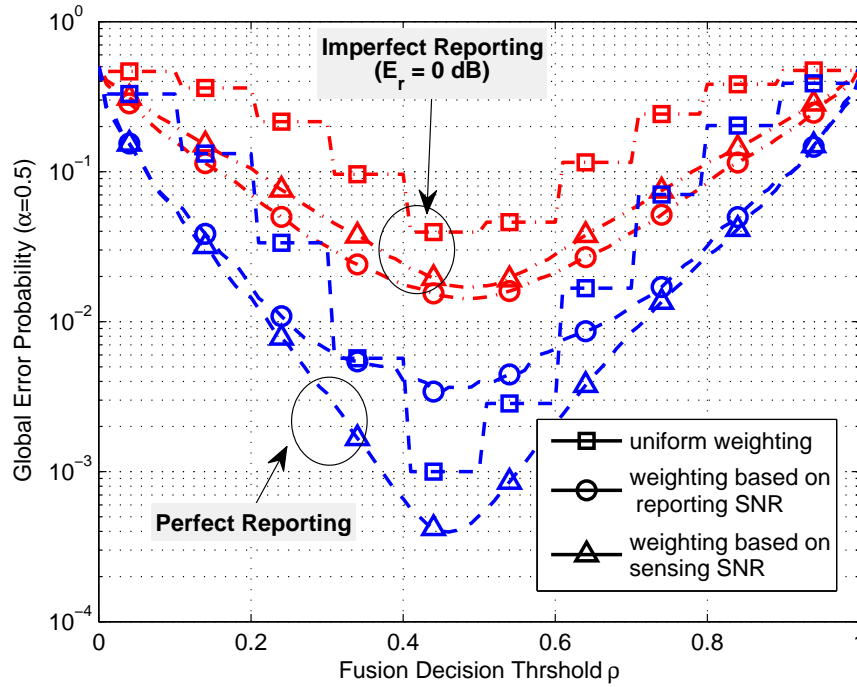


Figure 2.13: Performance of cooperative spectrum sensing for different fusion rules with binary local decision and $E_s = 10$ dB.

considering the imperfect reporting channels, the weighting based on the reporting SNR outperforms the two others which shows the higher impact of reporting SNR on the global performance than sensing SNR. More sophisticated weightings could be adopted which take into account both reporting and sensing SNR but in general this figure shows that an adaptive weighting depending on the topology parameters could further enhance the global performance.

Tertiary Local Decision Thresholds

Fig 2.14 shows that the optimal value ϵ^* depends on the different parameters of the cognitive system such as the primary user transmission energy E_s , the reporting power E_r , and the fusion rule threshold ρ . This performance computation can be exploited in a numerical optimization algorithm to determine the optimal value of ϵ that minimizes the global error probability depending on the system topology.

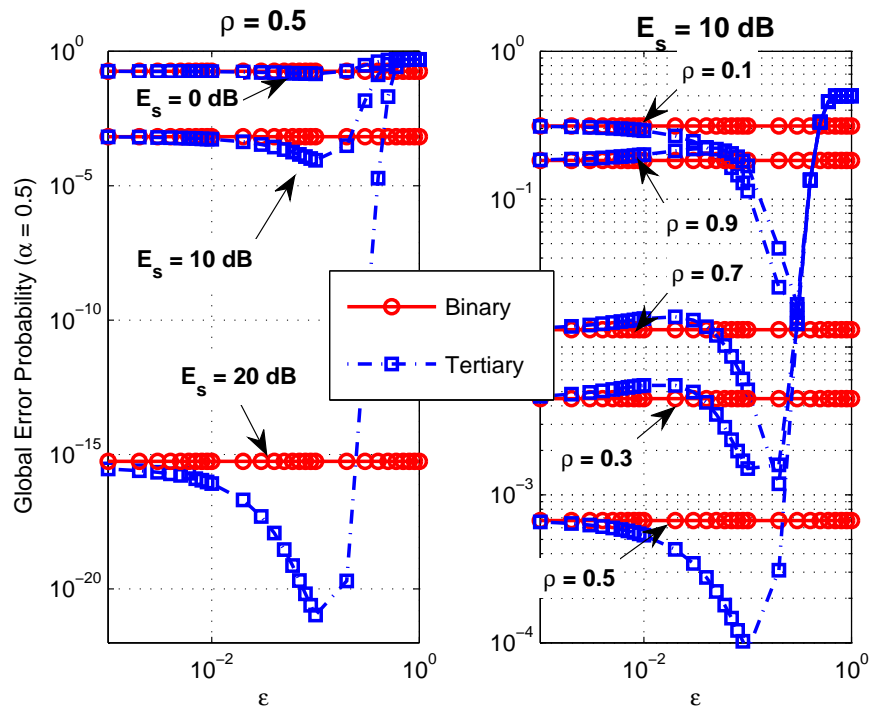


Figure 2.14: Comparison between tertiary and binary local decision scenarios for perfect reporting with different values of primary user transmission energy E_s and fusion decision thresholds ρ .

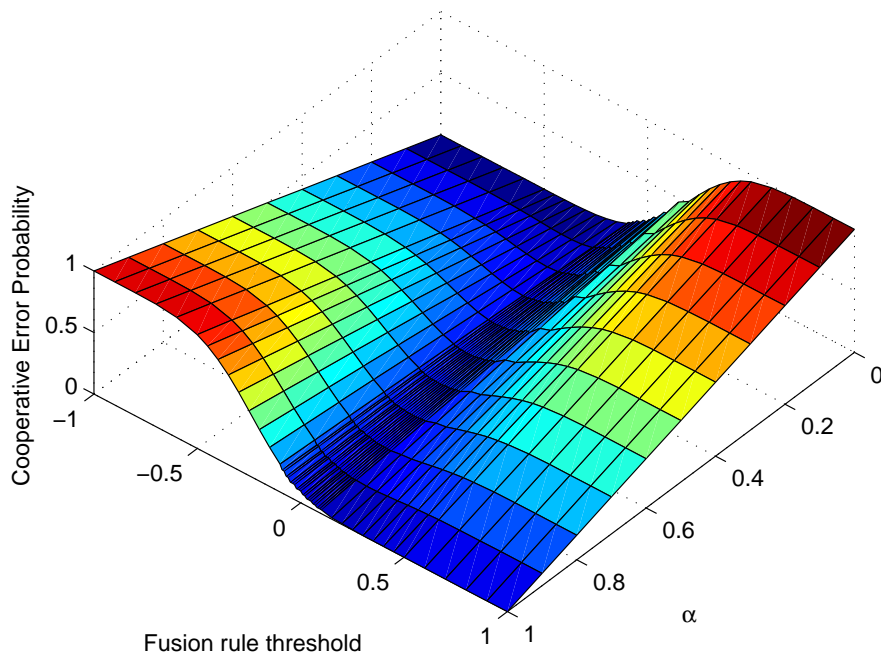


Figure 2.15: Cooperative error probability function of the fusion decision threshold ρ and the parameter α for perfect reporting channel and $M = 16$.

Quantized Fusion Decision Thresholds

In Fig. 2.15, we show the dependence of the cooperative error probability as function of α in X axis and fusion decision thresholds in Y axis for the case $M = 16$ and perfect reporting channels. We conclude that for each value of α , there exists an optimal fusion decision threshold which minimizes the cooperative error probability. This fact is seen clearly in Fig. 2.16 presenting curves of cooperative error probability for each value of α as function of the fusion decision threshold. Since the fusion decision threshold is a constrained value, its optimal value can be obtained by a numerical optimization algorithm such as the bisection method.

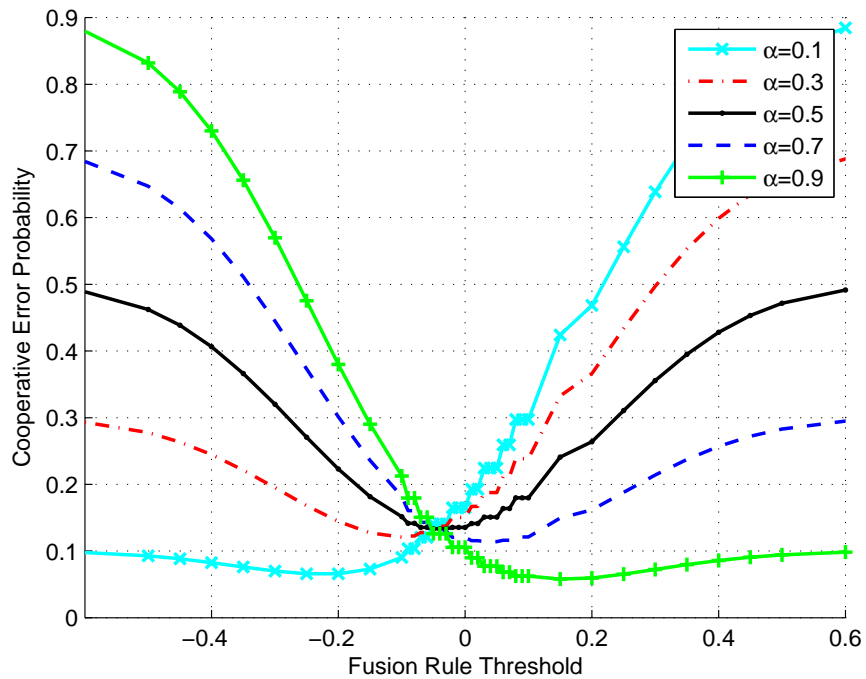


Figure 2.16: Cooperative error probability function of the fusion decision threshold for different values of the parameter α with perfect reporting channel and $M = 16$.

2.4.3 Application of the Performance Analysis for Different Network Topologies

A fully centralized cooperative spectrum sensing scheme with only one fusion center as discussed above has the advantage of possibility of achieving optimal performance but in practice it is not recommended due to its high bandwidth consumption. Thus, decentralized models are preferred in order to simplify implementation and computational complexity. We present two examples of decentralized networks, namely the distributed and the cluster-based models, and discuss how the performance study shown earlier can be used to parametrize these systems and optimize their performance.

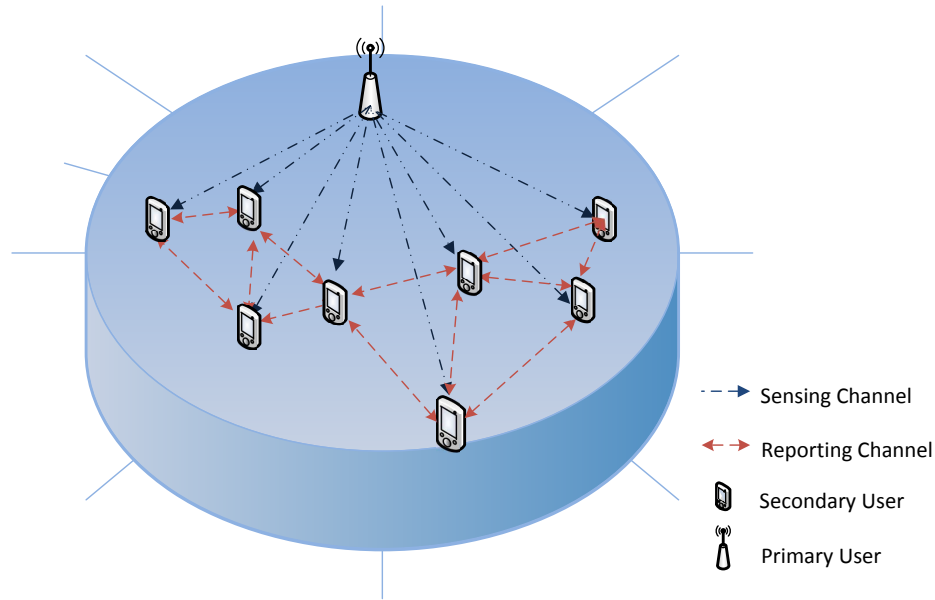


Figure 2.17: Distributed cooperative spectrum sensing model.

Distributed Cooperative Spectrum Sensing

In this scheme, as shown in Fig. 2.17, each user takes its local decision and simply broadcasts it. Then each user acts as a fusion center that collects the local decisions from its own nearest neighbors. Thus, every user not only performs a local spectrum sensing as usual, but also behaves as a fusion center for its own neighbors while profiting from local decisions of the neighboring users. Then, each user updates its own decision using this new decision. Afterwards, this updated decision is re-broadcast to help the neighbors make a fine tune of their fusion decisions. This iterative process is repeated until a satisfactory reliability of the spectrum decision is obtained. The cooperative detection and false alarm cooperative probabilities can be deduced by applying the same formulas derived earlier for fusion decision and the selected neighbors' probabilities at the previous iteration as local probabilities.

In Fig. 2.18, distributed cooperative spectrum sensing performance is plotted by the average error probability after different iterations of cooperation with its neighbors. The total number of users in the network is 50 and each user cooperates with its

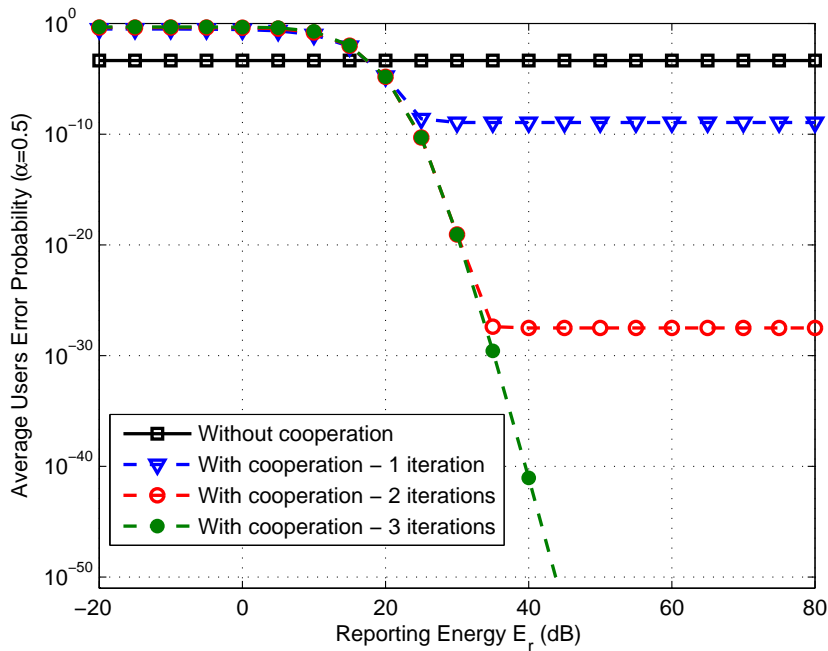


Figure 2.18: Distributed cooperative spectrum sensing performance with different number of iterations in collaboration between users (50 users, 5 neighbors per user, $E_s = 10$ dB, binary local decision, uniform weighting fusion rule with $\rho = 0.5$).

5 nearest neighbors. As the number of iterations increases the average error probability falls exponentially, which shows the efficiency of this procedure. In addition, the cooperative gain increases as the reporting energy grows (The cooperative gain is the difference between global probabilities with and without collaboration). This type of figure is useful for system modeling as it can be used to determine the satisfactory number of neighbors to be used and at which iteration a satisfactory error probability is obtained.

Cluster-based Cooperative Spectrum Sensing

Clustering is a technique employed in many domains to improve the efficiency of cooperation. This procedure has two main objectives, 1) reducing the energy consumption needed for cooperation by reducing reporting operations and distances, and 2) reducing the computational overhead at fusion centers resulting from reduction of number

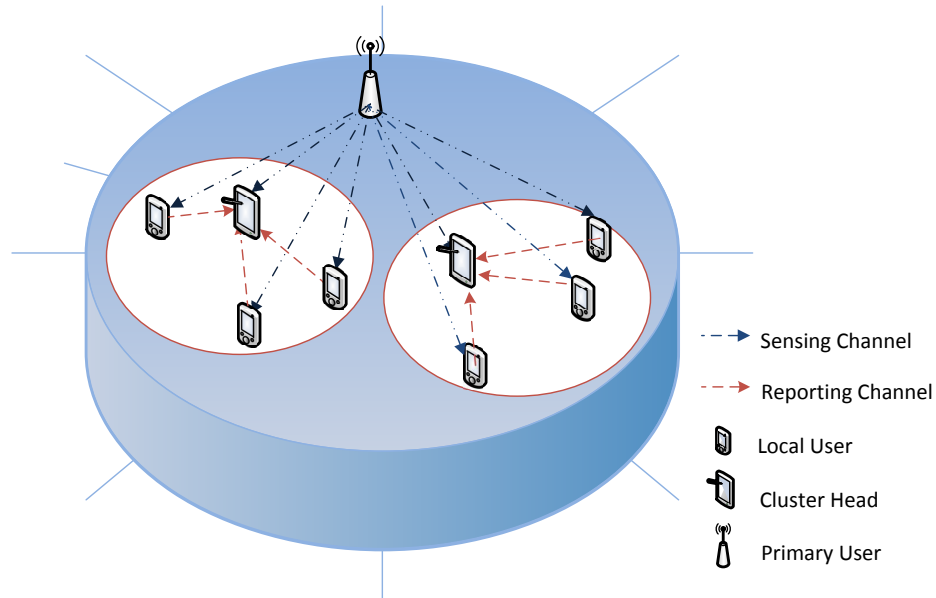


Figure 2.19: Cluster-based cooperative spectrum sensing scheme.

of users per fusion center/cluster. Fig. 2.19 depicts the cluster-based spectrum sensing scheme, where the users are grouped into subgroups called “clusters”. For each cluster (group), a cluster head is chosen to play the role of the fusion center for the cluster. This cluster head collects local decisions from the users in that cluster and then takes the “cluster decision”. Then, depending on the objective, either clusters’ decisions are forwarded to a fusion center for a global decision if a centralized decision is required or each cluster will use its decision for the users inside that cluster only.

The detection and false alarm probabilities of the cluster decision are deduced by applying the fusion probabilities using local probabilities of the users inside its cluster. Then, if a centralized decision is required, fusion center probabilities are computed based on the fusion probabilities obtained at each cluster.

In clustering, the way users are grouped has an important impact on the cooperation performance. In this study we will consider three different clustering methods as depicted in Fig. 2.20

- Clustering based on the distance to the primary user (i.e. all the users having similar distance to the primary user will be in the same cluster),

- Clustering based on the relative distance between users (i.e. close users will be grouped in the same cluster),
- Hybrid clustering strategy incorporating the two latest methods.

The fusion center for each cluster called cluster head is chosen to be the nearest secondary user to the centroid of all the users of the cluster while the global fusion center is chosen to be the nearest to the centroid of the cluster heads.

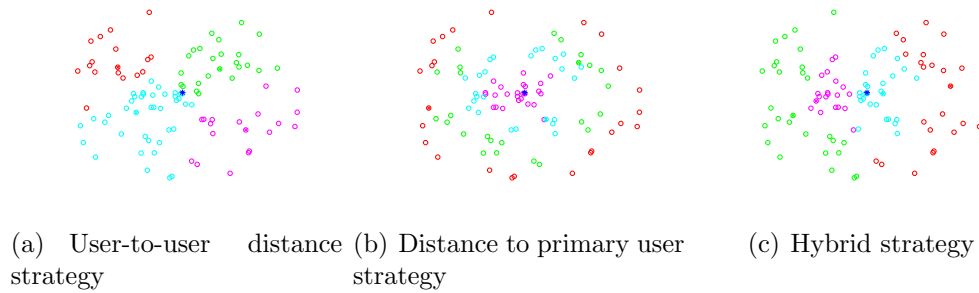


Figure 2.20: Different clustering strategies.

In Fig. 2.21, we compare the effect of the different clustering strategies on the performance of a centralized cluster-based cognitive spectrum sensing system. In this topology, user-to-user distance clustering strategy leads to the best performance. This can be explained by the fact that this clustering minimizes the distance between cooperating users. However, the distance-to-primary user strategy allows better spread of the cooperating users inside each cluster and that will enhance the local decisions variability (allows to avoid shadowing) but a higher reporting energy is needed for cooperation.

2.5 Conclusion

In this chapter we studied the performance of cooperative spectrum sensing under imperfect reporting channels and non-identical average SNRs. The main contribution of this chapter is the derivation of closed-form expressions of average probabilities

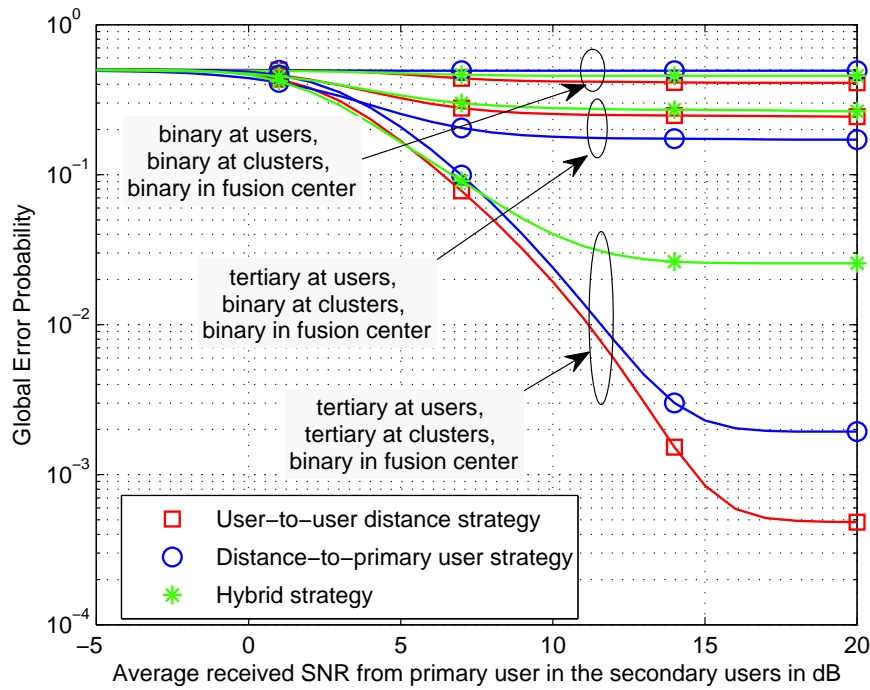


Figure 2.21: Comparison between the clustering strategies on performance of cluster-based spectrum sensing.

of detection and false-alarm considering independent but non-identically distributed Nakagami- m fading for the sensing and reporting channels. This performance analysis allowed us to conclude the effect of the reporting local decisions imperfectness on global spectrum sensing performance. Different cooperation schemes were studied for reporting local decisions: 1) The classic hard binary decision, 2) The tertiary (censored) decision scheme, 3) The quantized decision scheme, and 4) the soft information scheme. This study showed that although increasing the shared information helps improving the cooperation under perfect reporting assumption, the imperfect reporting affects this property and the cooperation gain decreases and can become even negative with very low reporting SNRs. The study also employed generic weighted fusion rules and via simulations we proved that an adaptive choice of the weights affected to each user's decision function of its sensing and reporting SNRs could enhance the global performance. The derived expressions are of great importance as they could

be used as inputs for optimization algorithms for system parametrization in terms of performance requirements such as available energy and tolerable probability of error. They are also easily adaptable to be applied for other network topologies such as distributed or clustered schemes and in order to optimize them.

Chapter 3

Location-based Resource Allocation

3.1 Introduction

Optimizing the allocation of available resources is an important task in communication systems in order to maximize the profit. In particular, for cognitive radios systems, this step becomes primordial due to the specificity of these systems characterized by the rapid change of available opportunities. An extensive research has been performed for cognitive radio networks [41, 42, 43]. Many of them assume that the instantaneous channel gain or the channel state information (CSI) of the interference links from secondary transmitters to primary receivers is available. However, since primary users need to be oblivious to secondary users, CSI estimation of the interference links at the primary receivers is generally not possible. Furthermore, it is impractical in cognitive radio systems to assume that primary users send feedbacks to secondary users.

Without the CSI of the interference links, secondary transmitters can not estimate the potential interference at primary users. Therefore, it is not possible to share the frequency bands used by the primary users but must avoid transmission over those frequency bands which will lead to an inefficient system (very low capacity). However,

if the interference at the primary users can be estimated by a certain method, then the secondary users can use some interference-free transmit power and share the frequency bands that are being occupied by the primary users, which allows a more efficient use of the spectrum. As such, it is of paramount importance to estimate the interference caused to the primary users under the condition of no CSI of the interference links and further perform resource allocation to maximize the system capacity of the secondary network. In line with this, [44] proposes a power allocation algorithm that requires the statistics not instantaneous CSI of the interference link in OFDM based cognitive radio systems. [45] considers a scenario where only some primary users' CSI is available at the secondary transmitter and proposes an allocation algorithm based on rate loss constraint. In [46], the authors propose a power allocation algorithm based on the mean value of the channel gain of the interference link.

Location information represents a solution to this problem. Indeed, secondary users will use it to estimate the interference they may cause to the primary users as function of their transmitted power based on a pathloss and shadowing model. Unlike the channel state information, location information is easier to obtain with the evolution and spread of localization features such as global positioning system (GPS). Thus, in this chapter, we introduce a resource allocation algorithm cognitive radio systems which uses location information of the primary and secondary users instead of the channel state information of the interference link.

The remainder of this chapter is organized as follows. Section 3.2 we introduce the system model. In section 3.3, we detail how to estimate interference from location information. In section 3.4, we study the resource allocation problem for downlink and uplink scenarios. For each of them, we formulate the optimization problems, solve them analytically using Lagrange technique, and propose adequate resource allocation algorithms in addition to adapted algorithms for more practical implementations such as discrete rate and collocated channels allocation. Finally, in section 3.5 numerical

results are presented and discussed to deduce algorithms performance. Conclusions are drawn in section 3.6.

3.2 System Model

Consider Orthogonal Frequency-Division Multiple Access (OFDMA) based cellular cognitive radio network that consist of a secondary base station (single cell environment) and K secondary users who aim to opportunistically use the spectrum occupied by the primary users without causing a harmful interference. For the primary users, we consider the general case (i.e. not necessarily cellular network). Without loss of generality, we suppose that there are N primary users occupying the subchannels to be shared by the secondary network (i.e., more than one primary user could be using the same subchannel).

We assume that the subchannels are orthogonal and the transmission is omnidirectional. We assume also that the primary users operate in a time division duplex (TDD) mode, where the same frequency band is used for transmission and reception, and the cognitive networks use OFDMA with L subchannels and a wider system bandwidth than that of the primary users due to the interference mitigation based on frequency diversity and the capability of a selective use of unoccupied subchannels by the primary users, where subchannel is defined as a group of subcarriers.

Interference temperature is defined as the radio frequency (RF) power measured at a receiving antenna per unit bandwidth and indicates the tolerable interference level at the primary user [5]. Due to heterogeneity of the primary users, the interference temperature may vary depending on the user, and for the same user, depending on the subchannel. We denote $\mathcal{I}_{n,i}^{thresh}$ the maximum amount of interference allowed by the primary user n in the subchannel i .

3.3 Estimating Interference from Location Information

Location awareness [47] has realized huge advancements in the cellular networks during the last years due to the emergence of more accurate and faster algorithms which benefit from cooperation techniques (triangulation) [48, 49]. In cognitive radios, location information represents a great opportunity for system optimization in various aspects such as:

- performing more precise measurements of the spectrum occupancy even with a less frequent spectrum sensing,
- determining the minimum transmit power level for a reliable link between the secondary users,
- determining angle of arrival/departure toward primary users from the viewpoint of secondary users and use beam forming techniques to reduce the interference to the primary users if multiple antennas are available,
- optimizing the cognitive radio networks in order to maximize the spectrum usage and the spatial reuse,
- constructing the optimal secondary network topology based on the given primary networks,
- performing more accurate spectrum sensing by adjusting the detection threshold and an estimation of the pathloss exponent that enables a precise interference control within resource allocation algorithms.

Among the mentioned benefits, we will focus on how the relative location between the primary and secondary users can be exploited for resource allocation in cognitive radio networks under pathloss and log-normal shadowing. Indeed, secondary users use

the location information to estimate the pathloss to the primary users, which lead to the evaluation of the interference at the primary users as a function of the transmitted power. Then, the cognitive system determine the maximum interference-free transmit power while sharing the frequency bands with primary users.

Location of each secondary user may be determined autonomously using GPS or estimated based on power measurement of pilot signals from the surrounding beacons. For the primary user, if the location information can not be delivered, a variety of localization techniques are introduced in the literature (see [48, 49, 50] and the references therein). Most of these works are based on a cooperative estimation of multiple secondary users based on a receive power measurement and a triangulation technique.

3.3.1 Interference Estimation using Location Information

Consider a 2-dimensional horizontal plane (no height elevation). Let $\{x_n^{(p)}, y_n^{(p)}\}$ denote the location of the n^{th} primary user ($1 \leq n \leq N$), $\{x_k^{(c)}, y_k^{(c)}\}$ the location of the secondary user k ($1 \leq k \leq K$), and $\{x_0^{(c)}, y_0^{(c)}\}$ the location of the secondary base station, respectively.

Consider log-distance pathloss model where the received power can be written as

$$P_{rx}(d) = \frac{P_{tx} \xi 10^{0.1X}}{d^\eta}, \quad (3.1)$$

where

- η is the pathloss exponent,
- d is the distance between the transmitter and the receiver,
- ξ is the pathloss in a reference distance (1 km) with transmit and receive antenna gains and effect of wavelength,

- $10^{0.1X}$ is a log-normal shadowing where X is a Gaussian random variable with zero mean and variance σ_x^2 .

We assume that the measured symbols are averaged out to remove the small-scale fading effect.

When log-normal shadowing is present, the interference constraint at the primary user is satisfied in a probabilistic manner. In order to avoid causing a harmful interference at the primary user under log-normal shadowing, we adjust the original interference temperature such that the probability of the interference constraint violation is bounded by a probability of our choice p_ϵ . A lower p_ϵ results in a lower adjusted interference temperature, which is more conservative way of protecting the primary user. Thus, we formulate the following:

$$\Pr \left[10 \log P_{rx}(d) > 10 \log \mathcal{I}^{thresh} \right] \leq p_\epsilon, \quad (3.2)$$

where \mathcal{I}^{thresh} is the maximum interference level tolerable by the primary user.

Substituting (3.1) into (3.2) and using the fact that $\Pr[X > \gamma] = Q(\gamma)$ for Normal distribution, where $Q(\cdot)$ is the Gaussian-Q function, we get

$$\frac{P_{tx}\xi}{d^\eta} = \frac{\mathcal{I}^{thresh}}{10^{\frac{\sigma_x Q^{-1}(p_\epsilon)}{10}}}. \quad (3.3)$$

From (3.3), we can find the secondary transmitter's maximum transmit power that obeys the interference constraint with a probability $(1 - p_\epsilon)$ when log-normal shadowing is present.

To simplify, we denote $\tilde{\mathcal{I}}^{thresh} = \frac{\mathcal{I}^{thresh}}{10^{(\sigma_x Q^{-1}(p_\epsilon)/10)}}$ the effective threshold, and thus (3.3) can be rewritten as:

$$\frac{P_{tx}\xi}{d^\eta} = \tilde{\mathcal{I}}^{thresh}. \quad (3.4)$$

3.3.2 Interference Constraint in the Cognitive System

Downlink

The distance between the secondary base station and the primary user n can be written as

$$d_{0,n} = \sqrt{(x_0^{(c)} - x_n^{(p)})^2 + (y_0^{(c)} - y_n^{(p)})^2}, \quad 1 \leq n \leq N. \quad (3.5)$$

Given the knowledge of $d_{0,n}$, the interference power at the primary user n for the subchannel i based on the pathloss model in (3.1) is given by:

$$\sum_{k=1}^K a_{k,i} b_{n,i} \frac{p_{k,i} \xi}{d_{0,n}^\eta} \leq \tilde{\mathcal{I}}_{n,i}^{thresh}, \quad 1 \leq i \leq L, \quad 1 \leq n \leq N. \quad (3.6)$$

where:

- $\mathbf{A} \in \{0, 1\}^{K \times L}$ is the subchannel allocation matrix for secondary users showing that the i^{th} subchannel is allocated to the user k if $a_{k,i} = 1$.
- $\mathbf{B} \in \{0, 1\}^{N \times L}$ is the subchannel allocation matrix for the primary users. We assume that \mathbf{B} is known by spectrum sensing [48].
 - If $b_{n,i} = 1$, then the i^{th} subchannel is being used by the primary user n and thus the secondary users may use it but under the interference constraint $\tilde{\mathcal{I}}_{n,i}^{thresh}$.
 - If $b_{n,i} = 0$, the primary user n is not using the subchannel i . Thus, if $b_{n,i} = 0$, $\forall n \in \{1, \dots, N\}$, then the secondary users can use this subchannel without any interference constraint.
- $p_{k,i}$ denote the allocated power by the secondary base station to the secondary user k on the i^{th} subchannel in case of downlink or the transmitted power by the secondary user k on the i^{th} subchannel in case of uplink.

Uplink

The distance between the secondary user k and the primary user n can be computed as

$$d_{k,n} = \sqrt{(x_n^{(p)} - x_k^{(c)})^2 + (y_n^{(p)} - y_k^{(c)})^2}, \quad 1 \leq k \leq K, 1 \leq n \leq N. \quad (3.7)$$

Similar to the downlink case, the interference power at the primary user n due to the uplink signal from the secondary user k can be modeled by

$$\sum_{k=1}^K a_{k,i} b_{n,i} \frac{p_{k,i} \xi}{d_{k,n}^\eta} \leq \tilde{I}_{n,i}^{thresh}, \quad 1 \leq i \leq L, 1 \leq n \leq N. \quad (3.8)$$

The pathloss exponent η is assumed to be the same for both downlink and uplink.

3.4 Resource Allocation Algorithms based on Location Information

3.4.1 Downlink

Problem Formulation

Our goal is for the secondary base station to allocate the given power and subchannels to secondary users in order to maximize the sum rate under the following constraints:

- No inter-secondary user interference : each subchannel can be allocated to at maximum one secondary user,
- Total power constraint: the secondary base station has a limited power budget,
- Interference constraint: secondary users can use the subchannels being occupied by the primary users as long as the interference constraint at the primary users is met.

This can be mathematically written as

$$\begin{aligned}
& \underset{\substack{a_{k,i} \in \{0,1\} \\ p_{k,i} \geq 0}}{\text{Maximize}} && \sum_{k=1}^K \sum_{i=1}^L a_{k,i} \log_2 \left(1 + \frac{|h_{k,i}|^2 p_{k,i}}{N_o} \right) \\
& \text{subject to} && \sum_{k=1}^K a_{k,i} \leq 1, \quad 1 \leq i \leq L, \\
& && \sum_{k=1}^K \sum_{i=1}^L a_{k,i} p_{k,i} \leq P_{tot}, \\
& && \sum_{k=1}^K a_{k,i} b_{n,i} \frac{p_{k,i} \xi}{d_{0,n}^\eta} \leq \tilde{\mathcal{I}}_{n,i}^{thresh}, \quad 1 \leq i \leq L, \quad 1 \leq n \leq N,
\end{aligned} \tag{3.9}$$

Analytic Solution

Using the Lagrange multiplier technique, (3.9) is formulated as

$$\begin{aligned}
\mathcal{L} = & \sum_{k=1}^K \sum_{i=1}^L a_{k,i} \log_2 \left(1 + \frac{|h_{k,i}|^2 p_{k,i}}{N_o} \right) \\
& + \sum_{n=1}^N \sum_{i=1}^L \lambda_{n,i} \left(\tilde{\mathcal{I}}_{n,i}^{thresh} - \sum_{k=1}^K a_{k,i} b_{n,i} \frac{p_{k,i} \xi}{d_{0,n}^\eta} \right) \\
& + \rho_0 \left(P_{tot} - \sum_{k=1}^K \sum_{i=1}^L a_{k,i} p_{k,i} \right),
\end{aligned} \tag{3.10}$$

where $\lambda_{n,i}$ and ρ_0 are Lagrangian coefficients. The Karush-Kuhn-Tucker (KKT) conditions [51] are listed as

$$\frac{a_{k,i} |h_{k,i}|^2}{N_o + |h_{k,i}|^2 p_{k,i}} - a_{k,i} \sum_{n=1}^N b_{n,i} \frac{\lambda_{n,i} \xi}{d_{0,n}^\eta} - a_{k,i} \rho_0 = 0, \tag{3.11a}$$

$$\lambda_{n,i} \left(\tilde{\mathcal{I}}_{n,i}^{thresh} - \sum_{k=1}^K a_{k,i} b_{n,i} \frac{p_{k,i} \xi}{d_{0,n}^\eta} \right) = 0, \tag{3.11b}$$

$$\rho_0 \left(P_{tot} - \sum_{k=1}^K \sum_{i=1}^L a_{k,i} p_{k,i} \right) = 0. \tag{3.11c}$$

Even though the above problem is in the form of mixed-integer programming

problem, which is in general NP-hard, a simple two-step approach provides the maximum capacity thanks to the fairness of the constraints regarding the different users. In fact, allocating the power to a user k_1 or k_2 will have the same contribution on the saturation of the total power and interference constraints (note that in the downlink case, the interference constraint depends only on the distance from the base station to the primary users and the total power budget is the budget of the base station). Thus, the only factor that will decide on the subchannel allocation is the contribution in the total capacity. Then, we allocate each subchannel to the secondary user with the maximum SNR for that subchannel. Thus, the subchannel allocation index for secondary users is simply given as $a_{k,i} = 1$ for $k = k_i$, and 0 otherwise, where

$$k_i = \arg \max_{k \in [1, K]} \left\{ \frac{|h_{k,i}|^2}{N_o} \right\}, \quad 1 \leq i \leq L. \quad (3.12)$$

The interference constraint can also be simplified. In fact, for each subchannel i , the primary user n_i is the most sensitive to the power increase of secondary users, where:

$$n_i = \arg \min_{n \in b_i^{used}} \left\{ \frac{d_{0,n}^n \tilde{\mathcal{I}}_{n,i}^{thresh}}{\xi} \right\}, \quad i = 1, \dots, L, \quad (3.13)$$

with $b_i^{used} = \{n \in \{1 \dots N\} \text{ such that } b_{n,i} = 1\}$ is the set of primary users using the subchannel i . Thus the interference constraint becomes

$$\frac{p_{k_i,i} \xi}{d_{0,n_i}^n} \leq \tilde{\mathcal{I}}_{n_i,i}^{thresh}, \quad 1 \leq i \leq L. \quad (3.14)$$

The Lagrange multiplier can therefore be simplified to

$$\begin{aligned}
\mathcal{L} &= \sum_{i=1}^L \log_2 \left(1 + \frac{|h_{k_i,i}|^2 p_{k_i,i}}{N_o} \right) \\
&+ \sum_{i=1}^L \lambda_{n_i,i} \left(\tilde{\mathcal{I}}_{n_i,i}^{thresh} - \frac{p_{k_i,i} \xi}{d_{0,n_i}^\eta} \right) \\
&+ \rho_0 \left(P_{tot} - \sum_{i=1}^L p_{k_i,i} \right).
\end{aligned} \tag{3.15}$$

Thus, the KKT conditions can be rewritten as

$$\frac{a_{k,i} |h_{k,i}|^2}{N_o + |h_{k,i}|^2 p_{k,i}} - \frac{\lambda_{n_i,i} \xi}{d_{0,n_i}^\eta} - \rho_0 = 0, \tag{3.16a}$$

$$\lambda_{n_i,i} \left(\tilde{\mathcal{I}}_{n_i,i}^{thresh} - \frac{p_{k,i} \xi}{d_{0,n_i}^\eta} \right) = 0, \tag{3.16b}$$

$$\rho_0 \left(P_{tot} - \sum_{i=1}^L p_{k,i} \right) = 0. \tag{3.16c}$$

Let \mathcal{U} denote the set of unallocated subchannels and \mathcal{U}_p the set of the subchannels occupied by at least a primary user. It is assumed that \mathcal{U}_p is already known by spectrum sensing. Thus, $\mathcal{U}_c = \mathcal{U} - \mathcal{U}_p$ is the set of the interference-free subchannels. The second step, consists in solving this optimization problem. (3.16), the optimal transmit power can be obtained as

$$p_{k_i,i} = \left[\frac{d_{0,n_i}^\eta}{\lambda_{n_i,i} \xi + \rho_0 d_{0,n_i}^\eta} - \frac{N_o}{|h_{k_i,i}|^2} \right]^+, \quad 1 \leq i \leq L. \tag{3.17}$$

where $[x]^+ = \max\{x, 0\}$. From (3.11b), it is clear that $\lambda_{n_i,i} = 0$ for $i \in \mathcal{U}_c$. Therefore, (3.17) can be simplified as

$$p_{k_i,i} = \begin{cases} \left[\frac{1}{\rho_0} - \frac{N_o}{|h_{k_i,i}|^2} \right]^+, & i \in \mathcal{U}_c, \\ \min \left\{ \left[\frac{1}{\rho_0} - \frac{N_o}{|h_{k_i,i}|^2} \right]^+, \frac{\tilde{\mathcal{I}}_{n_i,i}^{thresh} d_{0,n_i}^\eta}{\xi} \right\}, & i \in \mathcal{U}_p, \end{cases} \tag{3.18}$$

Note that (3.18) is a combination of the conventional waterfilling and the cap-limited waterfilling both with the common water level $\frac{1}{\rho_0}$ which can be computed to saturate the total power and interference constraints as

$$\frac{1}{\rho_0} = \frac{1}{|\mathcal{U}|} \left(P_{tot} - \sum_{i \in \mathcal{S}_p} \frac{\tilde{\mathcal{I}}_{n_i, i}^{thresh} d_{0, n_i}^\eta}{\xi} + \sum_{i \in \mathcal{U}} \frac{N_0}{|h_{k_i, i}|^2} \right), \quad (3.19)$$

where $|\mathcal{U}|$ denotes the size (number of elements) of the set \mathcal{U} and \mathcal{S}_p is the set of the subchannels satisfying the condition: $\frac{1}{\rho_0} - \frac{N_0}{|h_{k_i, i}|^2} > \frac{\tilde{\mathcal{I}}_{n_i, i}^{thresh} d_{0, n_i}^\eta}{\xi}$.

Resource Allocation Algorithm

The power and subchannel allocation algorithm runs as follows

1. Initialize the sets $\mathcal{U} = \{1, \dots, L\}$ and $\mathcal{S}_p = \{\}$.
2. Perform the conventional water filling algorithm and compute (3.19) and $p_{k, i} = \frac{1}{\rho_0} - \frac{N_0}{|h_{k_i, i}|^2}$.
3.
 - If $\exists i \in \mathcal{U} / p_{k, i} < 0$, then $\mathcal{U} = \mathcal{U} - \{i\}$ and redo the above calculations.
 - If $\frac{p_{k, i} \xi}{d_{0, n_i}^\eta} > \tilde{\mathcal{I}}_{n_i, i}^{thresh}$ for any $i \in \mathcal{U}_p$, the allocated power will be saturated such that $p_{k, i} = \frac{\tilde{\mathcal{I}}_{n_i, i}^{thresh} d_{0, n_i}^\eta}{\xi}$. Then,
 - Remove i from \mathcal{U} and \mathcal{U}_p , and add it to \mathcal{S}_p .
 - Recalculate $\frac{1}{\rho_0}$ (water level) using (3.19).
 - Repeat the above procedure until no subchannel $i \in \mathcal{U}_p$ that satisfies $\frac{p_{k, i} \xi}{d_{0, n_i}^\eta} > \tilde{\mathcal{I}}_{n_i, i}^{thresh}$ is found.

This procedure is detailed in Algorithm 1.

Algorithm 1 Optimal Downlink Resource Allocation

Require: $\{h_{k,i}\}_{\substack{1 \leq k \leq K \\ 1 \leq i \leq L}}, P^{tot}, \tilde{\mathcal{I}}^{thresh}, \{d_{0,n}\}_{1 \leq n \leq N}, \eta, \xi, N_o.$

$$p_{k,i} \leftarrow 0, \quad g_{k,i} \leftarrow \frac{N_o}{|h_{k,i}|^2}, \quad \forall k \in [1, K], \forall i \in [1, L]$$

$$k_i \leftarrow \arg \max_{k \in [1, K]} \{g_{k,i}\}, \quad \forall i \in [1, L],$$

$$a_{k,i} \leftarrow 0, \quad \forall k \in [1, K], \quad a_{k_i, i} = 1, \quad \forall i \in [1, L],$$

$$\mathbf{G} \leftarrow \{g_{1, k_1}, \dots, g_{L, k_L}\},$$

$$\mathbf{P}^{max} \leftarrow \{p_1^{max}, \dots, p_L^{max}\}, \quad \text{where}$$

$$p_i^{max} \leftarrow \min_{n \in [1, N] / b_{n, i} = 1} \left\{ \frac{\tilde{\mathcal{I}}_{n, i}^{thresh} \times d_{0, n}^\eta}{\xi} \right\}, \quad \forall i,$$

$$\mathbf{P}^{vec} \leftarrow \text{Algorithm 2} (\mathbf{G}, \mathbf{P}^{max}, P^{tot})$$

$$p_{k_i, i} \leftarrow p_i^{vec}, \quad \forall i \in [1, L],$$

$$\text{return } \{a_{k,i}\}_{\substack{1 \leq k \leq K \\ 1 \leq i \leq L}}, \{p_{k,i}\}_{\substack{1 \leq k \leq K \\ 1 \leq i \leq L}}.$$

Algorithm 2 Cap-limited Waterfilling ($\mathbf{G}, \mathbf{P}^{max}, P^{tot}$)

Require: $\mathbf{G}, \mathbf{P}^{max}, P^{tot}.$

$$\mathbf{U} \leftarrow \{1, \dots, L\}, \quad N_s \leftarrow L, \quad p_t \leftarrow 0,$$

while ($|P - p_t| > \epsilon$ **and** $N_s > 0$) **do**

$$V_1 \leftarrow \min_{i \in \mathbf{U}} \left\{ g_i + \frac{P^{tot} - p_t}{N_s} \right\}, \quad V_2 \leftarrow \min_{i \in \mathbf{U}} \{g_i + p_i^{max}\}$$

$$V \leftarrow \min(V_1, V_2)$$

$$w_i \leftarrow \max(V - g_i, 0), \quad g_i \leftarrow g_i + w_i, \quad \forall i$$

$$p_i \leftarrow p_i + w_i, \quad p_i^{max} \leftarrow p_i^{max} - w_i, \quad \forall i$$

$$p_t \leftarrow p_t + \sum_{i=1}^L w_i, \quad \mathbf{U} \leftarrow \arg_i (p_i^{max} > \epsilon), \quad N_s \leftarrow |\mathbf{U}|$$

end while

$$\text{return } \mathbf{P}^{vec} \leftarrow \{p_1, \dots, p_L\}$$

3.4.2 Uplink

Problem Formulation

The objective is to maximize the sum rate under the individual secondary user power constraint. The problem is formulated in this case as

$$\begin{aligned}
& \underset{\substack{a_{k,i} \in \{0,1\} \\ p_{k,i} \geq 0}}{\text{Maximize}} && \sum_{k=1}^K \sum_{i=1}^L a_{k,i} \log_2 \left(1 + \frac{|h_{k,i}|^2 p_{k,i}}{N_o} \right) \\
& \text{subject to} && \sum_{k=1}^K a_{k,i} \leq 1, \quad 1 \leq i \leq L, \\
& && \sum_{k=1}^K \sum_{i=1}^L a_{k,i} p_{k,i} \leq P_k, \quad 1 \leq k \leq K, \\
& && \sum_{k=1}^K a_{k,i} b_{n,i} \frac{p_{k,i} \xi}{d_{k,n}^\eta} \leq \tilde{\mathcal{I}}_{n,i}^{thresh}, \quad 1 \leq i \leq L, \quad 1 \leq n \leq N,
\end{aligned} \tag{3.20}$$

where P_k is the transmit power budget for secondary user k .

The constraints are similar to the downlink case except the total power constraint which is replaced by an individual power constraint for each secondary user k .

Analytic Solution

We start by simplifying the problem by selecting for each secondary user, the most sensitive primary user in each used subchannel. Similarly to the downlink case, this user can be determined from the interference constraint as:

$$n_{k,i} = \arg \min_{n \in b_i^{used}} \left\{ \frac{d_{k,n}^\eta \tilde{\mathcal{I}}_{n,i}^{thresh}}{\xi} \right\}, \quad 1 \leq k \leq K, \quad 1 \leq i \leq L. \tag{3.21}$$

Using the Lagrangian and KKT conditions, the optimal transmit power can be

obtained as

$$p_{k_i,i} = \left[\frac{d_{k_i,n_{k_i,i}}^\eta}{\lambda_i \xi + \rho_{k_i} d_{k_i,n_{k_i,i}}^\eta} - \frac{N_o}{|h_{k_i,i}|^2} \right]^+, \quad 1 \leq i \leq L. \quad (3.22)$$

which can be simplified as

$$p_{k_i,i} = \begin{cases} \left[\frac{1}{\rho_{k_i}} - \frac{N_o}{|h_{k_i,i}|^2} \right]^+, & i \in \mathcal{U}_c, \\ \min \left\{ \left[\frac{1}{\rho_{k_i}} - \frac{N_o}{|h_{k_i,i}|^2} \right]^+, \frac{\tilde{\mathcal{I}}_{n_{k_i,i},i}^{thresh} d_{k_i,n_{k_i,i}}^\eta}{\xi} \right\}, & i \in \mathcal{U}_p. \end{cases} \quad (3.23)$$

Resource Allocation Algorithm

Unlike the downlink case, it is not optimal in the uplink case to separate subchannel and power allocations due to the per-user power constraint. In order to solve the problem with a reduced complexity, we propose an algorithm that runs a per-subchannel two-step procedure of user selection and power allocation for all the subchannels one after another. A brief description of the procedure is given in what follows.

1. Initialize $\mathcal{U} = \{1, \dots, L\}$, $\mathcal{U}_k = \{1, \dots, L\}$ and $\mathcal{S}_k = \{\}$, $\forall k$, where \mathcal{U}_k and \mathcal{S}_k are the set of the unallocated subchannels for the user k and the set of the subchannels that their allocated power should be capped due to interference constraint, respectively.
2. Run the waterfilling algorithm over the available subchannels for each user independently. The water level for secondary user k is shown as

$$\frac{1}{\rho_k} = \frac{1}{|\mathcal{U}_k|} \left(P_k - \sum_{i \in \mathcal{S}_k} \frac{\tilde{\mathcal{I}}_{n_{k,i},i}^{thresh} d_{k,n_{k,i}}^\eta}{\xi} + \sum_{i \in \mathcal{U}_k} \frac{N_o}{|h_{k,i}|^2} \right). \quad (3.24)$$

For each user k , if $i \in \mathcal{U}_p$ and $p_{k,i} > \frac{\tilde{\mathcal{I}}_{n_{k,i},i}^{thresh} d_{k,n_{k,i}}^\eta}{\xi}$, then $p_{k,i} = \frac{\tilde{\mathcal{I}}_{n_{k,i},i}^{thresh} d_{k,n_{k,i}}^\eta}{\xi}$ and $\mathcal{S}_k = \mathcal{S}_k + \{i\}$.

3. Compute the capacity for each subchannel and user as

$$C_{k,i} = \log_2 \left(1 + \frac{p_{k,i} |h_{k,i}|^2}{N_o} \right), \quad (3.25)$$

and then select the pair with the highest capacity as $\{k_i^*, i^*\} = \arg \max_{k,i \in \mathcal{U}} C_{k,i}$.

4. Allocate the i^* th subchannel to the user k_i^* ($a_{k_i^*, i^*} = 1$).

5. Remove this subchannel from the sets $\mathcal{U} = \mathcal{U} - \{i^*\}$ and $\mathcal{U}_k = \mathcal{U}_k - \{i^*\}$, where $k = 1, \dots, i^* - 1, i^* + 1, \dots, K$.

6. Repeat the above procedure until \mathcal{U} is empty.

This procedure is detailed in Algorithm 3.

Algorithm 3 Proposed Uplink Resource Allocation

Require: $\{h_{k,i}\}_{\substack{1 \leq k \leq K \\ 1 \leq i \leq L}}, \{P_k^{user}\}_{1 \leq k \leq K}, \tilde{\mathcal{I}}^{thresh}, \{d_{k,n}\}_{\substack{1 \leq k \leq K \\ 1 \leq n \leq N}}, \eta, \xi, N_o$.

$$a_{k,i} \leftarrow 1, \quad g_{k,i} \leftarrow \frac{N_o}{|h_{k,i}|^2}, \quad \forall k \in [1, K], \forall i \in [1, L]$$

while $\prod_{i=1}^L \sum_{k=1}^K a_{k,i} \neq 1$ **do**

for $k = 1$ to K **do**

$$\mathbf{G} \leftarrow \{g_{k,1}, \dots, g_{k,L}\},$$

$$\mathbf{P}_k^{max} \leftarrow \{p_{k,1}^{max}, \dots, p_{k,L}^{max}\} \text{ where}$$

$$p_{k,i}^{max} \leftarrow \min_{n \in [1, N] / b_{n,i}=1} \left\{ \frac{\tilde{\mathcal{I}}^{thresh} \times d_{k,n}^\eta}{\xi} \right\}, \forall i,$$

$$\mathbf{P}_k \leftarrow \text{Algorithm 2} (\mathbf{G}, \mathbf{P}_k^{max}, P_k^{user}),$$

end for

$$C_{k,i} = \log_2 \left(1 + \frac{p_{k,i}}{g_{k,i}} \right), \quad \forall k, \forall i$$

$$k^*, i^* \leftarrow \arg \max_{k,i} C_{k,i}$$

$$a_{j,i^*} \leftarrow 0, \quad \forall j \in [1, K], \quad a_{k^*, i^*} \leftarrow 1$$

end while

return $\{p_{k,i}\}_{\substack{1 \leq k \leq K \\ 1 \leq i \leq L}}, \{a_{k,i}\}_{\substack{1 \leq k \leq K \\ 1 \leq i \leq L}}$.

Notice that, unlike the downlink case, the user with the maximum SNR for a subchannel can not always offer the highest rate in the uplink case. Therefore, to

maximize the capacity, each subchannel needs to be allocated into the secondary user with the highest capacity for the subchannel.

3.4.3 Practical Implementation Algorithms for Resource Allocation

Collocated Subchannels Allocation

Assuming consecutive subchannels are allocated for each secondary user, we can formulate the optimization problem for the uplink scenario as

$$\begin{aligned}
& \underset{\substack{a_{k,i} \in \{0,1\} \\ p_{k,i} \geq 0}}{\text{Maximize}} && \sum_{k=1}^K \sum_{i=1}^L a_{k,i} \log_2 \left(1 + \frac{|h_{k,i}|^2 p_{k,i}}{N_o} \right) \\
& \text{subject to} && \sum_{k=1}^K a_{k,i} \leq 1, \quad 1 \leq i \leq L, \\
& && \sum_{k=1}^K \sum_{i=1}^L a_{k,i} p_{k,i} \leq P_k, \quad 1 \leq k \leq K, \\
& && \sum_{k=1}^K a_{k,i} b_{n,i} \frac{p_{k,i} \xi}{d_{k,n}^\eta} \leq \tilde{\mathcal{I}}_{n,i}^{thresh}, \quad 1 \leq i \leq L, \quad 1 \leq n \leq N, \\
& && \mathcal{U}_k = \{u_k^{(1)}, \dots, u_k^{(1)} + u_k^{(w)} - 1\}, \quad 1 \leq k \leq K,
\end{aligned} \tag{3.26}$$

where \mathcal{U}_k is the set of allocated subchannels for the secondary user k.

Since each secondary user is allocated with consecutive subchannels, \mathcal{U}_k can be characterized by the start subchannel index $u_k^{(1)}$ and the number of subchannels $u_k^{(w)}$.

The optimization problem in (3.26) is similar to the uplink problem proposed in (3.20) with an additional constraint of consecutive subchannel allocation. In order to solve the problem with a reduced complexity, we propose an algorithm that runs a per-subchannel two-step procedure of user selection and power allocation for all the subchannels one after another. A brief description of the algorithm is given as follows:

1. Construct a capacity matrix $\mathbf{C} = \{c_{k,i}\}^{K \times L}$, where row is the user index and column is the subchannel index, and a validity indication matrix $\mathbf{V} = \{v_{k,i}\}^{K \times L}$ and initialize all the elements as valid ($v_{k,i} = 1, \forall k, \forall i$).
2. Each user runs an individual cap-limited waterfilling and compute \mathbf{C} such that $c_{k,i} = \log_2(1 + \frac{|h_{k,i}|^2 p_{k,i}}{N_o})$.
3. Find the element with the highest capacity among the valid elements in the validity indication matrix, i.e., $\{k^*, i^*\} = \arg \max_{k,i} v_{k,i} c_{k,i}$.
4. Check if the user k^* already has other allocated subchannel(s). If so, go to 5, otherwise, proceed to 6.
5. Check if the subchannel i^* is adjacent to the already allocated subchannels for the user k^* . If so, proceed to 6, otherwise, the subchannel i^* can not be allocated to the user k^* . So mark the subchannel i^* is invalid for the user k^* , i.e., $v_{k^*,i^*} = 0$, and go back to 3 (find the next highest element).
6. Allocate the subchannel i^* to the user k^* and put $v_{k,i^*} = 0$ for $1 \leq k \leq K$ and $k \neq k^*$.
7. Check if the surrounding (left and right) elements are invalid, i.e., $v_{k^*,i^*+1} = 0$ or $v_{k^*,i^*-1} = 0$. If they are invalid, then change them as valid.
8. Go back to 2 and repeat until all the subchannels are allocated.

Fixed Power Allocation

For practical implementations, it is more convenient to allocate the same power for all subchannels. In this subsection, we will propose an approach to search for the

optimal power in the downlink case. The optimization problem is reformulated as:

$$\begin{aligned}
& \underset{\substack{a_{k,i} \in \{0,1\} \\ p \geq 0}}{\text{Maximize}} && \sum_{k=1}^K \sum_{i=1}^L a_{k,i} \log_2 \left(1 + \frac{|h_{k,i}|^2 p}{N_o} \right) \\
& \text{subject to} && \sum_{k=1}^K a_{k,i} \leq 1, \quad 1 \leq i \leq L, \\
& && \sum_{k=1}^K \sum_{i=1}^L a_{k,i} \leq \frac{P_{tot}}{p}, \\
& && \sum_{k=1}^K a_{k,i} b_{n,i} \frac{p \xi}{d_{0,n}^\eta} \leq \tilde{\mathcal{I}}_{n,i}^{thresh}, \quad 1 \leq i \leq L, \quad 1 \leq n \leq N,
\end{aligned} \tag{3.27}$$

The optimal power is obtained as

$$p^* = \min \left[\frac{P_{tot}}{|U^*|}; \min_{i \in U^*} \left\{ \tilde{\mathcal{I}}_{n_i,i}^{thresh} \frac{d_{0,n_i}^\eta}{\xi} \right\} \right]; \tag{3.28}$$

where U^* is the set of the used subchannels by the secondary users. The problem is how to determine the optimal set. For that, after determining the most sensitive primary user and the best secondary user per subchannel as in the general case, we sort the subchannels by decreasing order of SNR. Then we initialize this set as $\{1, \dots, L^*\}$ where

$$L^* = \arg \max_l \sum_{i=1}^l a_{k_i,i} \log_2 \left(1 + \frac{|h_{k_i,i}|^2 p_l^*}{N_o} \right). \tag{3.29}$$

This initialization considers that the interference is uniform for all subchannels. Since the threshold is variable, it can affect the chosen power and thus decrease the total capacity. For that, is the optimal power is selected to saturate the interference in one of the subchannels, we try to remove it from the set of eligible subchannels, redetermine the optimal L^* and p^* , and recompute the total capacity. If it is better than the previous capacity, we save this change and we repeat the previous test. We keep testing until the optimal power is not an interference cap or the remove of the subchannel does not improve the capacity.

For the uplink scenario, we use the same procedure for each user then we insert it in the iterative procedure described in the algorithm (3).

Discrete Rate Allocation

Since it is more interesting to see integer bit allocations in practice, the original allocated power is reduced to the one that results in the nearest inferior integer bits for each subchannel. Then, the total remaining power is redistributed in order to maximize the number of total allocated bits.

In both downlink and uplink cases, for integer-bit allocation, the power allocated for each subchannel is adjusted as

$$p'_{k_i,i} = \frac{N_0}{|h_{k_i,i}|^2} (2^{r_{k_i,i}} - 1), \quad (3.30)$$

where $r_{k_i,i} = \lfloor \log_2(1 + \frac{|h_{k_i,i}|^2 p_{k_i,i}}{N_0}) \rfloor$. Thus, the power remaining unused is

$$P^- = P_{tot} - \sum_{i=1}^L p'_{k_i,i}, \quad (3.31)$$

which is redistributed by the greedy algorithm as follows. For each subchannel i , calculate the amount of power needed to allocated one more bit as

$$p_i^+ = p''_{k_i,i} - p'_{k_i,i} = \frac{N_0}{|h_{k_i,i}|^2} 2^{r_{k_i,i}}, \quad (3.32)$$

where $p''_{k_i,i} = \frac{N_0}{|h_{k_i,i}|^2} (2^{r_{k_i,i}+1} - 1)$. In order to redistribute the remaining power, we start from the subchannel that requires the minimum additional power to increment the allocated bits (to the next integer value) while verifying that the power budget and the interference constraints are not violated. Thus, the subchannel that requires

the minimum power for an additional bit is given as

$$n_{\min} = \arg \min_i p_i^+, \quad (3.33)$$

which is equivalent to finding the best subchannel (the one with the highest channel gain) among those subchannels with the lowest allocated bits and is given as

$$n_{\min} = \arg \max_{i \in \mathcal{S}} |h_{k_i, i}|, \quad (3.34)$$

where \mathcal{S} is the set of the subchannel indices with the minimum $r_{k_i, i}$. For the subchannels $i \in \mathcal{U}_c$, or the subchannels $i \in \mathcal{U}_p$ satisfying $p_{k_i, i} + p_i^+ \leq \frac{\tilde{\mathcal{I}}_{n_i, i}^{thresh} d_{0, n_i}^\eta}{\xi}$, update $p_{k_i, i} = p_{k_i, i} + p_i^+$ and $P^- = P^- - p_i^+$. For other subchannels i , no additional power can be allocated. Then, $\mathcal{S} = \mathcal{S} - i$. Repeat the above power redistribution procedure until $P^- - p_i^+ < 0$ and then finally distribute the remaining power equally over all the subchannels.

3.5 Simulation Results

Extensive simulations were performed, where the cognitive radio system composed of $K = 20$ secondary users is assumed to have a total of $L = 64$ subchannels shared with $N = 10$ primary users. The base station transmit power budget is $P_{tot} = 20$ dBm and the user transmit power budget of $P_k = 3$ dBm. We consider two different threshold levels ($\mathcal{I}_{n, i}^{thresh}$) of -110 dBm and -130 dBm, affected randomly to users and subchannels. We generate the secondary users' locations randomly inside the circle of radius 1 km while the primary users are located randomly inside a circle of radius D_{max} which will be variable in our simulations.

For performance comparison, two extreme scenarios are considered.

- **OFDMA:** it corresponds to absence of primary users. Thus the cognitive users

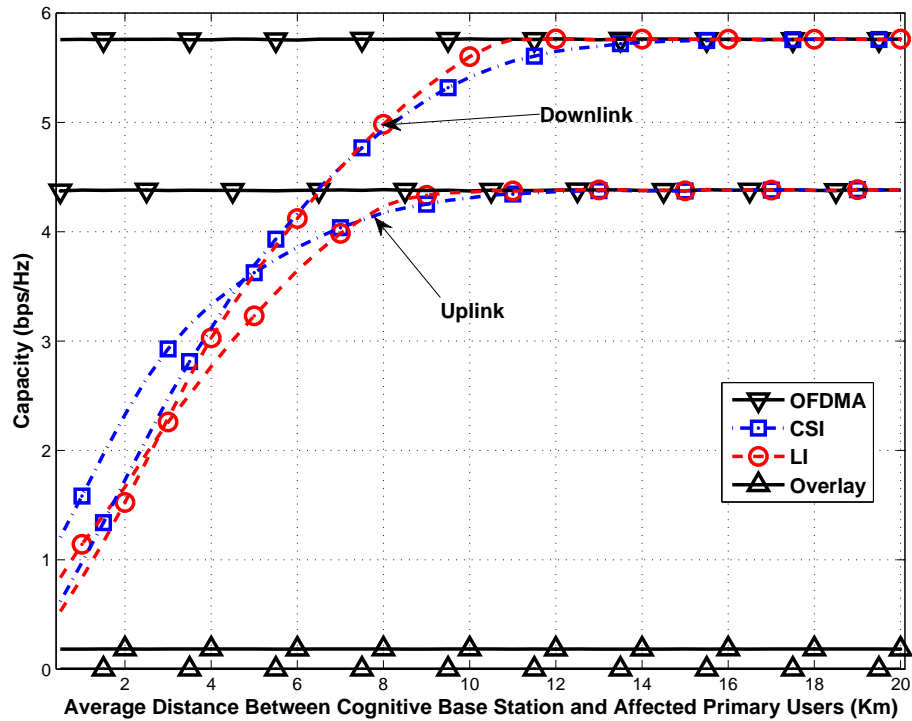


Figure 3.1: Effect of the location information use instead of the channel state information on the total capacity of the network.

are free to allocate their resources in the subchannels without any concern for the interference.

- **Overlay:** in this scenario, no interference with primary users is allowed. The cognitive users can only use the totally free subchannels (i.e. not used by primary users).

3.5.1 Effect of the Use of Location Information

In Fig. 3.1, we show the effect of the use of location information (LI) instead of the CSI. Remarking that the loss of capacity is acceptable, we conclude that the used approximation is valid knowing that the CSI are in practical impossible to obtain.

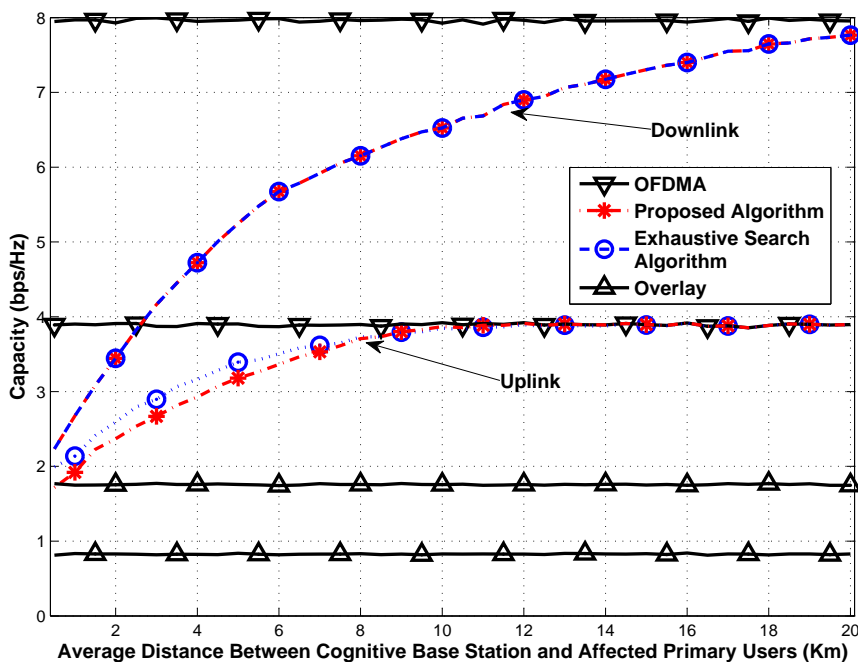


Figure 3.2: Comparison between the total capacity obtained using the proposed algorithm and the exhaustive search algorithm.

3.5.2 Optimality of the Proposed Algorithms

In Fig. 3.2, we show the efficiency of the proposed algorithms by comparing them to the Exhaustive Search algorithms. In fact, for the downlink case, the proposed algorithm is exactly superposed with the Exhaustive search which shows its optimality. For the uplink case, the suboptimal algorithm that we propose is very near to the exhaustive search. The complexity reduction justifies our choice of this approach. We note that due to the high complexity of the exhaustive search algorithm, we perform this comparison (Fig. 3.2) with only 8 subchannels, 4 secondary users and 2 primary users.

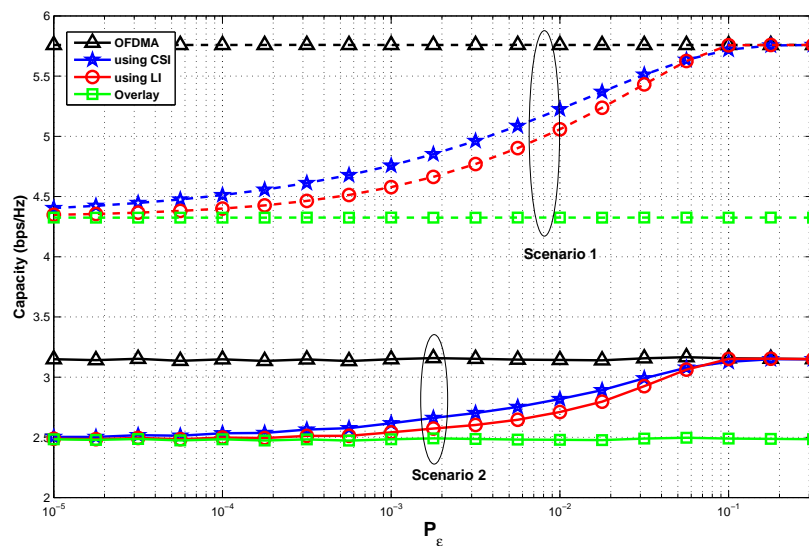


Figure 3.3: Downlink capacity of various schemes as a function of p_ϵ when the distance between the primary user and the secondary base station is 3 (km).

3.5.3 Effect of the Users' Spatial Distribution

In Fig. 3.3, we consider two different simulation scenarios for the secondary users and the primary user:

1. All the secondary users are located along the circle with a radius of 1 (km) and the primary users are located at random within the cell with the radius of 8 (km).
2. The secondary users as well as the primary users are randomly distributed within the cell. This is a more practical scenario with non-identically distributed users in a cellular environment.

We show in this figure the impact of p_ϵ on the performance of the location-based algorithm. As in the figure, the lower p_ϵ , the stronger protection we put in place for the primary user and therefore the secondary users tend to avoid the subchannels under the primary user's band.

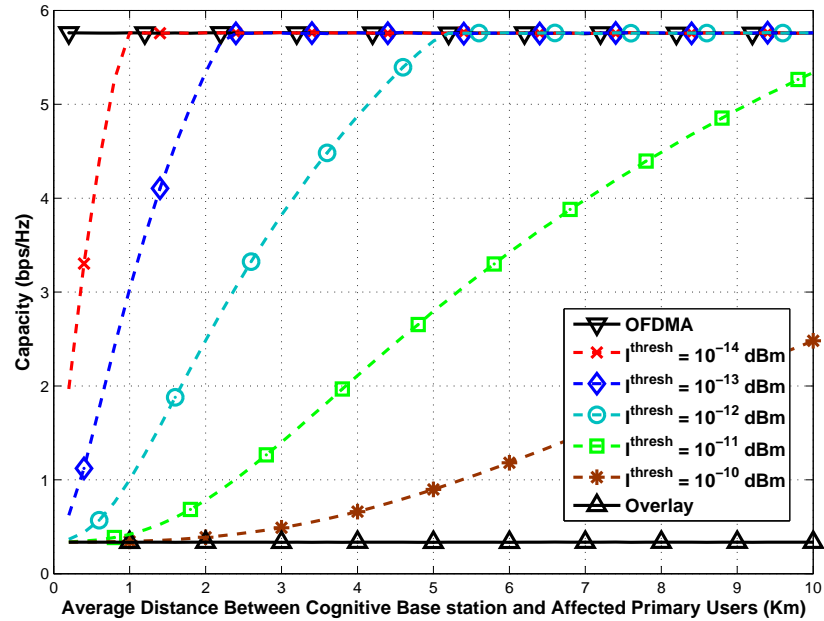


Figure 3.4: Impact of interference threshold on the network capacity for the proposed algorithm (downlink case).

3.5.4 Effect of the Interference Threshold

Fig. 3.4 shows the impact of the threshold level on the performance of the location-based algorithm. As shown in the figure, the higher the threshold level, the stronger protection we put in place for the primary users and therefore the secondary users tend to avoid the subchannels under the primary users' band which corresponds to the overlay algorithm. Inversely, when the threshold level decreases, we allow more freedom to secondary users to use all the subchannels which is similar to the OFDMA case.

3.5.5 Effect of the Number of Primary Users

Fig. 3.5 shows the capacity as function of the number of primary users. The capacity decreases with the increase of the primary users which can be explained by the increase of the interference constraints due to the decrease of the minimal distance.

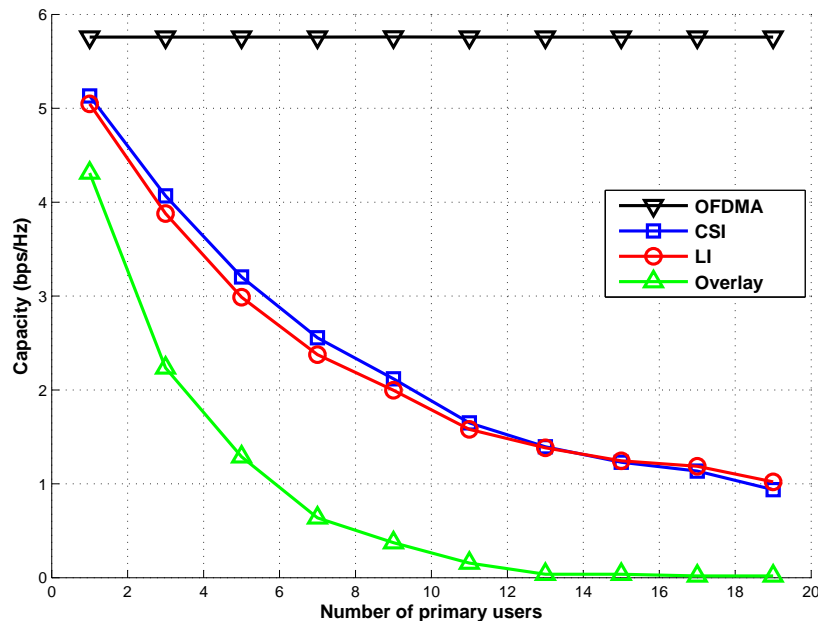


Figure 3.5: Impact of the number of primary users on the cognitive network performances.

3.5.6 Practical Algorithms Performance

In this paragraph, we focus on the practical instantiations of the resource allocation algorithms presented in section 3.4.3.

Fig. 3.6 shows the capacity of the discrete rate and fixed power allocation algorithms compared to the continuous case. An important rate loss is observed with the discretization (5 levels) but this loss becomes negligible with use of high number of discrete levels (i.e. 20 levels). For the fixed power algorithm, the rate loss is important for long distances to the primary users and very low when this distance increases. This can be explained by the interference constraint which do not have any effect on the power allocation for high distances to the primary user.

Fig. 3.7 compares effect of different combinations of practical constraints as stated in Table. 3.1 on the resource allocation achieved capacity. The collocated subchannels constraint results in a loss of around 1 bps/Hz per user (Scenario 4), while a

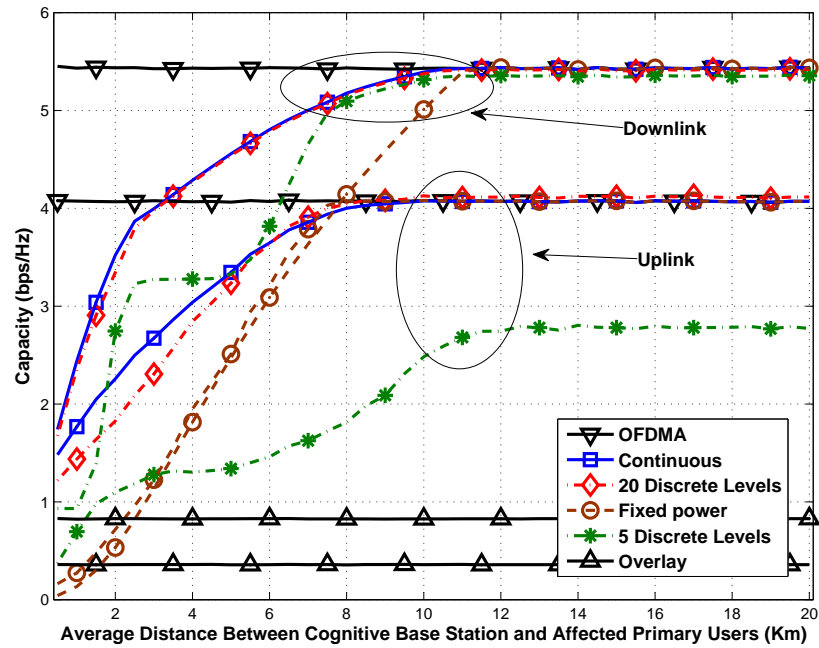


Figure 3.6: Discrete rate and fixed power constraints effect on the performance of the resource allocation.

combination of collocated subchannels and discrete rate constraints (Scenario 5) degrades more the rate to 1.5 bps/Hz per user compared to the continuous case. The cumulation of the different practical constraints affect the achieved throughput which shows the need to consider these practical constraints in modeling the system due to the important difference compared to the theoretical achievable rate.

3.6 Conclusion

This chapter introduced a resource allocation algorithm based on location information for OFDMA cognitive radio systems and showed that it achieves a near-optimal capacity even without knowledge of the interference link. In particular, we firstly proposed a method to estimate of the interference based on pathloss and location information. Then, we optimized the capacity of the cognitive network under the interference and power constraints. In addition, we proposed sub-optimal algorithms

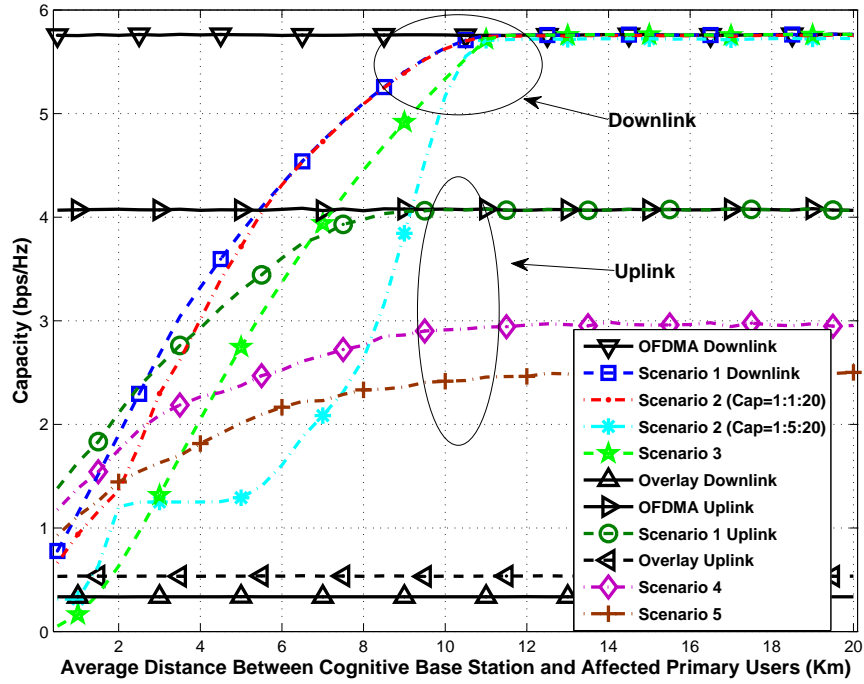


Figure 3.7: Effect of discretization of the capacities and allocation of collocated sub-channels on the performance of the cognitive network.

Table 3.1: Different resource allocation scenarios for Fig. 3.7.

Scenario	subchannel allocation	power allocation	rate (capacity)
1	no restriction	waterfilling	fractional
2	no restriction	waterfilling	discrete
3	no restriction	fixed power	fractional
4	collocated	waterfilling	fractional
5	collocated	waterfilling	discrete

which solve the formulated optimization problems. The numerical results show the efficiency of the proposed algorithms compared to the exhaustive search algorithm. Extended algorithms considering practical implementation constraints such as discrete rates or collocated channels were also proposed. Although we have shown that the location-based resource allocation achieves close performance to the optimization with knowledge of real channel state information, this result limited to some environments where the proposed pathloss and shadowing model which we used to estimate the average interference based on the location information.

Chapter 4

Reduced-Dimension Power

Allocation over Clustered Channels under Cochannel Interference

4.1 Introduction

Due to the nature of cognitive radio requiring rapid exploitation of the opportunities that occur before the status of the primary users change, complexity reduction of the resource allocation algorithms remains as one of the most important challenges for these systems. In multicarrier systems like OFDMA, the selection of the subcarrier bandwidth is a key factor since it controls the trade-off between computational complexity and performance. For instance, a large subcarrier width allows to reduce notably the computational complexity under the assumption of constant channel gains over each subcarrier which is not usually the case in wireless channels. On the other hand, reducing the subcarrier width results in large number of channels that have to be optimally allocated; Hence the computational complexity of the resource allocation problem becomes cumbersome, which is not desirable in rapidly changing channels.

In this work, we propose a complex-efficient algorithm for the channel assignment

under cochannel interference. In the proposed scheme the available subcarriers are grouped into clusters or blocks of subcarriers where the size of each cluster is a design parameter. Thus, the power allocation will be performed over reduced number of clusters instead of all subcarriers. An interpolation matrix will be defined to relate the power allocation per subcarrier and the relevant cluster's power. The regrouping of the subcarriers will depend obviously on many factors such as the channels' smoothness and users' mobility. The choice of the clustering is not our main focus; we rather work with a predefined interpolation matrix and concentrate on how to solve the reduced dimension optimization problem and evaluate its performance and complexity compared to the optimal scheme. We should note that similar ideas of reduced dimension spectrum allocation were studied in the context of digital subscriber line systems [52]. However, the problem here is treated with different interpolation matrix in addition to the additional challenges of the wireless channels and the cognitive radio context.

In this context, we propose a resource allocation problem where a generic utility function is optimized under different power and target rate constraints in addition to the interference constraint to the primary users. We formulate the optimization problem considering the clustering of subcarriers and show that the new problem with clustering can be still decomposed into per cluster independent sub-problems. The complexity gain using this approach is then proportional to the average number of subcarriers per cluster. Inherent to this interpolation, there is a performance loss that will be evaluated using numerical simulations.

The rest of the chapter is organized as follows: We describe in section 4.2 the cognitive system model and formulate the resource allocation optimization problem under the clustering property in section 4.3. In section 4.4, we analyze and solve the optimization problem. In section 4.5, we present some numerical simulation results showing the complexity/performance tradeoffs of the reduced dimension approach.

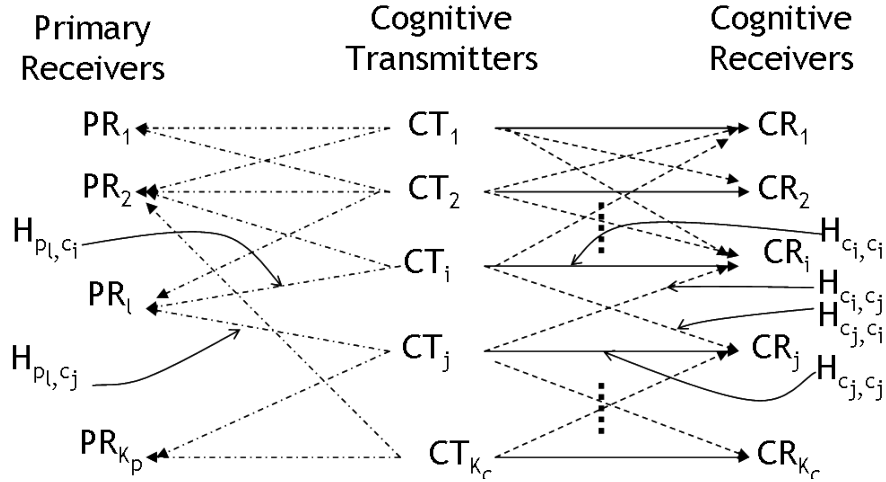


Figure 4.1: Block diagram for cognitive radios system with co-channel interference.

Finally, in section 4.6 we draw the main conclusions of this approach.

4.2 System Model

In this chapter, we consider a peer-to-peer network composed of K_c secondary users and K_p primary users sharing N subcarriers in an OFDMA based transmission. We denote by $H_{pl,cu}^{(n)}$ the channel gain from the cognitive user u to the primary user l in the subcarrier n , and $H_{ck,cu}^{(n)}$ the channel gain from the cognitive user u to the cognitive user k in the subcarrier n as depicted in Fig. 4.1.

The knowledge of the interference channels to the primary users is not the focus of this chapter. As such, we suppose that an accurate estimation is available to the primary users either by primary users feedback or through location information like in the previous chapter.

4.3 Problem Formulation

4.3.1 Utility Function

We consider for each cognitive user u a generalized utility which combines the achievable rate and the consumed power expressed as the difference between the reward associated to achieved rates and the cost of the consumed power:

$$\max_{P_u^{(n)}} \sum_{u=1}^{K_c} \omega_u \{ \alpha_u R_u - \beta_u P_u \} \quad (4.1)$$

where

- ω_u is the weight associated to the user u ,
- β_u is the cost of a unit power for user u ,
- α_u is the reward associated to the rate of the user u ,
- $P_u = \sum_{n=1}^N P_u^{(n)}$ is the total power consumed by the user u ,
- $P_u^{(n)}$ is the power allocated to the user u in the sub-carrier n ,
- $R_u = f_s \sum_{n=1}^N \log_2 \left(1 + \frac{\gamma_u^{(n)}}{\Gamma_u} \right)$ is the sum-rate of user u , with f_s the symbol rate in Hz, Γ_u the gap to capacity of the user u which incorporates effects of coding and other factors that may degrade the user's rate, and $\gamma_u^{(n)}$ the signal-to-interference and noise ratio (SINR) of the user u over the n -th sub-carrier expressed as

$$\gamma_u^{(n)} = \frac{|H_{c_u, c_u}^{(n)}|^2 P_u^{(n)}}{\sum_{\substack{k=1 \\ k \neq u}}^{K_c} |H_{c_u, c_k}^{(n)}|^2 P_k^{(n)} + N_u^{(n)}}, \quad (4.2)$$

where $N_u^{(n)}$ is the background noise power which can incorporate interference from primary users or other devices.

This optimization utility is generic since by setting $\alpha_u = 0$, we obtain the problem of minimization of total cost power under target rate constraints. Inversely by setting $\beta_u = 0$, we obtain the problem of maximization of the achievable rate under budget power constraint.

4.3.2 Power and Rate Constraints

The following rate and power constraints will be considered:

1. Minimum target rate per-user $R_u \geq \check{R}_u \quad \forall u$
2. Power budget per user $P_u \leq \hat{P}_u \quad \forall u$
3. Total power budget $\sum_{u=1}^{K_c} P_u \leq \hat{P}$ (suitable for downlink scenario only)
4. Maximum power per user and per sub-carrier $0 \leq P_u^{(n)} \leq \hat{P}_u^{(n)} \quad \forall u, \forall n$
5. Instantaneous interference to primary users $B_l^{(n)} \sum_{u=1}^{K_c} |H_{pl,cu}^{(n)}|^2 P_u^{(n)} \leq \check{I}_l^{(n)} \quad \forall l, n,$

where $\{B_l^{(n)}\}_{\substack{1 \leq l \leq K_p \\ 1 \leq n \leq N}}$ is an index matrix representing the activity of the primary user (i.e., $B_l^{(n)} = 1$ indicates that the l -th primary user is active on the n -th subcarrier and $B_l^{(n)} = 0$ otherwise).

The last constraint ensures that for each subcarrier n where the primary user l is active, the total power received from the different cognitive users should not exceed an interference threshold $\check{I}_l^{(n)}$. The advantage of this interference constraint is that it ensures instantaneous protection to the primary users but it assumes an instantaneous estimation of the interference channel to the primary users and feedback about the tolerable interference per subcarrier. The interference threshold $\check{I}_l^{(n)}$ can be determined in function of the required bit loading or the tolerable SINR of the primary user.

Thus, the optimization problem is formulated as

$$\begin{aligned}
& \max_{P_u^{(n)}} \sum_{u=1}^{K_c} \omega_u \{ \alpha_u R_u - \beta_u P_u \} \\
& \text{S.t.} \quad R_u \geq \check{R}_u \quad \forall u \\
& \quad \sum_{u=1}^{K_c} P_u \leq \hat{P} \\
& \quad P_u \leq \hat{P}_u \quad \forall u \\
& \quad 0 \leq P_u^{(n)} \leq \hat{P}_u^{(n)} \quad \forall u, \forall n \\
& \quad B_l^{(n)} \sum_{u=1}^{K_c} |H_{p_l, c_u}^{(n)}|^2 P_u^{(n)} \leq I_l^{(n)} \quad \forall l, \forall n
\end{aligned} \tag{4.3}$$

4.3.3 Subcarriers Clustering

The subcarriers are grouped into $M \leq N$ clusters. An $N \times M$ binary indicator matrix \mathbf{A} relates the active subcarriers to the different clusters where $A_{n,m} = 1$ means that subcarrier n belongs to cluster m and otherwise $A_{n,m} = 0$. Since each subcarrier can belong to only one cluster, we have $\sum_{m=1}^M A_{n,m} = 1, \forall n$. Thus, the power allocation for each subcarrier can be deduced from the power allocated to each cluster as

$$P_u^{(n)} = \sum_{m=1}^M A_{n,m} \cdot Q_u^{(m)} = A_{n,m_n} \cdot Q_u^{(m_n)}, \tag{4.4}$$

where $P_u^{(n)}$ is the power spectrum assigned to the subcarrier n of user u , $Q_u^{(m)}$ is the power assigned to subcarriers belonging to the cluster m of the user u . The index m_n of the cluster to which the subcarrier n belongs should fulfill the following constraint

$$\forall n, \exists! m_n, A_{n,m} = \begin{cases} 1 & \text{if } m = m_n \\ 0 & \text{otherwise.} \end{cases}$$

This indexing matrix can be generalized to an interpolation matrix where the parameters $A_{n,m}$ can take not only binary values (0 or 1) but any positive real value

in the interval $[0, 1]$. In this case, the parameters $A_{n,m}$ will play the role of scaling coefficients of the subcarrier power in reference to the subgroup power to which they belong. The only constraint in this generalized case is that a subcarrier should belong to only one cluster, i. e. $0 < A_{n,m_n} \leq 1$ and $A_{n,m \neq m_n} = 0$. Inversely, the power per cluster can be obtained from the subcarrier powers as

$$Q_u^{(m_n)} = \frac{P_u^{(n)}}{A_{n,m_n}}, \quad \forall n. \quad (4.5)$$

The scaling coefficients A_{n,m_n} can be determined using e.g. empirical models of the channel dependency versus frequency. The choice of such coefficients is beyond the scope of this work. We rather focus on a indexing interpolation where $A_{n,m_n} = 1$ and $A_{n,m \neq m_n} = 0$. We assume that the clustering is selected according to the primary users activity in order to ensure that the primary users have the same state for all the subcarriers of the same cluster (either active or inactive over all subcarriers in each cluster). Thus, for each cluster m and all subcarriers $\{n\}$ belonging to it, we have $B_l^{(n)} = B_l^{(m_n)}, \forall l$. This assumption is realistic since in practice spectrum allocation is generally fixed over adjacent subcarriers. For example in Long-Term Evolution (LTE), OFDMA is used with blocks of 12 subcarriers. Thus, the primary occupation will be the same for all subcarriers in each block.

4.4 Reduced Dimension Power Allocation

4.4.1 Optimization Problem

Using the clustering characteristic expressed in (4.4), the rate of user u can be rewritten as

$$R_u = \sum_{m=1}^M \sum_{n=1}^N f_s \log_2 \left(1 + \frac{\gamma_u^{(m,n)}}{\Gamma_u} \right), \quad (4.6)$$

with $\gamma_u^{(m,n)}$ defined as the SINR of the user u over the n -th subcarrier in cluster m expressed as

$$\gamma_u^{(m,n)} = \frac{A_{n,m} |H_{c_u, c_u}^{(n)}|^2 Q_u^{(m)}}{\sum_{\substack{k=1 \\ k \neq u}}^{K_c} A_{n,m} |H_{c_u, c_k}^{(n)}|^2 Q_k^{(m)} + N_u^{(n)}}, \quad (4.7)$$

where $Q_k^{(m)}$ is the power loading in the m -th cluster for the k -th user. We note that as postulated in the characterization of the clusters, for a subcarrier n that does not belong to a cluster m ($m \neq m_n$), the interpolation index is null (i.e., $A_{n,m} = 0$) which leads to $\gamma_u^{(m,n)} = 0$. Thus, in the expression of the rate in (4.6), only the terms corresponding to the subcarriers belonging to each cluster m will remain in the sum.

Following this clustering relations, the problem (4.3) can be reformulated as follows

$$\begin{aligned} \max_{Q_u^{(m)}} \quad & \sum_{u=1}^{K_c} \omega_u \left\{ \alpha_u \sum_{m=1}^M \sum_{n=1}^N f_s \log_2 \left(1 + \frac{\gamma_u^{(m,n)}}{\Gamma_u} \right) - \beta_u \sum_{m=1}^M \sum_{n=1}^N A_{n,m} Q_u^{(m)} \right\} \quad (4.8) \\ \text{S.t} \quad & \sum_{m=1}^M \sum_{n=1}^N f_s \log_2 \left(1 + \frac{\gamma_u^{(m,n)}}{\Gamma_u} \right) \geq \check{R}_u \quad \forall u \\ & \sum_{u=1}^{K_c} \sum_{m=1}^M \sum_{n=1}^N A_{n,m} Q_u^{(m)} \leq \hat{P} \\ & \sum_{m=1}^M \sum_{n=1}^N A_{n,m} Q_u^{(m)} \leq \hat{P}_u \quad \forall u \\ & 0 \leq \sum_{m=1}^M A_{n,m} Q_u^{(m)} \leq \hat{P}_u^{(n)} \quad \forall u, \forall m \\ & A_{n,m} B_l^{(n)} \sum_{u=1}^K |H_{pl, c_u}^{(n)}|^2 Q_u^{(m)} \leq \check{I}_l^{(n)} \quad \forall l, \forall n, \forall m. \end{aligned}$$

Thus, the problem is shown to be re-written in function of the new $K_c \times M$ optimization variables $Q_u^{(m)}$ referring to the power allocation per cluster. Let us define for each cluster m the following useful parameters:

- $T_m \triangleq \sum_{n=1}^N A_{n,m}$ the number of subcarriers in the cluster,
- $R_u^{(m)} \triangleq \sum_{\substack{n=1 \\ A_{n,m} \neq 0}}^N f_s \log_2 \left(1 + \frac{\gamma_u^{(m,n)}}{\Gamma_u} \right)$ the total achievable rate per cluster,
- $\hat{Q}_u^{(m)} \triangleq \min_{n: A_{n,m} \neq 0} \left\{ \frac{\hat{P}_u^{(n)}}{A_{n,m}} \right\}$ the maximum power per user per cluster.

These definitions allow the optimization problem (4.8) over the clusters of subcarriers to be rewritten in an interesting form that only depends on the clusters (except for the interference constraint that we elaborate more in section 4.4.3):

$$\begin{aligned}
& \max_{Q_u^{(m)}} \sum_{u=1}^{K_c} \omega_u \left\{ \alpha_u \sum_{m=1}^M R_u^{(m)} - \beta_u \sum_{m=1}^M T_m Q_u^{(m)} \right\} & (4.9) \\
& \text{S.t.} \quad \sum_{m=1}^M \sum_{\substack{n=1 \\ A_{n,m} \neq 0}}^N f_s \log_2 \left(1 + \frac{\gamma_u^{(m,n)}}{\Gamma_u} \right) \geq \check{R}_u \quad \forall u \\
& \quad \sum_{u=1}^{K_c} \sum_{m=1}^M T_m Q_u^{(m)} \leq \hat{P} \\
& \quad \sum_{m=1}^M T_m Q_u^{(m)} \leq \hat{P}_u \quad \forall u \\
& \quad 0 \leq Q_u^{(m)} \leq \hat{Q}_u^{(m)} \quad \forall u, \forall m \\
& \quad A_{n,m} B_l^{(n)} \sum_{u=1}^{K_c} |H_{pl,c_u}^{(n)}|^2 Q_u^{(m)} \leq \check{I}_l^{(n)} \quad \forall l, \forall \{m, n\} \setminus A_{n,m} \neq 0.
\end{aligned}$$

By setting $M = N$, the interpolation matrix is the identity matrix ($\mathbf{A} = \mathbf{I}_{N \times N}$) and the problem (4.9), is exactly the original power allocation problem without clustering.

4.4.2 Per-cluster Subproblems Decomposition

The problem (4.9) is a non convex optimization problem due to the cochannel interference between users [51]. A common way to solve this primal problem is to derive

and solve its equivalent dual problem by moving the constraints to the objective using a Lagrange multiplier per constraint. For non-convex problems, the duality gap is non null but [53] has shown that for non convex optimization problems the duality gap is 0 under a certain condition called *time-sharing* condition and that the time-sharing condition is satisfied for practical multiuser spectrum optimization problems in multicarrier systems in the limit as the number of subcarriers goes to infinity.

Thus, reformulating the problem into its Lagrangian dual, we obtain

$$\min_{\lambda \geq 0, \nu \geq 0} \left[\begin{array}{l} \max_{Q_u^{(m)}} \quad \sum_u \omega_u \{ \alpha_u R_u - \beta_u P_u \} + \sum_u \nu_u (R_u - \check{R}_u) + \lambda_0 (\hat{P} - \sum_u P_u) + \sum_u \lambda_u (\hat{P}_u - P_u) \\ \text{S.t} \quad \quad \quad 0 \leq Q_u^{(m)} \leq \hat{Q}_u^{(m)} \quad \quad \quad \forall u, \forall m \\ \quad \quad \quad A_{n,m} B_l^{(n)} \sum_{u=1}^{K_c} |H_{pl,c_u}^{(n)}|^2 Q_u^{(m)} \leq \check{I}_l^{(n)} \quad \forall l, \forall (m,n). \end{array} \right], \quad (4.10)$$

where $\boldsymbol{\lambda} = [\lambda_0, \dots, \lambda_{K_c}]^T$ and $\boldsymbol{\nu} = [\nu_1, \dots, \nu_{K_c}]^T$, are the Lagrangian parameters.

We remark that in the dual problem we moved only the constraints involving different subcarriers to the Lagrangian expression. The mask and interference constraints are per subcarrier constraints and they will form just a limit for our allocated power space search in the optimization. The problem (4.10) can be rewritten as

$$\min_{\lambda \geq 0, \nu \geq 0} \left[g(\boldsymbol{\lambda}, \boldsymbol{\nu}) + \lambda_0 \hat{P} + \sum_u \lambda_u \hat{P}_u - \sum_u \nu_u \check{R}_u \right], \quad (4.11)$$

where the subproblem $g(\boldsymbol{\lambda})$ is defined by

$$\begin{aligned} g(\boldsymbol{\lambda}, \boldsymbol{\nu}) = & \max_{Q_u^{(m)}} \sum_{u=1}^{K_c} \left((\omega_u \alpha_u + \nu_u) \sum_{m=1}^M R_u^{(m)} - (\omega_u \beta_u + \lambda_u + \lambda_0) \sum_{m=1}^M T_m Q_u^{(m)} \right) \\ \text{S.t} \quad & 0 \leq Q_u^{(m)} \leq \hat{Q}_u^{(m)}, \quad \forall u \\ & A_{n,m} B_l^{(n)} \sum_{u=1}^{K_c} |H_{pl,c_u}^{(n)}|^2 Q_u^{(m)} \leq \check{I}_l^{(n)}, \quad \forall l, \forall n, \end{aligned} \quad (4.12)$$

which can be decomposed into sum of subproblems over each cluster of subcarriers:

$$g(\boldsymbol{\lambda}, \boldsymbol{\nu}) = \sum_{m=1}^M g^{(m)}(\boldsymbol{\lambda}, \boldsymbol{\nu}), \quad (4.13)$$

where the subproblem $g^{(m)}(\boldsymbol{\lambda}, \boldsymbol{\nu})$ is defined by

$$\begin{aligned} g^{(m)}(\boldsymbol{\lambda}, \boldsymbol{\nu}) = & \max_{Q_u^{(m)}} \sum_{u=1}^{K_c} \left((\omega_u \alpha_u + \nu_u) R_u^{(m)} - (\omega_u \beta_u + \lambda_u + \lambda_0) T_m Q_u^{(m)} \right) \\ \text{S.t} \quad & 0 \leq Q_u^{(m)} \leq \hat{Q}_u^{(m)}, \quad \forall u \\ & A_{n,m} B_l^{(n)} \sum_{u=1}^{K_c} |H_{pl,c_u}^{(n)}|^2 Q_u^{(m)} \leq \check{I}_l^{(n)}, \quad \forall l, \forall n. \end{aligned} \quad (4.14)$$

The previous equations, show that the optimization problem is written as a sum of per cluster subproblems $g^{(m)}(\boldsymbol{\lambda}, \boldsymbol{\nu})$. Each of the subproblems is a non-convex optimization problem in K_c variables. They can be solved optimally by exhaustive search over the discrete set of feasible power values. Clearly, this approach is not convenient for large users due to the exponential number of possible combinations. An alternative approach is to iterate over the users and optimize at each iteration the power for one user given the other users powers. This procedure has been shown to converge to a near-optimal solution of the multidimensional search [53, 54] with reduction of the computational cost from an exponential of the number of users p^{K_c} to only $p \times K_c$ where p is the number of power levels per user. The set of feasible powers is obtained by restricting the set of all affordable power levels (i.e., the powers corresponding to discrete bit-loading) for all users to only those satisfying the maximum power per cluster and the interference constraints to the primary users.

For the Lagrangian parameters, an adaptive step-size search algorithm will be applied to determine their optimal values. Overall, the algorithm will consist of two main loops. In the outer loop a search over the feasible Lagrangian parameters using e.g. a subgradient decent method is performed. In an inner loop for each set of Lagrangian parameters, the power allocation per subcarrier is optimized for each

user.

The interesting part of this approach is that we show that the problem can be solved by transforming it into M separate subproblems over each cluster of subcarriers. The clustering allows reducing the complexity by a factor equal to the number of subcarriers per cluster $\frac{N}{M}$ thanks to the decoupling between the clusters. This decoupling allows writing the overall problem into a sum of elementary subproblems that can be optimized separately. The performance loss will depend on the spectral characteristics of the channels and the choice of the interpolation matrix \mathbf{A} and especially on the number of subcarriers per cluster $\frac{N}{M}$.

4.4.3 Interference Constraint per Cluster

We note that the interference constraints remain per subcarrier due to the different interference channels for each user $|H_{pl,c_u}^{(n)}|^2$. These constraints do not cause a harmful increase of the algorithm complexity since we are using them to only check if a set of power levels per cluster $\left(\left\{Q_u^{(m)}\right\}_{1 \leq u \leq K_c}\right)$ is feasible or not. Thus, we will have for a given possible power level of the cluster, $K_p \cdot T_m$ constraints to check (number of primary users multiplied by number of subcarriers in the cluster m). If at least one of these $K_p \cdot T_m$ constraints is not fulfilled, the power level is discarded from the search space. Ideally, these $K_p \cdot T_m$ constraints per cluster could be transformed into K_p constraints having the following format

$$B_l^{(m)} \sum_{u=1}^{K_c} |\tilde{H}_{pl,c_u}^{(m)}|^2 Q_u^{(m)} \leq \tilde{I}_l^{(m)} \quad \forall l, \forall m, \quad (4.15)$$

where $\tilde{I}_l^{(m)}$ and $\tilde{H}_{pl,c_u}^{(m)}$ are respectively the equivalent interference threshold of the l -th primary user over the cluster m and the equivalent channel gain from the u -th cognitive user towards the l -th primary user over the cluster m . Although, the exact expressions of $\tilde{I}_l^{(m)}$ and $\tilde{H}_{pl,c_u}^{(m)}$ do not exist due to the multipath between cognitive

users towards primary users, modified constraints can be used. For example, we allow the interference to exceed the interference level for a given subcarrier but the average interference over the cluster should not exceed the average threshold levels of the same cluster. Mathematically speaking, this requirement result in the following expressions of the equivalent thresholds and channel gains as

$$\left\{ \begin{array}{l} \tilde{I}_l^{(m)} = \frac{1}{T_m} \sum_{\substack{n=1 \\ A_{n,m} \neq 0}}^N \check{I}_l^{(n)} \quad \forall l, \forall m \\ |\tilde{H}_{p_l, c_u}^{(m)}|^2 = \frac{1}{T_m} \sum_{\substack{n=1 \\ A_{n,m} \neq 0}}^N A_{n,m} |H_{p_l, c_u}^{(n)}|^2 \quad \forall u, \forall l, \forall m. \end{array} \right. \quad (4.16)$$

Another example is to consider a worst-case interference threshold and interference gains per cluster enforcing the interference constraint for all subcarriers are shown to be respectively

$$\left\{ \begin{array}{l} \tilde{I}_l^{(m)} = \min_{A_{n,m} \neq 0} \{ \check{I}_l^{(n)} \} \quad \forall l, \forall m \\ |\tilde{H}_{p_l, c_u}^{(m)}|^2 = \max_{A_{n,m} \neq 0} \{ A_{n,m} |H_{p_l, c_u}^{(n)}|^2 \} \quad \forall u, \forall l, \forall m. \end{array} \right. \quad (4.17)$$

4.5 Numerical and Simulation Results

For the numerical evaluation, we consider only the rate maximization problem ($\alpha_u = 1$ and $\beta_u = 0$). We consider the primary and secondary users to be uniformly distributed in a cellular cell of radius one Km. The channel gains, distributed as multivariate Rayleigh fading channels, are generated from multivariate complex Gaussian distribution with a covariance matrix as in [55]. The covariance between two subcarriers is exponentially decaying as a function of the distance between the subcarriers while the average power is proportional to the path-loss with a path-loss exponent $\eta = 4$. The budget power is set to 20 dBm per user while the maximum power per subcarrier is -2.3 dBm. We consider single primary user ($K_p = 1$). We assume the primary user

present in $\nu = 50\%$ of the subcarriers. The interference threshold is computed such that the primary bitloading in presence of cognitive users does not decrease by more than a degradation factor ϵ compared to its original bitloading in absence of cognitive user's interference. We run the simulations for a frequency band of $N = 512$ subcarriers with different number of clusters M and represent the results in function of the clustering factor $\rho = \frac{M}{N}$. We use the binary interpolation model ($A_{n,m} = 0$ or 1) and equal number of subcarriers per cluster.

4.5.1 Effect of Subcarriers Clustering

In Fig. 4.2, we plot the achievable rate regions of two users while varying the number of clusters. We first note that the reduced dimension almost has no effect on the achievable rate even with $\rho = 1\%$ as compared to no clustering ($\rho = 100\%$). This proves the efficiency of the reduced dimension approach since it allows to achieve a near-optimal performance with a much lower computational complexity that is proportional to the clustering factor as shown in section 4.4.2. The figure also shows the rate improvement for the cognitive users using the proposed hybrid scheme compared to the interweave or underlay modes due to the more opportunistic use of the available spectrum.

In Fig. 4.3, we present the power allocation over the set of subcarriers using different values of the clustering factor ρ . The interesting part is that the shape of the power allocation is the same independently from the clustering factor. The allocated power to each cluster is a kind of average over the powers allocated to the subcarriers in that cluster. This figure gave us an idea on a possible improve of the clustering through a better choose of the number of subcarriers per cluster. Instead of this uniform clustering, an adaptive clustering function of the channels variation could lead to closer performance to the optimal case with the same complexity.

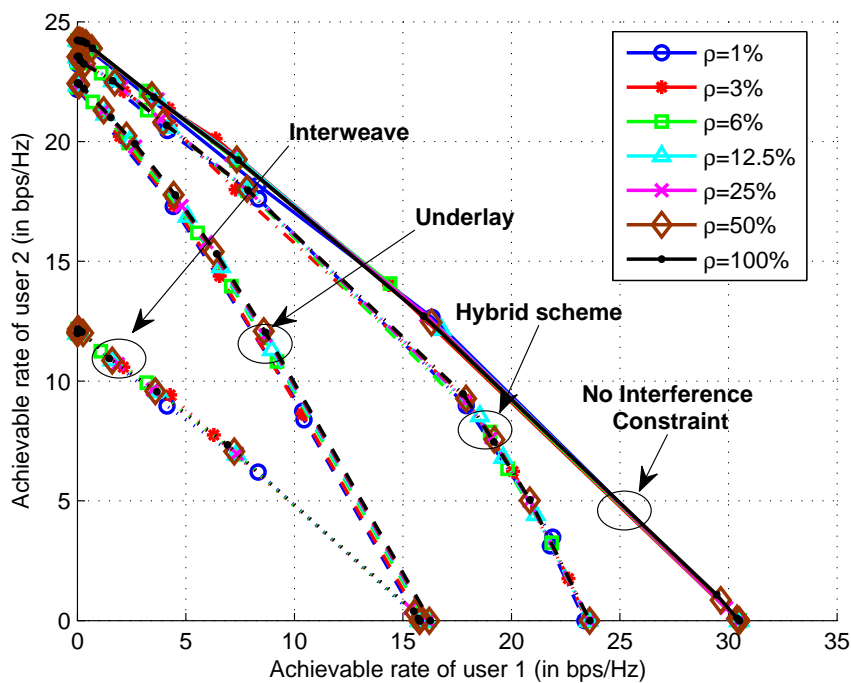


Figure 4.2: Rate region of two users with reduced dimension power allocation using different clustering factor ρ and an interference factor $\epsilon = 10\%$.

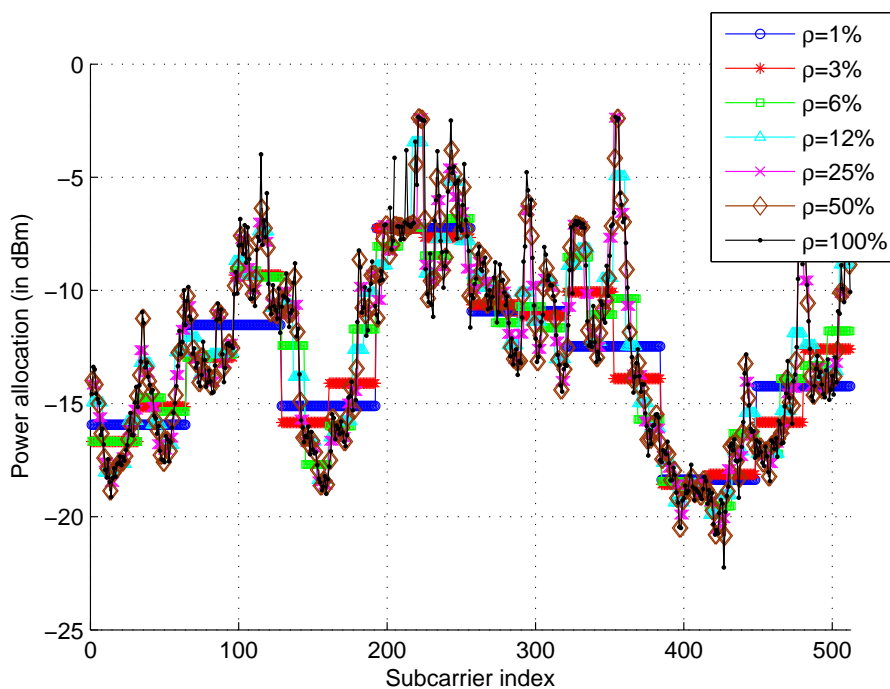


Figure 4.3: Power Allocation for an example user with reduced dimension using different clustering factor ρ and an interference factor $\epsilon = 10\%$.

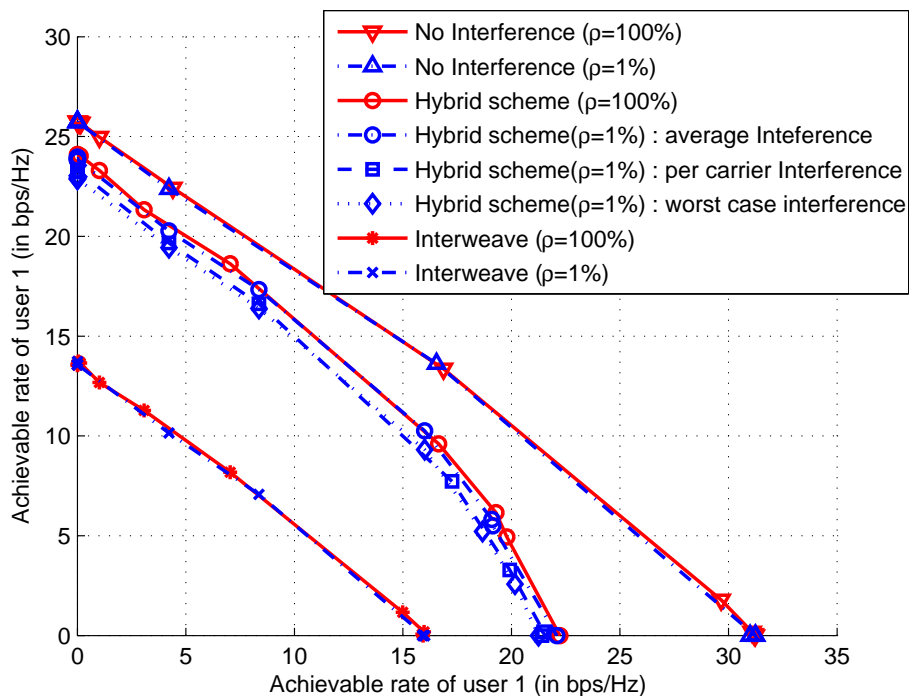


Figure 4.4: Rate region of two users for different interference constraints per cluster.

4.5.2 Effect of Interference Thresholds

In Fig. 4.5, we draw the rate regions for different interference threshold levels by varying the factor ϵ which indicates the allowed reduction of the bitloading in each subcarrier. We note that a factor $\epsilon = 50\%$ allows the secondary users to achieve almost their maximal performance (like without interference constraint). As the interference constraint become more strict (i.e., when ϵ decreases as in the $\epsilon = 1\%$ curve) the performance loss of the reduced dimension with respect to the full optimization increases which can be explained by the more strict constraint especially that this constraint should be respected for all subcarriers in the cluster (if at least one subcarrier has a strong interference channel towards one of the primary users, then all subcarriers in the same cluster should backoff to comply with the interference threshold).

In Fig. 4.4, we compare the performance when using an interference constraint per

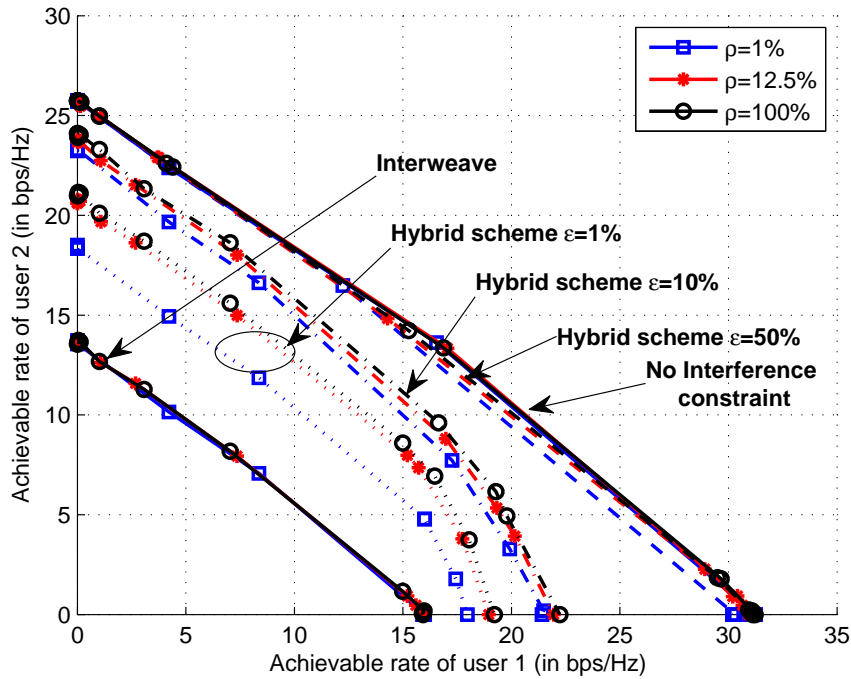


Figure 4.5: Rate region of two users versus the clustering ρ and the interference factors ϵ .

subcarrier to the simplified interferences per cluster: the average interference (4.16) and the worst case interference (4.17). The received interference at the primary users are plotted in Fig. 4.6. The average interference constraint allows to achieve better rates but it violates the interference constraint for some carriers even-though the average interference in the cluster is the same. The worst case interference achieves approximately the same performance as the per carrier interference for this topology. With a higher number of users (primary and secondary), this interference is expected to give worse interference but for this case there is no effect due to the limited diversity of the channels.

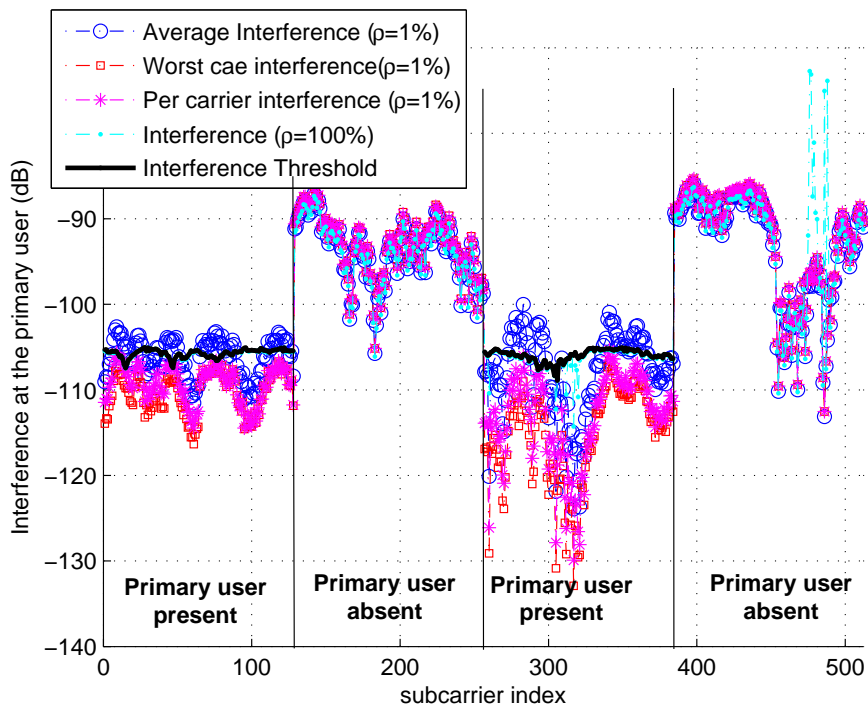


Figure 4.6: Comparison of the interference at the primary user with the different interference constraints with reduced dimension.

4.6 Conclusion

In this chapter, we proposed a reduced dimension resource allocation for cognitive radio by transforming the problem from an optimization over the subcarriers into optimization over clusters of subcarriers. We proved that this approach allows a complexity gain proportional to the average number of subcarriers per cluster of the resource allocation algorithm while achieving close performance with comparison to the optimization over all subcarriers at least for the evaluated scenario (rate minimization). Obviously the performance gap between the proposed resource allocation and optimal solution depends on the spectral properties of the channels and the different noises.

Chapter 5

Conclusion

5.1 Summary

In this thesis, we proposed major enhancements to cognitive radios systems taking into consideration the practical constraints and limitations of the real applications.

Firstly, we computed the expressions of the average cooperative spectrum sensing probabilities of false-alarm and detection in the case of non-identical and imperfect Nakagami-m distributed sensing and reporting channels. The results allowed to observe the effect of imperfect reporting channels on performance and hence could be useful for a better system parametrization.

Secondly, based on an interference estimation from location information, we formulated a resource allocation problem for cognitive users without need of instantaneous estimation of the interference channel towards primary users. Low-complexity algorithms for downlink and uplink scenarios as well as practical implementations considering collocated channels and discrete rate constraints are described and compared in terms of performance.

Finally, we proposed a reduced-dimension approach for resource allocation problem in presence of co-channel interference based on grouping of subcarriers. This approach allows an important gain in terms of complexity with a limited performance loss.

5.2 Future Research Work

This work can be extended in multiple directions. For instance, the derived performance analysis of the cooperative spectrum sensing under non identical and imperfect channels can be further extended to consider other channel models or cooperation schemes. In addition, the derived results could be exploited as relevant input for optimization algorithms where different parameters of the cognitive system will be optimized in order to enhance spectrum sensing reliability performance with lowest possible energy consumption. For the resource allocation, this work can be combined by studying a joint spectrum sensing and resource allocation problem where instead of doing the two steps of spectrum sensing and resource allocation consecutively. Indeed, a jointly designed algorithm may lead to a better performance taking in consideration probabilities of availability of primary users instead of only hard decision of their availability or not.

REFERENCES

- [1] G. Foschini and M. Gans, “On limits of wireless communications in a fading environment when using multiple antennas,” *Wireless Personal Communications*, vol. 6, pp. 311–335, 1998.
- [2] A. Goldsmith and S.-G. Chua, “Adaptive coded modulation for fading channels,” *IEEE Transactions on Communications*, vol. 46, no. 5, pp. 595–602, may 1998.
- [3] S. Ohmori, “Research activities of millimeter-wave technologies for multimedia communications,” in *Proc. IEEE International Conference on Personal Wireless Communication (ICPWC)*, Jaipur, India, Feb. 1999, pp. 60–65.
- [4] J. Mitola III and G. Q. Macguire Jr., “Cognitive radio: Making software radios more personal,” *IEEE Personal Commun. Mag.*, vol. 6, no. 4, pp. 13–18, Aug. 1999.
- [5] Federal Communications Commission: “Spectrum policy task force,” Report ET Docket, Nov. 2002.
- [6] A. Goldsmith, S. Jafar, I. Maric, and S. Srinivasa, “Breaking spectrum gridlock with cognitive radios: An information theoretic perspective,” *Proc. of the IEEE*, vol. 97, no. 5, pp. 894–914, May 2009.
- [7] A. Jovicic and P. Viswanath, “Cognitive radio: An information-theoretic perspective,” in *Proc. IEEE International Symposium on Information Theory (ISIT)*, Seattle, WA, USA, Jul. 2006, pp. 2413–2417.
- [8] T. Yucek and H. Arslan, “A survey of spectrum sensing algorithms for cognitive radio applications,” *IEEE Commun. Surveys Tuts.*, vol. 11, no. 1, pp. 116–130, quarter 2009.

- [9] Y. Zeng, Y.-C. Liang, A. T. Hoang, and R. Zhang, "A review on spectrum sensing for cognitive radio: challenges and solutions," *EURASIP J. Adv. Signal Process.*, vol. 2010, pp. 2:2–2:2, Jan. 2010.
- [10] Z. Quan, S. Cui, H. Poor, and A. Sayed, "Collaborative wideband sensing for cognitive radios," *IEEE Signal Process. Mag.*, vol. 25, no. 6, pp. 60–73, Nov. 2008.
- [11] Z. Quan, S. Cui, A. Sayed, and H. Poor, "Optimal multiband joint detection for spectrum sensing in cognitive radio networks," *IEEE Trans. Signal Process.*, vol. 57, no. 3, pp. 1128–1140, Mar. 2009.
- [12] Z. Quan, S. Cui, and A. H. Sayed, "Optimal linear cooperation for spectrum sensing in cognitive radio networks," *IEEE J. Sel. Topics Signal Process.*, vol. 2, no. 1, pp. 28–40, Feb. 2008.
- [13] G. Ganesan and Y. G. Li, "Cooperative spectrum sensing in cognitive radio - part I: two user networks," *IEEE Trans. Wireless Commun.*, vol. 6, no. 6, pp. 2204–2213, Jun. 2007.
- [14] J. Ma, G. Zhao, and Y. Li, "Soft combination and detection for cooperative spectrum sensing in cognitive radio networks," *IEEE Trans. Wireless Commun.*, vol. 7, no. 11, pp. 4502–4507, Nov. 2008.
- [15] W. Zhang and K. B. Letaief, "Cooperative spectrum sensing with transmit and relay diversity in cognitive radio networks," *IEEE Trans. Wireless Commun.*, vol. 7, no. 12, pp. 4761–4766, Dec. 2008.
- [16] H. Rif-Pous, M. Blasco, and C. Garrigues, "Review of robust cooperative spectrum sensing techniques for cognitive radio networks," *Wireless Personal Communications*, vol. 67, no. 2, pp. 175–198, 2012.
- [17] I. F. Akyildiz, B. F. Lo, and R. Balakrishnan, "Cooperative spectrum sensing in cognitive radio networks: A survey," *Elsevier Physical Commun.*, vol. 4, pp. 40–62, 2011.

- [18] W. Zhang, R. Mallik, and K. B. Letaief, "Optimization of cooperative spectrum sensing with energy detection in cognitive radio networks," *IEEE Trans. Wireless Commun.*, vol. 8, no. 12, pp. 5761–5766, Dec. 2009.
- [19] C. Sun, W. Zhang, and K. B. Letaief, "Cluster-based cooperative spectrum sensing in cognitive radio systems," in *Proc. IEEE Int. Conf. on Commun. (ICC)*, Glasgow, Scotland, Jun. 2007, pp. 2511–2515.
- [20] H. Birkan Yilmaz, T. Tugcu, and F. Alagoz, "Novel quantization-based spectrum sensing scheme under imperfect reporting channel and false reports," *Int. Journal Commun. Systems*, 2012.
- [21] Y. Chen, "Analytical performance of collaborative spectrum sensing using censored energy detection," *IEEE Trans. Wireless Commun.*, vol. 9, no. 12, pp. 3856–3865, Dec. 2010.
- [22] Y. Lin, C. He, L. Jiang, and D. He, "A censoring cooperative spectrum sensing scheme based on stochastic resonance in cognitive radio," in *Proc. IEEE Int. Conf. on Commun. (ICC)*, Kyoto, Japan, Jun. 2011, pp. 1–5.
- [23] D. Duan and L. Yang, "Cooperative spectrum sensing with ternary local decisions," *IEEE Communications Letters*, vol. 16, no. 9, pp. 1512–1515, 2012.
- [24] S. Xie, L. Shen, and J. Liu, "Optimal threshold of energy detection for spectrum sensing in cognitive radio," in *Proc. Int. Conf. on Wireless Commun. Signal Processing (WCSP)*, Nanjing, China, Nov. 2009, pp. 1–5.
- [25] C. Guo, T. Peng, S. Xu, H. Wang, and W. Wang, "Cooperative spectrum sensing with cluster-based architecture in cognitive radio networks," in *Proc. IEEE Veh. Technol. Conf. (VTC)*, Barcelona, Spain, Apr. 2009, pp. 26–29.
- [26] V. K. S. Chaudhari, J. Lunden and V. Poor, "Cooperative sensing with imperfect reporting channels: Hard decisions or soft decisions?" *IEEE Transactions on Signal Processing*, vol. 60, no. 1, pp. 18–28, 2012.

- [27] D.-C. Oh and Y.-H. Lee, "Cooperative spectrum sensing with imperfect feedback channel in the cognitive radio systems," *Int. Journal Commun. Systems*, vol. 23, no. 6-7, pp. 763–779, 2010.
- [28] M. Nakagami, "The m -distribution—a general formula for intensity distribution of rapid fading," *Statistical Methods in Radio Wave Propagation*, 1960.
- [29] M. Simon, *Probability Distributions Involving Gaussian Random Variables: A Handbook for Engineers and Scientists*, ser. International Series in Engineering and Computer Science. Springer Science + Business Media, LLC, 2006.
- [30] S. Al-Ahmadi and H. Yanikomeroglu, "On the approximation of the generalized-K pdf by a Gamma pdf using the moment matching method," in *Proc. IEEE Wireless Commun. Networking Conf. (WCNC)*, Budapest, Hungary, Apr. 2009, pp. 1–6.
- [31] A. Sahai, N. Hoven, and R. Tandra, "Some fundamental limits on cognitive radio," in *Proc. The 42nd Allerton Conference on Communication, Control and Computing*, Monticello, IL, USA, Oct. 2004, pp. 1–5.
- [32] F. F. Digham, M.-S. Alouini, and M. K. Simon, "On the energy detection of unknown signals over fading channels," *IEEE Trans. Commun.*, vol. 55, no. 1, pp. 21–24, Jan. 2007.
- [33] I. S. Gradshteyn and I. M. Ryzhik, *Table of Integrals, Series, and Products*, 5th ed. San Diego, CA: Academic Press, 1994.
- [34] S. Herath, N. Rajatheva, and C. Tellambura, "Energy detection of unknown signals in fading and diversity reception," *IEEE Trans. Commun.*, vol. 59, no. 9, pp. 2443–2453, 2011.
- [35] M. K. Simon and M.-S. Alouini, *Digital Communication Over Fading Channels*. John Wiley & Sons, Inc., 2002.
- [36] V. A. Aalo, T. Piboongunon, and C.-D. Iskander, "Bit-error rate of binary digital modulation schemes in generalized Gamma fading channels," *IEEE Commun. Lett.*, vol. 9, no. 2, pp. 139–141, Feb. 2005.

- [37] M. A. Thomas and A. E. Taub, “Calculating binomial probabilities when the trial probabilities are unequal,” *Journal of Statistical Computation and Simulation*, vol. 14, no. 2, pp. 125–131, 1982.
- [38] F. Yilmaz and M.-S. Alouini, “Product of the powers of generalized Nakagami-m variates and performance of cascaded fading channels,” in *Proc. IEEE Global Telecommunications Conference (GLOBECOM)*, Honolulu, HI, USA, Dec. 2009, pp. 1–8.
- [39] Baker, G. A., and P. Graves-Morris, *Pad Approximants*. Cambridge University Press, 1996.
- [40] M. Xia and S. Aissa, “Moments based framework for performance analysis of one-way/two-way CSI-assisted AF relaying,” *IEEE Journal on Selected Areas in Communications*, vol. 30, no. 8, pp. 1464–1476, 2012.
- [41] I. F. Akyildiz, W.-Y. Lee, M. C. Vuran, and S. Mohanty, “NeXt generation/dynamic spectrum access/cognitive radio wireless networks: A survey,” *Computer Networks*, vol. 50, no. 13, pp. 2127 – 2159, 2006.
- [42] S.-J. Kim and G. Giannakis, “Optimal resource allocation for MIMO Ad Hoc cognitive radio networks,” in *in Proc. The 46th Annual Allerton Conference on Communication, Control, and Computing*, Allerton House, IL, USA, Sep. 2008, pp. 39–45.
- [43] R. Zhang, Y.-C. Liang, and S. Cui, “Dynamic resource allocation in cognitive radio networks,” *IEEE Signal Processing Magazine*, vol. 27, no. 3, pp. 102–114, 2010.
- [44] G. Bansal, M. Hossain, and V. Bhargava, “Adaptive power loading for OFDM-based cognitive radio systems with statistical interference constraint,” *IEEE Transactions on Wireless Communications*, vol. 10, no. 9, pp. 2786–2791, 2011.
- [45] X. Kang, H. Garg, Y.-C. Liang, and R. Zhang, “Optimal power allocation for OFDM-based cognitive radio with new primary transmission protection criteria,” *IEEE Transactions on Wireless Communications*, vol. 9, no. 6, pp. 2066–2075, 2010.

- [46] S. Lim, H. Wang, H. Kim, and D. Hong, “Mean value-based power allocation without instantaneous CSI feedback in spectrum sharing systems,” *IEEE Transactions on Wireless Communications*, vol. 11, no. 3, pp. 874–879, 2012.
- [47] H. Celebi and H. Arslan, “Utilization of location information in cognitive wireless networks,” *IEEE Wireless Communications*, vol. 14, no. 4, pp. 6–13, 2007.
- [48] O. Duval, A. Punchihewa, F. Gagnon, C. Despins, and V. Bhargava, “Blind multi-sources detection and localization for cognitive radio,” in *Proc. IEEE Global Telecommunications Conference (GLOBECOM)*, New Orleans, LA, USA, Dec. 2008, pp. 1–5.
- [49] S. Kim, H. Jeon, and J. Ma, “Robust localization with unknown transmission power for cognitive radio,” in *Proc. IEEE Military Communications Conference (MILCOM)*, Orlando, FL, USA, Oct. 2007, pp. 1–6.
- [50] H. Celebi and H. Arslan, “Cognitive positioning systems,” *IEEE Transactions on Wireless Communications*, vol. 6, no. 12, pp. 4475–4483, 2007.
- [51] S. Boyd and L. Vandenberghe, *Convex Optimization*. New York, NY, USA: Cambridge University Press, 2004.
- [52] M. Guenach, C. Nuzman, K. Hooghe, J. Maes, and M. Peeters, “Reduced dimensional power optimization using class AB and G line drivers in DSL,” in *Proc. IEEE Global Telecommunications Conference (GLOBECOM)*, Miami, FL, USA, Dec. 2010, pp. 1443–1447.
- [53] W. Yu and R. Lui, “Dual methods for nonconvex spectrum optimization of multicarrier systems,” *IEEE Transactions on Communications*, vol. 54, no. 7, pp. 1310–1322, 2006.
- [54] S. Huberman, C. Leung, and T. Le-Ngoc, “Dynamic spectrum management (DSM) algorithms for multi-user xDSL,” *IEEE Communications Surveys Tutorials*, vol. 14, no. 1, pp. 109–130, 2012.

- [55] G. Karagiannidis, D. Zogas, and S. Kotsopoulos, “An efficient approach to multivariate Nakagami-m distribution using Green’s matrix approximation,” *IEEE Transactions on Wireless Communications*, vol. 2, no. 5, pp. 883–889, 2003.

APPENDICES

A Papers Submitted and Published

Papers Related to this Thesis

Journals

- M. Ben Ghorbel, M. Guenach, and M.-S. Alouini, “Reduced-dimension power allocation over clustered channels in cognitive radios system under cochannel interference,” *Submitted to IEEE Transactions on Communications*.
- M. Ben Ghorbel, H. Nam, and M.-S. Alouini, “Performance of soft cooperative spectrum sensing for cognitive radios under imperfect and non identical reporting channels,” *Submitted to IEEE Wireless Communications Letters*.
- M. Ben Ghorbel, H. Nam, and M.-S. Alouini, “Performance of cooperative spectrum sensing for cognitive radios under imperfect and non identical reporting channels,” *Submitted to IEEE Transactions on Communications*.
- H. Nam, M. Ben Ghorbel, and M.-S. Alouini, “Primary user localization and uplink resource allocation in OFDMA cognitive radio systems,” *Submitted to*

Conferences

- M. Ben Ghorbel, H. Nam, and M.-S. Alouini, “Exact performance of cooperative spectrum sensing for cognitive radios with quantized information under imperfect reporting channels,” *To appear in Proc. IEEE Vehicular Technology Conference (VTC)*, Las Vegas, USA, September 2013.
- M. Ben Ghorbel, H. Nam, and M.-S. Alouini, “Cluster-based spectrum sensing for cognitive radios with imperfect channel to cluster-head,” *in Proc. IEEE Wireless Communications and Networking Conference (WCNC)*, Paris, France, April 2012.
- M. Ben Ghorbel, H. Nam, and M.-S. Alouini, “Discrete rate resource allocation for OFDMA cognitive radio systems with location information,” *in Proc. IEEE International Symposium on Personal, Indoor and Mobile Radio Communications (PIMRC)*, Istanbul, Turkey, September 2010.
- M. Ben Ghorbel, H. Nam, and M.-S. Alouini, “Generalized location-based resource allocation for OFDMA cognitive radio systems,” *in Proc. International Symposium on Wireless Communication Systems (ISWCS)*, York, UK, September 2010.
- H. Nam, M. Ben Ghorbel, and M.-S. Alouini, “Location-based resource allocation for OFDMA cognitive radio systems,” *in Proc. on Cognitive Radio Oriented Wireless Networks & Communications (CROWNCOM)*, Cannes, France, June 2010.

Others

- M. Guenach, M. Ben Ghorbel, C. Nuzman, K. Hooghe, M. Timmers, and J. Maes, “Energy management of DSL systems: Experimental findings,” *To appear in Proc. IEEE Global Communications Conference (GLOBECOM)*, Atlanta, USA, December 2013.
- J. Maes, M. Guenach, M. Ben Ghorbel, and B. Drooghag, “Managing unvectorized lines in a vectored group,” *To appear in Proc. IEEE Global Communications Conference (GLOBECOM)*, Atlanta, USA, December 2013.
- M. Ben Ghorbel, A. Goldsmith, and M.-S. Alouini, “Joint pricing and resource allocation for cognitive radios system,” *in Proc. IEEE International Conference on Computer Communications (INFOCOM)*, Shanghai, China, April 2011.